

Dr. Rolf M. Schwiete Center
for Limbal Stem Cell Deficiency
and Congenital Aniridia Research
Saarland University, Homburg/Saar
Chairman: Prof. Dr. Nóra Szentmáry

**The effect of Ca²⁺ supplementation on epithelial cell
differentiation and retinoic acid signaling components
in a siRNA-based aniridia cell model**

*Dissertation for the degree of
Doctor of Theoretical Medicine (Dr. rer. med.)
Faculty of Medicine*

UNIVERSITY OF SAARLAND

2021

Submitted by: Priya Katiyar
Born on 10.07.1987 in Auraiya, UP, India

Supervisor: Univ.-Prof. Dr. Nóra Szentmáry
Chairman, Dr. Rolf M. Schwiete Center for Limbal Stem
Cell Deficiency and Congenital Aniridia Research
Saarland University, Homburg/Saar

Co-supervisor: Entfällt

Tag der Promotion: 22.08.2022

Dekan: Univ.- Prof. Dr. med. Michael D. Menger

Berichterstatter: Prof. Dr. Nóra Szentmáry
PD Dr. Stephan Philipp
Prof. Dr. Frank Schmitz

Dedicated to my sister and brother

Declaration

I hereby declare that the Dr. rer. med./ Ph.D. thesis entitled as **“The effect of Ca²⁺ supplementation on epithelial cell differentiation and retinoic acid signaling components in a siRNA-based aniridia cell model”** is a presentation of original research work and studies carried out by me. Where other sources of information have been used, they have been acknowledged. Contents of the thesis do not form the award of any other degree or qualification to me or to anybody else from this or any other University / Institution.

Homburg, Germany

03-08-2021

PRIYA KATIYAR

TABLE OF CONTENTS

V

TABLE OF CONTENTS	V
Abbreviations.....	1
List of figures.....	4
List of tables.....	5
Zusammenfassung.....	6
Summary.....	8
CHAPTER 1: INTRODUCTION.....	9
1.1 The Cornea.....	9
1.2 Limbus and limbal epithelial cells.....	10
1.3 Paired Box Gene 6 (PAX6)	11
1.4 Congenital aniridia.....	12
1.5 Limbal stem cell insufficiency (LSCI).....	14
1.6 Aniridia associated/related keratopathy (AAK or ARK)	14
1.7 Corneal differentiation markers KRT3 and 12 and DSG1 and their altered expression in congenital aniridia.....	15
1.8 Mechanism and signaling pathways involved in corneal epithelial regeneration.....	15
1.8.1 Retinoic acid signaling.....	16
1.9 Modelling of limbal epithelial cells in aniridia: An aniridia cell model.....	17
1.9.1 Cell model based on genome editing.....	18
1.9.2 Cell model based on gene silencing.....	18
1.9.2.1 RNA interference: Gene silencing by small interfering RNA (siRNA).....	18
1.9.2.2 An aniridia cell model based on gene silencing.....	20
1.10 Differentiation triggering role of calcium in different cell types.....	20
1.10.1 Differentiation triggering in salivary acinar cells.....	21
1.10.2 Differentiation triggering in skin keratinocytes.....	21
1.10.3 Differentiation triggering role of calcium in limbal epithelial cells...	22

1.11 THESIS AIMS.....	23
CHAPTER 2: MATERIALS AND METHODS.....	24
2.1 MATERIALS.....	24
2.2 METHODS.....	29
2.2.1 Primary limbal epithelial cells.....	29
2.2.1.1 Isolation and culturing of primary limbal epithelial cells (pLECs).....	29
2.2.1.2 Cryopreservation of limbal epithelial cells.....	30
2.2.1.3 Ca ²⁺ treatment and siRNA transfection of pLECs.....	30
2.2.1.4 Harvesting of pLECs	30
2.2.2 Human telomerase-immortalized limbal epithelial stem cells (T-LSCs) and genome edited T-LSCs (T-LSCs PAX6 ^{+/-}).....	31
2.2.2.1 Culture of T-LSCs and T-LSCs PAX6 ^{+/-}	31
2.2.2.2 Splitting of T-LSCs and T-LSCs PAX6 ^{+/-}	31
2.2.2.3 Ca ²⁺ treatment of T-LSCs and T-LSCs PAX6 ^{+/-}	31
2.2.2.4 Harvesting of T-LSCs and T-LSCs PAX6 ^{+/-}	31
2.2.3 RNA and protein isolation.....	32
2.2.3.1 RNA concentration estimation.....	32
2.2.3.2 cDNA synthesis.....	32
2.2.3.3 Quantitative polymerase chain reaction (qPCR).....	33
2.2.4 Protein estimation.....	34
2.2.4.1 Western blot.....	34
2.2.5 Statistical analysis.....	34
CHAPTER 3: RESULTS.....	35
3.1 Cell culture and morphology of the cells.....	35
3.2 Combination of Ca ²⁺ treatment with primary siRNA cell model.....	35
3.2.1 Transcription factor PAX6 and differentiation marker DSG1 expression (qPCR and western blot)	35
3.2.2 Retinoic acid pathway components ADH7, ALDH3A1 and ALDH1A1 expression (qPCR and western blot).....	37

3.2.3 Cellular binding protein CRABP2, RBP1 and FABP5 expression (qPCR and western blot).....	37
3.2.4 Retinoic acid pathway component CYP1B1, PPARG, STRA6 and VEGFA (qPCR).....	40
3.2.5 Lypogenic enzyme ELOVL7, RDH10 and protease inhibitor SPINK7 expression.....	42
3.3 Expression analysis of FABP5 and DSG1 genes in human telomerase immortalized limbal epithelial stem cells (T-LECs).....	42
3.3.1 24 hours Ca ²⁺ treatment (qPCR and western blot).....	42
3.3.2 72 hours Ca ²⁺ treatment (qPCR and western blot).....	44
CHAPTER 4: DISCUSSION.....	46
CHAPTER 5: CONCLUSIONS AND OUTLOOK TO THE FUTURE.....	52
CHAPTER 6: REFERENCES.....	53
ACKNOWLEDGEMENTS.....	64
CURRICULUM VITAE.....	66
LIST OF PUBLICATIONS.....	69

Abbreviations

AAK	Aniridia associated keratopathy
ACTB	β -Actin
ADH	Alcohol dehydrogenase
ADH7	Alcohol dehydrogenase 7
ALDH1A1	Aldehyde dehydrogenase 1 Family Member A1
ALDH3A1	Aldehyde dehydrogenase 3 Family Member A1
β-actin	ACTB
BPE	Bovine pituitary extract
Ca²⁺	Calcium
CO₂	Carbondioxide
CRBP	Cellular retinol binding protein
CRABP2	Cellular retinoic acid binding protein 2
CYP1B1	Cytochrome P450 Family 1 Subfamily B Member 1
CYP26A1	Cytochrome P450 Family 26 Subfamily A Member 1
CYP 450	Cytochrome P450
cDNA	Complementary DNA
CYP1B1	Cytochrome P450 1B1
Cx43	Connexin 43
DMEM	Dulbecco's Modified Eagle Medium
DNA	Deoxyribonucleic acid
DSG	Desmoglein
EDTA	Ethylenediaminetetraacetic acid
EGF	Epidermal growth factor
Ep	Epithelium
ELOVL7	Elongation of very long chain fatty acids protein 7

FABP	Fatty acid binding protein
FC	Fold change
GUSB	Glucuronidase Beta
K10	Keratin type II cytoskeletal 10
kDa	Kilo dalton
KSFM	Keratinocyte Serum-Free Medium
KRT3	Keratin type II cytoskeletal 3
KRT12	Keratin type II cytoskeletal 12
L	Liter
LEC	Limbal epithelial cell
LESC	Limbal epithelial stem cells
LSCD	Limbal stem cell deficiency
LSCI	Limbal stem cell insufficiency
μ	Micro
M	Mol/l
m	Mili
MOPS	(3-(N-morpholino) propanesulfonic acid)
mRNA	Messenger ribonucleic acid
PAX6	Paired box protein-6
PBS	Phosphate-buffered saline
pLEC	Primary limbal epithelial cell
PPARG	Peroxisome proliferator-activated receptor gamma
RA	Retinoic acid
RBP	Retinol-binding protein
RDH	Retinol dehydrogenase
qPCR	Quantitative polymerase chain reaction
RT-qPCR	Quantitative reverse transcription PCR
RA	Retinoic acid

RAR	Retinoic acid receptor
RDH10	Retinol dehydrogenase 10
RXR	Retinoid X receptor
PPARG	Peroxisome proliferator-activated receptor gamma
siRNA	Small interfering RNA
siCtrl	Control small interfering RNA
SPINK	Serine peptidase inhibitor, kazal type 7
STRA6	Vitamin A receptor
TACs	Transient amplifying cells
TBP	TATA-binding protein
T-LSCs	Telomerase-immortalized limbal epithelial stem cells
TRIS	Tris (hydroxymethyl) aminomethane
ETDA	Disodium ethylenediaminetetra acetic acid
VEGFA	Vascular endothelial growth factor A

List of figures

		Page No.
Figure 1	<i>Anatomical structure of the cornea.</i>	9
Figure 2	<i>Anatomy of the human limbus.</i>	10
Figure 3	<i>Corneal epithelial morphology in aniridia related keratopathy.</i>	13
Figure 4	<i>Schematic diagram of retinoic acid (RA) signaling and its dual role in cell survival.</i>	16
Figure 5	<i>Mechanism of RNA interference through small interfering RNA (siRNA).</i>	19
Figure 6	<i>Morphology of the primary limbal epithelial cells (pLECs).</i>	35
Figure 7	<i>qRT-PCR and western blot analysis of differentiation markers PAX6 and DSG1.</i>	36
Figure 8	<i>qRT-PCR and western blot analysis of the metabolizing enzymes of retinoic acid signaling components ADH7, ALDH1A1 and qRT-PCR analysis of ALDH3A1.</i>	38
Figure 9	<i>qRT-PCR analysis of the cellular binding proteins CRABP2, RBP1 and qRT-PCR and Western blot analysis of the cellular binding protein/RA signaling component FABP5.</i>	39
Figure 10	<i>qRT-PCR analysis of the downregulated transcripts VEGFA, STRA6, CYP1B1 and PPRAG.</i>	40
Figure 11	<i>qRT-PCR analysis of unchanged transcripts ELOVL7, RDH10 and SPINK7.</i>	41
Figure 12	<i>FABP5, PAX6, DSG1 qRT-PCR and western blot analysis (24 hours calcium treatment).</i>	43
Figure 13	<i>FABP5, PAX6, DSG1 qRT-PCR and western blot analysis (72 hours calcium treatment).</i>	45

List of tables

		Page No.
Table 1	<i>Laboratory materials.</i>	24
Table 2	<i>siRNA used in experiments.</i>	24
Table 3	<i>Instruments and softwares.</i>	25
Table 4	<i>Chemicals and kits.</i>	25
Table 5	<i>Medias and buffers.</i>	26
Table 6	<i>Primers used for qPCR.</i>	27
Table 7	<i>Antibodies used for western blot.</i>	28
Table 8	<i>Materials used for the first strand of the cDNA synthesis.</i>	32
Table 9	<i>Materials of the reagent mixture of the single reaction, used in the qPCR experiment.</i>	33
Table 10	<i>Thermocycler profile for the qPCR experiment and melt curve analysis.</i>	33

Der Effekt der Ca²⁺-Supplementierung auf die Epithelzellendifferenzierung und das Retinsäure-Signaling Komponenten in einem siRNA-basierten Aniridie-Zellmodell

Zusammenfassung

Fragestellung: Die PAX6-Haploinsuffizienz-assoziierte Aniridie ist durch das Fortschreiten der Aniridie-assoziierten Keratopathie (ARK) charakterisiert und in der Regel mit einer Störung der limbalen Epithelzellen (LECs) verbunden. PAX6 wird in reifen kornealen und konjunktivalen Epithelzellen gesunder Personen exprimiert. Beim Screening der limbalen und konjunktivalen Epithelzellen von Aniridie-Patienten wurden deregulierte mRNAs der RA-Signalkomponenten *ADH7*, *RDH10*, *ALDH1A1*, *ALDH3A1*, *STRA6*, *CYP1B1*, *RBP1*, *CRABP2*, *FABP5*, *PPARG*, *VEGFA* und *ELOVL7* identifiziert. Veränderungen auf mRNA-Ebene wurden vor Veränderungen auf Proteinebene in undifferenzierten primären LECs nachgewiesen. Durch die Kombination eines Small Interfering RNA (siRNA) basierten Aniridie-Zellmodells (PAX6 knockdown) mit einer differenzierungsauslösenden Wachstumsbedingung wollten wir die Expression von Differenzierungsmarkern auf mRNA- und Proteinebene sichtbar machen.

Methoden: Primäre LECs wurden aus korneoskleralen Ringen von gesunden Spendern isoliert und in serumfreiem low Ca²⁺ Medium (KSFM) und in KSFM supplementiert mit 0,9 mmol/L Ca²⁺ kultiviert. Zusätzlich wurden die LECs mit siRNA gegen PAX6 behandelt. Die RNA und Proteine wurden aus den Zellen isoliert und *DSG1*, *PAX6*, *ADH7*, *RDH10*, *ALDH1A1*, *ALDH3A1*, *STRA6*, *CYP1B1*, *RBP1*, *CRABP2*, *FABP5*, *PPARG*, *VEGFA* und *ELOVL7* mittels qPCR unter Verwendung der $\Delta\Delta C_t$ -Methode und Western Blot analysiert, um einen Vergleich auf mRNA und Proteinebene durchzuführen.

Ergebnisse: Nach der Ca²⁺-Supplementierung konnte ein Anstieg der mRNA-Expression von *DSG1*, *FABP5*, *ADH7*, *ALDH1A1*, *RBP1*, *CRABP2* und *PAX6* gemessen werden ($p \leq 0,03$), während die mRNA-Expression von *PPARG* und *CYP1B1* herunterreguliert wurde ($p \leq 0,0003$). Nach zusätzlichem PAX6-Knockdown nahm die *DSG1*- und *FABP5*-Proteinexpression ab ($p \leq 0,04$). Die *FABP5*-Proteinexpression stieg nach Ca²⁺-Supplementierung an ($p = 0,01$), die *DSG1*-Proteinexpression war nur mit Ca²⁺ sichtbar ($p < 0,0001$). Nach der PAX6 siRNA-Behandlung wurden *ADH7* und *ALDH1A1* nur auf mRNA-Ebene unter beiden Wachstumsbedingungen herunterreguliert ($p \leq 0,008$).

Schlussfolgerungen: Die Ca²⁺-Behandlung kann mit der PAX6 siRNA-Behandlung kombiniert werden, um das bei Patienten beobachtete zelluläre Verhalten der Aniridie zu imitieren. Dies kann auf einige der ausgewählten Marker beschränkt sein. Nach dem PAX6-Knockdown sinkt die mRNA-Expression des Differenzierungsmarkers *DSG1* und der RA-Komponente *FABP5*. Ein ähnlicher Effekt

zeigt sich auf Proteinebene durch differenzierungsauslösende Ca^{2+} -Behandlung im siRNA-basierten Aniridie-Zellmodell. In Zukunft müssen weitere Antikörper-Validierungen für die übrigen Marker durchgeführt werden, um die Ergebnisse zu bestätigen.

Summary

Purpose: PAX6 haploinsufficiency related aniridia is characterized by progression of aniridia related keratopathy (ARK) and is associated with disorder of limbal epithelial cells (LECs). PAX6 is expressed in mature corneal and conjunctival epithelial cells of healthy subjects. Screening of aniridia patients' limbal and conjunctival epithelial cells, deregulated mRNAs of RA signaling components *ADH7*, *RDH10*, *ALDH1A1*, *ALDH3A1*, *STRA6*, *CYP1B1*, *RBP1*, *CRABP2*, *FABP5*, *PPARG*, *VEGFA* and *ELOVL7* were identified. Changes at mRNA level are detected prior changes at protein level in undifferentiated primary LECs. While combining a small interfering RNA (siRNA) based aniridia cell model (PAX6 knock down) with a differentiation triggering growth condition, we aimed to visualize the expression of differentiation markers at mRNA and protein level.

Methods: Primary LECs were isolated from corneoscleral rims of healthy donors and were cultured in serum free low Ca^{2+} medium (KSFM) and in KSFM supplemented with 0.9 mmol/L Ca^{2+} . In addition, LECs were treated with siRNA against PAX6. All cells were lysed to yield DSG1, PAX6, ADH7, RDH10, ALDH1A1, ALDH3A1, STRA6, CYP1B1, RBP1, CRABP2, FABP5, PPARG, VEGFA and ELOVL7 to get RNA and protein. qPCR using the $\Delta\Delta\text{Ct}$ method and western blot have been performed to make a comparison at mRNA and protein level.

Results: *DSG1*, *FABP5*, *ADH7*, *ALDH1A1*, *RBP1*, *CRABP2* and *PAX6* mRNA expression increased ($p\leq 0.03$) while *PPARG*, *CYP1B1* mRNA expression decreased ($p\leq 0.0003$) after Ca^{2+} supplementation. After additional PAX6 knock down, DSG1 and FABP5 protein expression decreased ($p\leq 0.04$). FABP5 protein expression increased upon Ca^{2+} supplementation ($p=0.01$), DSG1 protein expression was only visible using Ca^{2+} ($p<0.0001$). Following PAX6 siRNA treatment, *ADH7* and *ALDH1A1* were downregulated only at mRNA level under both growth conditions ($p\leq 0.008$).

Conclusions: Ca^{2+} treatment can be combined with PAX6 siRNA treatment to mimic aniridia cellular behavior observed in patients. This may be restricted to some of the chosen markers. Upon PAX6 knockdown, mRNA expression of differentiation marker *DSG1* and RA component *FABP5* decreases. The similar effect becomes apparent at protein level through differentiation triggering Ca^{2+} treatment in siRNA-based aniridia cell model. In the future, we need to perform further antibody validation for the remaining markers to confirm these findings.

CHAPTER 1:

INTRODUCTION

1.1 The cornea

The human eye is a paired sense organ which is part of the visual system, allowing vision. Cornea is the foremost structure of the eye. Its transparency and avascularity is necessary for good vision (Kitazawa et al., 2016). It is resided by immature immune cells and has an immunologic privilege. In humans, the cornea has a horizontal diameter of about 11.71 ± 0.42 mm and borders with the sclera at the corneoscleral limbus. The human cornea has five layers: epithelium, Bowman's layer, stroma, Descemet's membrane, endothelium (Notara et al., 2018; Sridhar MS, 2018; DelMonte and Kim, 2011).

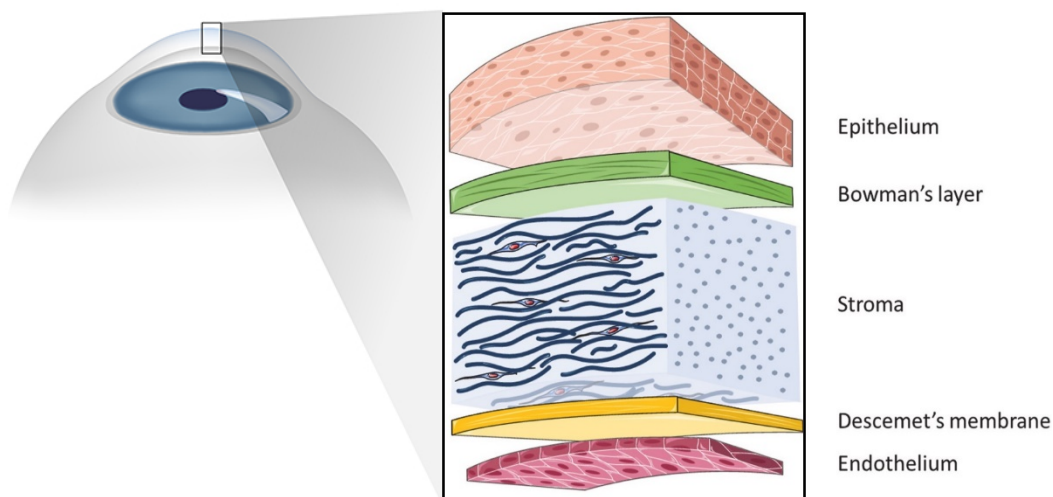


Figure 1. Anatomical structure of the cornea. The corneal tissue is built up of five distinguishable layers: two acellular layers (Bowman's layer and Descemet's membrane) and three cellular layers (epithelium, stroma and endothelium) (modified and adapted from Faye et al., 2021).

The cornea mechanically protects the inner structures of the eye. In the central cornea, the epithelium has 5 to 7 layers. It is about $50 \mu\text{m}$ in thickness and it is build-up of nonkeratinized stratified squamous epithelium (Ehlers et al., 2010; Notara et al., 2018) and covers the front part of eye. The corneal epithelium provides a smooth regular surface and it also serves as a barrier against dirt, germs and other particle. The corneal epithelial cells have a lifespan of about 7 to 10 days (Hanna et al., 199; Sridhar MS., 2018) and regenerate from the limbus (Notara et al., 2018; Latta et al., 2019; Townsend,1991; Käsman-Kellner et al., 2018).

1.2 Limbus and limbal epithelial cells

The limbus is located at the junction of the cornea and conjunctiva as a barrier between conjunctiva and cornea, also known as corneoscleral limbus (Schlötzer-Schrehardt & Kruse., 2005; Tseng, 1989; Davanger and Evensen, 1971) (**Figure 2**). It is highly pigmented in some individuals, which allows clear visualization of the limbal palisades of Vogt at the corneoscleral limbus.

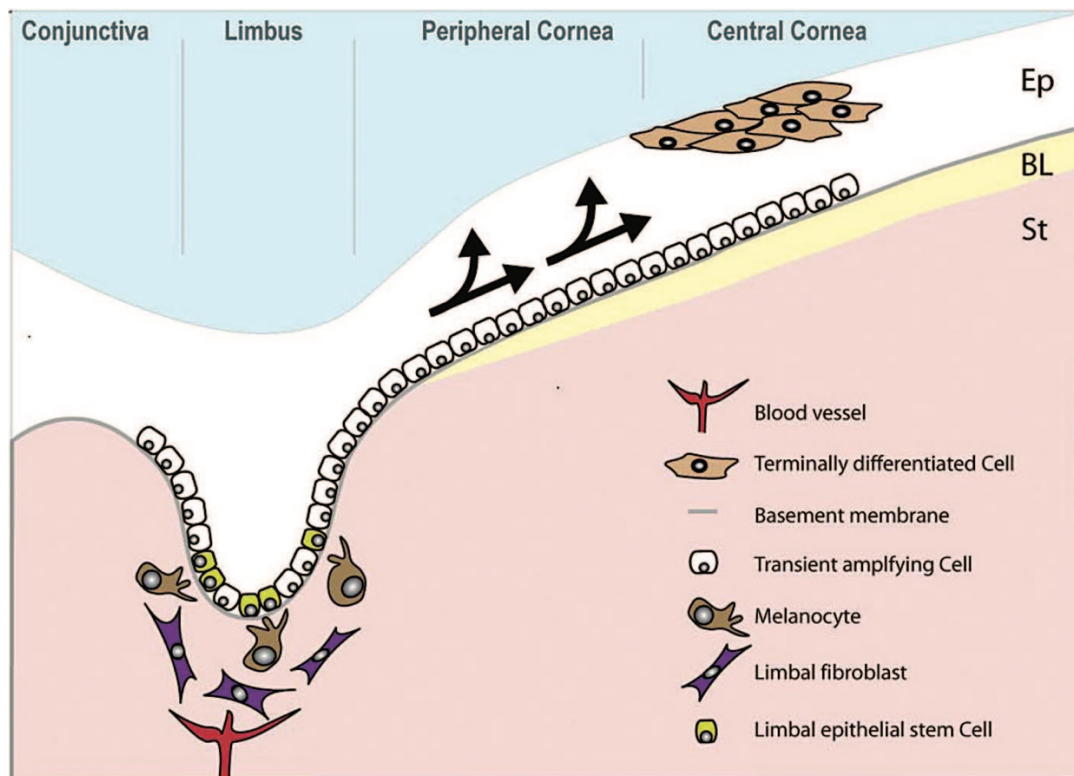


Figure 2. Anatomy of the human limbus. Limbal epithelial stem cells (LESC) reside in the basal layer of the epithelium (Ep), which convert into daughter transient amplifying cells (TACs). These cells migrate towards the central cornea (arrows) to replenish the epithelium (adapted from Secker GA et al., 2008).

region (Käsmann-Kellner et al., 2018; Townsend, 1991; Davanger and Evensen, 1971; Notara et al., 2018). In 2005, a novel anatomical structure, the limbal epithelial crypt has been identified by Dua et al. in the limbus. Dua proposed to name this region limbal epithelial stem cell (LESC) niche (Dua et al., 2005; Kulkarni et al., 2010).

Limbal epithelial cells are a mixture of limbal epithelial stem cells and other niche cells, which reside in the basal cell compartment of the limbus (Latta et al., 2019; Townsend, 1991; Kulkarni et al., 2010). Limbal epithelial stem cells (LESC) are cuboidal in shape and are located at the basal layer of the limbal region, then differentiate into transient amplifying cells (TACs) and migrate towards the apical layer of the corneal epithelium to maintain epithelial integrity (Notara et al., 2010; Secker et al., 2008; Sun and

Lavker, 2004; Lavker et al., 2004). Depletion of LESC in combination with destruction of their stem cell niche may result in a limbal stem cell deficiency (LSCD), which significantly alters tissue homeostasis (Haagdorens et al., 2016).

1.3 Paired Box Gene 6 (PAX6)

PAX6 is a transcriptional regulator, involved in the developmental process of the nose, central nervous system, and pancreas (Walther and Gruss, 1991). Human PAX6 is located on the 11p13 chromosome segment (Ton et al., 1991; Lee et al., 2008). PAX6 protein controls many aspects of eye development during early embryogenesis (Terzic and Saraga-Babic et al., 1999) and after birth (Gehring, 1996; Koroma et al., 1997). PAX6 protein regulates the expression of various genes in many structures of the eyes including the lens, conjunctiva, corneal epithelium, iris, ciliary body, optic vesicles and all layers of the retina (Collinson et al., 2004; Koroma et al., 1997; Quinn et al., 1996; Davis and Reed, 1996; Martin et al., 1992). The transcription factor PAX6 was identified by positional cloning as the defective candidate in humans (Ton et al., 1991).

Three isoforms of PAX6 have been reported in vertebrate. It has two major isoforms, the canonical PAX6 and the PAX6 (5a). There is a third isoform PAX6 (Δ PD), known as pairedless isoform.

The **canonical PAX6** isoform is expressed in most cells which express PAX6 (Plaza et al., 1999; Xu and Saunders, 1997; Kammandel et al., 1999; Anderson et al., 2002; XU et al., 1999) and has two DNA-binding domains, the paired domain (PD) at the N terminus and a paired-like homeodomain (HD), joined by a glycine-rich region and a proline–serine–threonine (PST)-rich transactivation domain (Glaser et al., 1992; walther and Gruss, 1991; Ton et al., 1991; Ton et al., 1992; Hill et al., 1991).

PAX6 (5a) was the first described isoform which has been detected in the spinal cord, eye, brain, olfactory epithelium (Kim and Lauderdale, 2006; Zhang et al., 2001; Azuma et al., 1996; Epstein et al., 1994). It is formed through an alternative splicing of exon 5a by insertion of 14 amino acids (Lee et al., 2008). This splicing disturbs the paired domain and its altered DNA binding properties allow PAX6 to activate a set of downstream target genes (Pinson et al., 2006). Some studies describe the phenotypic changes through this alternative splicing such as iris hypoplasia, defects in corneal, lens and retinal development (Sanjay Singh, 2010). Interestingly, studies in vertebrates' address that the functions of PAX6 and PAX6 (5a) are different (Pinson et al., 2006).

The third isoform (**Pax6 Δ PD**) lacks the paired domain (PD). It has been identified in neuroretinal extracts of quail (Carriere et al., 1993). Transcripts encoding for this isoform have been identified in mammals and can be generated by alternative splicing (Kammandel et al., 1999; Mishra et al., 2002; Kleinjan et al., 2004; Gorlov and Saunders, 2002). There is little knowledge about its expression and its normal function, *in vivo*.

PAX6 gene mutation results in altered expression of PAX6 protein which call forth maldevelopment or no development of different organs such as eye, nose, central nervous system and pancreas. Different PAX6 mutation types have been identified (Brown et al., 1998; Ton et al., 1991; Glaser, 1992; Hanson et al., 1993). These can be divided into nonsense, splicing, frame shift, missense and run on mutations (Pinson et al., 2006). It has been reported that in most of the cases a heterozygous mutation (inactivation of one allele) in the PAX6 gene locus leads to haploinsufficiency with reduced expression of PAX6 protein amount and ocular disease (Lee et al 2008; Prosser and Van Heyningen 1998; Tzoulaki et al., 2005; Lima Cunha et al., 2019) and the small *eye* (*Sey*) character in rodents (Hill et al., 1991; Matsuo et al.,1993). Homozygous mutation (inactivation of both alleles) is described to be fatal with mal-/ no development of brain and nasal cavity (Glaser, 1992; 1994; Grindley et al., 1994).

Some findings demonstrate that corneal epithelial identity is maintained by PAX6 through regulation of genes related to normal differentiation (Ramesh et al., 2003; Li et al., 2015; Kitazawa et al., 2016). Studies show that limbal epithelial cells (LECs) exhibit a low PAX6 expression level and a low KRT12 and KRT3 differentiation marker level, which results a less differentiated phenotype than corneal epithelial cells (Ramesh et al., 2005a; Rubelowski et al., 2020). This indicates that PAX6 plays a role in their differentiation process. Heterozygous mutant LECs displayed a reduced PAX6 protein expression and at the same time reduced proliferation, migration and detachment (Roux et al., 2018). PAX6 protein overexpression in mouse corneal epithelial cells directly modifies centripetal migration and differentiation of these cells (Collinson et al., 2004). These all studies suggest that PAX6 plays an important role in regulation of proliferation, migration, adhesion and differentiation processes.

1.4 Congenital aniridia

Congenital aniridia is an eye disorder characterized by complete or partial iris hypoplasia or absence of iris at a first glance (Nelson et al.1984; Käsmann-Kellner et al.2018). Nevertheless, it is also characterized by aniridia associated keratopathy (AAK), cataract (Lagali et al., 2013; Nishida et al., 1995; Le et al., 2013) glaucoma and in some cases with optic nerve head hypoplasia (Grant et al. 1974; Baulmann et al., 2002). These all together lead to visual impairment or blindness (Landsend et al., 2017). An abnormal epidermal skin like phenotype is also associated in severe congenital aniridia.

An acquired aniridia might be found due to trauma, or as iatrogenic effect of ocular surgery. It must be different from congenital aniridia. Congenital aniridia is a rare, bilateral panocular disorder caused by fundamental disturbances in the development of the eye. The exact cause of congenital aniridia is not known however PAX6 gene has a critical role in most cases in its pathogenesis (Michael Ross, 2019; Tripathy and Salini, 2020).

Classification- Congenital aniridia can be classified in to three class.

- I. ***Autosomal Dominant*** - Familial congenital aniridia inherited as an autosomal dominant manner in 2/3 of cases. It may be present in around 85% aniridia patient and most common form of aniridia (Tripathy and Salini, 2020; Lee et al., 2008).



Figure 3. *Corneal epithelial morphology in aniridia related keratopathy. Corneal epithelial opacification, conjunctivalization and neovascularization.*

- II. ***Sporadic*** - In these cases, there is a heterozygous PAX6 mutation at band P13 of chromosome 11. It is responsible for 13% to 33% of the cases and there are changes in corneal, lens, optic nerve, retinal and macular phenotype. This type of aniridia has an incidence between 1:64000 and 1:100000 in live birth and may be found in association with other syndromes, most commonly with WAGR (Wilms tumor, aniridia, genitourinary anomalies, and intellectual disability) syndrome (Lee et al., 2008).
- III. ***Autosomal recessive*** - This is the least common form of congenital aniridia, which represents 1% to 3% of all aniridia cases. It is associated with Gillespie's syndrome, a rare genetic disorder characterized by partial aniridia, cerebellar ataxia, intellectual disability and mental retardation (Lee et al., 2008; Tripathy and Salini, 2020; Hall et al., 2019).

1.5 Limbal stem cell deficiency (LSCD)

Limbal stem cell deficiency (LSCD) is a condition with eye pain, blurred vision and sensitivity to light and may also lead to loss of vision. It is a pathological condition, which occurs due to dysfunction or insufficient quantity of limbal stem cells. PAX6 haploinsufficiency associated aniridia affects nearly all anatomical structures of the eye and presents with LSCD and breakdown of the stem cell niche (Tripathy

and Salini, 2020; Käsmann-Kellner et al., 2018). Therefore, there is limbal stem cell insufficiency (LSCI). Some studies show that downregulation of transcription factor PAX6 controls LESC lineage, by affecting the differentiation process of the transient amplifying cells (TACs, the daughter cells of LESC) in to “terminally differentiated cells” and therefore, by disturbing maintenance of the corneal epithelium consequently (Teseng, 1989; Dua et al., 2000). The stem cell niche is a cellular microenvironment, which is important to maintain stem cell state by regulating the LESC cell cycle, in order to keep them in an undifferentiated resting state (Shortt et al., 2007).

There are many causes of LSCI. There are some hereditary or genetic causes like congenital aniridia, however, in some cases it is idiopathic (Puangsricharern et al., 1995; Espana et al., 2002). Contact lens wear, as environmental factor may also result in LSCD (Clinch et al., 1992). As iatrogenic damage, an extensive cryotherapy, radiation, thermal/ chemical burn, or surgery of the limbus may also lead to LSCD (Sajjad, 2012; Kitazawa et al., 2016; Sotozono et al., 2007). Subconjunctival or topical application of antiproliferative agents may also result in LSCD (Lichtinger et al., 2010). In LSCD, a critical alteration in tissue homeostasis occurs due to the depletion of the LSCs, which changes structural integrity of the corneal surface. Thus, corneal transparency and visual function are no longer maintained. Symptoms of LSCD are redness, impaired vision, tearing and photophobia (Notara et al., 2018).

1.6 Aniridia associated/related keratopathy (AAK or ARK)

Aniridia associated keratopathy (AAK) or aniridia related keratopathy (ARK) is a progressive, sight threatening secondary complication of congenital aniridia. It is characterized by a progressive conjunctivalization of the cornea (Tripathy and Salini, 2020; Nishida et al., 1995; Lagali et al., 2005; Ihnatko et al., 2016). Currently it is believed that first signs of AAK already appear in the first decade of life (childhood) with thickening and vascularization of the peripheral cornea. This process progresses until adulthood, when typically, the complete corneal surface is involved (Landsend et al., 2017; Lee et al., 2008). In AAK, in absence of a healthy corneal epithelium, the conjunctiva proliferates over the corneal surface resulting in opacification and vascularization, which may severely impair vision (Notara et al., 2018).

Dry eye, red eye and photophobia belong to typical symptoms of AAK with LSCI, which can be classified as slight, moderate or severe (Lee et al., 2008). Nevertheless, it is often argued, that ARK develops as consequence of a combination of limbal stem cell deficiency and an abnormal differentiation of the corneal epithelium (Lee et al., 2008). Both are related factors, nevertheless, these are discussed separately.

1.7 Corneal differentiation markers KRT3, KRT12, DSG1 and their altered expression in congenital aniridia

Cornea-specific keratins KRT3 and KRT12 are adhesion markers (Cordon et al., 2000; Irvine et al., 1997), which have also been considered as specific corneal differentiation markers (Latta et al., 2017; Rubelowski et al., 2020; Lie et al., 2020; Chaloin-Dufau et al., 1990). PAX6 may be involved in AAK pathogenesis as it binds to the KRT12 promoter region and it is able to drive its transcription (Liu et al., 1999). Some studies strongly indicate that KRT3 and KRT12 are regulated by PAX6, as with PAX6 knockout, there was a significantly reduced KRT3 and KRT12 expression in human corneal epithelial cells (Kitazawa et al., 2017). Some other studies suggested that manipulation of PAX6 transcription changes expression of these keratins in AAK or other keratopathies (Davis et al., 2003; Li et al., 2015; Ramaesh et al., 2003).

Desmoglein (DSG), a desmosomal protein and adhesion marker is required for maintaining cellular adhesion in the corneal epithelium (Davis et al., 2003). DSG1 is a differentiation marker for limbal epithelial cells (Rubelowski et al., 2020) and keratinocytes (Johnson et al., 2014). There was a reduced desmoglein protein expression in PAX6^{+/-} small eye mice (Davis et al., 2003). Using PAX6^{+/-} limbal epithelial cells as aniridia cell model, there was also reduced DSG1 mRNA expression and a correlation between PAX6 and DSG1 expression (Latta et al., 2019). In case of DSG1 upregulation, the epithelial differentiation process recovers (Johnson et al., 2014), which indicates that DSG1 could be a potential differentiation marker of limbal epithelial cells. Its expression is also higher in corneal epithelial cells, which are highly differentiated (Rubelowski et al., 2020) and DSG1 seems to be regulated by the PAX6 gene (Latta et al., 2019; Davis et al., 2003).

1.8 Mechanism and signaling pathways involved in corneal epithelial regeneration

Various mechanism and signaling pathways are suggested to be involved in corneal epithelial regeneration. It has been shown that Wnt and Notch signaling are important for the self-renewal and maintenance of limbal stem cell lineage. Notch1 helps to repair injured mouse corneas (Li et al., 2015) and Wnt signaling is involved in ocular surface development. WNT7A controls corneal epithelial differentiation through PAX6. Loss of either WNT7A or PAX6 gene induces keratinization of the corneal epithelium. WNT/ β catenin signaling regulates proliferation (Nakatsu et al., 2011; Quyang et al., 2014). Endogenous retinoic acid (RA) signaling is also crucial for corneal maintenance and regeneration (Kumar et al., 2017; Sommer, 1983).

1.8.1 Retinoic acid signaling

It has been reported that retinoid, vitamin A (retinol) and their derivatives, for example retinoic acid (RA) are involved in development (Ghyselinck and Duester, 2019; Clagett-Dame and DeLuca, 2002) and are known to regulate cell proliferation, morphogenesis and differentiation (Kim et al., 2012;

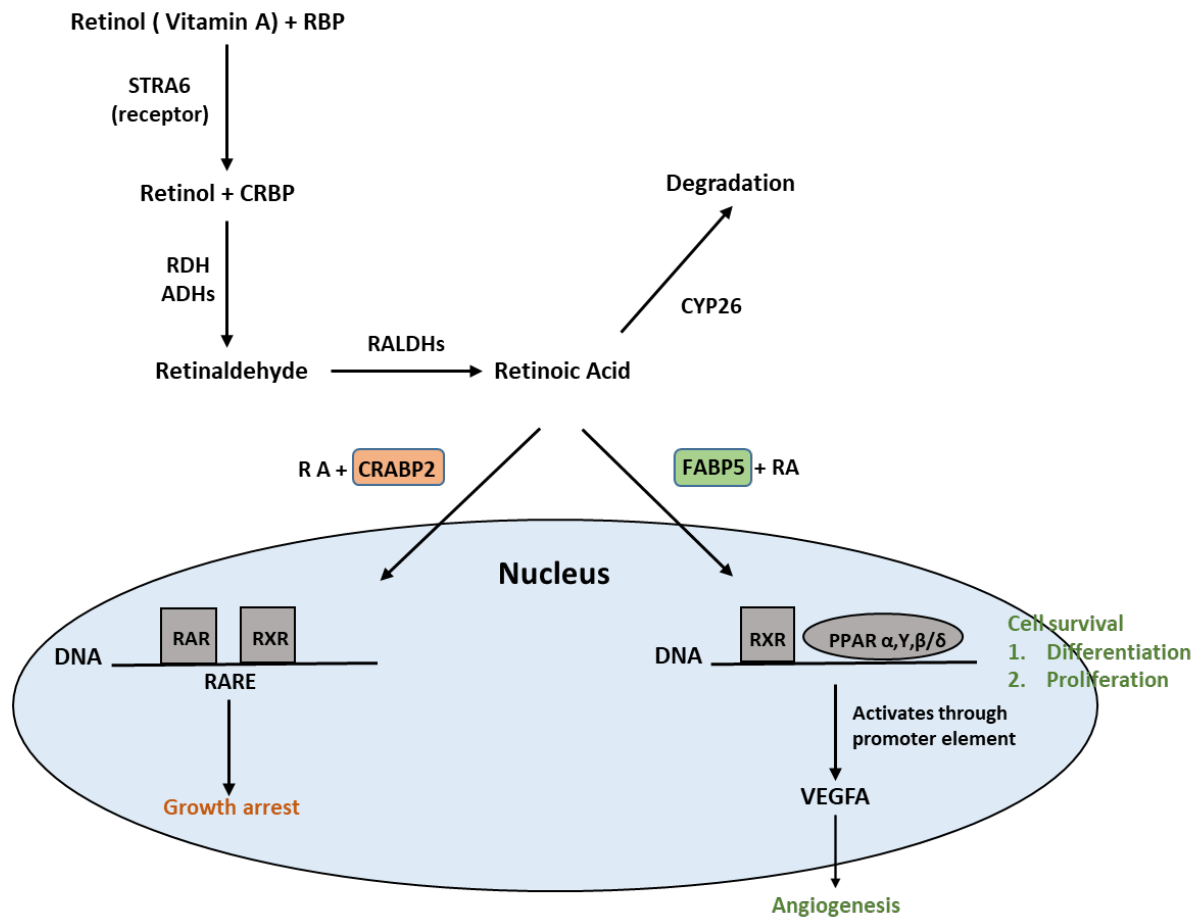


Figure 4. Schematic diagram of retinoic acid (RA) signaling and its dual role in cell survival. Retinol is metabolized into the transcriptionally active vitamin A form RA, then regulates transcription of vitamin A-responsive genes. CRABP-2 and FABP5 transport RA to RAR and PPAR, respectively. In case cells express a high CRABP-2/FABP5 ratio, RA translocates to RAR by CRABP2, which inhibits cell growth. In the presence of a low CRABP-2/FABP5 expression ratio, RA is transported to PPARs by FABP5, to upregulate survival pathways (Noy, 2016; Duester, 2008; Schug et al., 2007; Thatcher and Isoherranen, 2009).

RBP (Retinol binding protein), STRA6 (Vitamin A receptor), CRBP (Cellular retinol binding protein), ADH (Alcohol dehydrogenase), RDH (retinol dehydrogenase), RALDH (retinal dehydrogenase), CYP26 (Cytochrome P450 26, metabolizing enzyme), CRABP2 (Cellular retinoic acid binding protein 2), FABP5 (Fatty acid-binding protein 5), PPARG (Peroxisome proliferator-activated receptor alpha, beta/delta and gamma), VEGFA (Vascular endothelial growth factor A, angiogenic factor), RAR (Retinoic acid receptor), RXR (Retinoid X receptor), RARE (Retinoic acid response elements).

Bossenbroek et al., 1998; Lee et al., 2009). Vitamin A is necessary for normal differentiation of nonsquamous epithelium and its deficiency leads to keratinization of corneal epithelium as a direct consequence (Sommer, 1983; Kim et al., 2012). A severe vitamin A deficiency leads to keratopathy and dry eye (Sommer, 1990). Retinoic acid is important for physiological functions like epithelial proliferation (Asselineau et al., 1989) and the differentiation of limbal stem cells into TACs (Kruse and

Tseng, 1994) in a concentration dependent manner. Retinoic acid may affect the expression of more than 500 genes, since several different pathways and transcriptional factors respond to retinoid (Mangelssdorf, 2009; Desvergne and Wahl, 1992).

RA is an active metabolite of vitamin A (retinol), which is lipophilic in nature (Kumar et al., 2017; Rhinn and Dollé, 2012). STRA6 is a membrane receptor, which is responsible for the retinol uptake by recognizing the retinol binding protein (RBP) complex (Noy N, 2016; Kelly and Lintig, 2015). After cellular uptake of retinol, RA is intracellularly produced by the oxidation of retinol to retinal by retinal or alcohol-dehydrogenases (RDH/ADH) and subsequently by transformation of retinal to RA by retinal-dehydrogenases (RALDH) (Duester, 2009; Samarawickrama et al., 2015; Ziouzenkova et al., 2008). RA can act through binding to the retinoic acid receptors RAR (retinoic acid receptor), RXR (retinoic X receptor) and PPARs (peroxisome proliferator-activated receptors) (Samarawickrama et al., 2015; Yu et al., 2012).

In the cytoplasm, RA is bound by the cellular RA-binding protein (CRABP), which is transferred to the nucleus and binds to the nuclear RA receptors. It also binds/activates nuclear peroxisome proliferator-activated receptors (PPARs), when transported by fatty acid-binding proteins (FABPs) (Schug et al., 2008; Xia et al., 2015; Yu et al., 2012; Michalik and Wahli, 2007). Previous studies showed that the ratio of CRABP2/FABP5 is responsible for the activation of RARs and PPARs. When FABP5 to CRABP2 ratio is high, RA serves as a physiological ligand for PPARs instead of RARs. In the presence of a low FABP5 to CRABP2 expression ratio, RA is targeted to RARs. RA leads to two opposing effects on cell survival by alternating activation of these two nuclear receptors (Schug et al., 2007; 2008). When RA is no longer needed, it is catabolized by cytochrome enzymes (CYP26 enzymes) (Thatcher et al., 2019; Ghyselinck and Duester, 2019). CYP1B1, a member of the cytochrome p450 family has been proposed as a retinoic acid synthesis component, with an opposite effect to CYP26A1, which is degrading (Chambers et al., 2007).

1.9 Modelling of limbal epithelial cells in aniridia: An aniridia cell model

Homozygous mutation or complete deletion of master regulatory gene PAX6 causes a failure in eye formation (Hogan et al., 1986; Grindley et al., 1995; Gehring, 1996), whereas heterozygous mice are unable to fully depict human aniridia disease due to a small eye phenotype (Roux et al., 2018). Therefore, the gene network regulated by PAX6 in healthy corneas is not fully understood. Some study groups proposed a cellular model, which enables recapitulation of the AAK phenotype, to better understand its pathophysiology (Roux et al., 2018, Latta et al., 2019).

1.9.1 Cell model based on genome editing

An in vitro model of AAK was introduced by Roux et al in 2018, based on genome editing technique to cause PAX6 haploinsufficiency in human limbal epithelial cells. A point mutation found in a patient, which encodes a nonsense mutation and responsible for premature stop codon (p.E109X) was introduced to generate AAK phenotype with the help of CRISPER/CASE9 system. This was the first model (CRISPR/Cas9 genome edited human telomerase-immortalized limbal epithelial stem cells or T-LSCs PAX6^{+/-} cells), designed by genome editing in LSCs to study the ocular surface disease and to screen novel therapeutic approaches (Roux et al., 2018).

RNA sequencing of T-LSCs PAX6^{+/-} cells has been performed, in order to exactly clarify the consequences of PAX6 haploinsufficiency, at molecular level. There are in total 258 genes, which have an altered expression in the T-LSCs PAX6^{+/-} clone (Love et al., 2014). There are 87 upregulated and 171 downregulated genes in the mutant T-LSCs PAX6^{+/-} cells, compared to controls. These genes are involved in regulation of various biological processes such as lipid metabolism (for example ABCA1), epigenetic regulation (for example DNMT3B) exocytosis (for example RAB9A) etc. The upregulated genes are involved in extracellular matrix organization (for example PXDN, FBN2) and cell adhesion (for example NRCAM) or both (for example TGFBI and ITGA5). The transcription of PAX6 was rescued in T-LSCs PAX6^{+/-}, using recombinant PAX6 protein. Interestingly, the PAX6 protein restoration in T-LSCs PAX6^{+/-} cells also restores the functional defects such as detachment and migration (Roux et al., 2018).

1.9.2 Cell model based on gene silencing

1.9.2.1 RNA interference: Gene silencing by small interfering RNA (siRNA)

Inhibition or knockdown of specific gene expression in cultured cells is commonly used to study gene function in mammalian cells. One of the most widely used technologies for induction of such gene specific mRNA degradation is RNA interference (RNAi) technology. This is the most common way to silence individual gene expression post transcriptionally (Wittrup and Liberman, 2015; Han, 2018).

RNA interference technology was discovered approximately 20 years ago (Wittrup and Liberman; 2015). This method of interference use double-stranded RNA (dsRNA), which is around 20-22 nucleotide long, could participate in silencing of genes at the genome level, which function at a highly specific manner (Elbashir et al., 2001; Mocellin & Provenzano, 2004; Han, 2018). RNAi is a multistep process. After siRNA delivery into the cells either by transfection or electroporation method, each siRNA molecule is incorporated to the RNA-induced silencing complex (RISC). RISC is a nuclease complex that is responsible for the ultimate destruction of the target mRNA (Han, 2018; Mocellin & Provenzano, 2004) and lead to gene silencing (**Figure 5**).

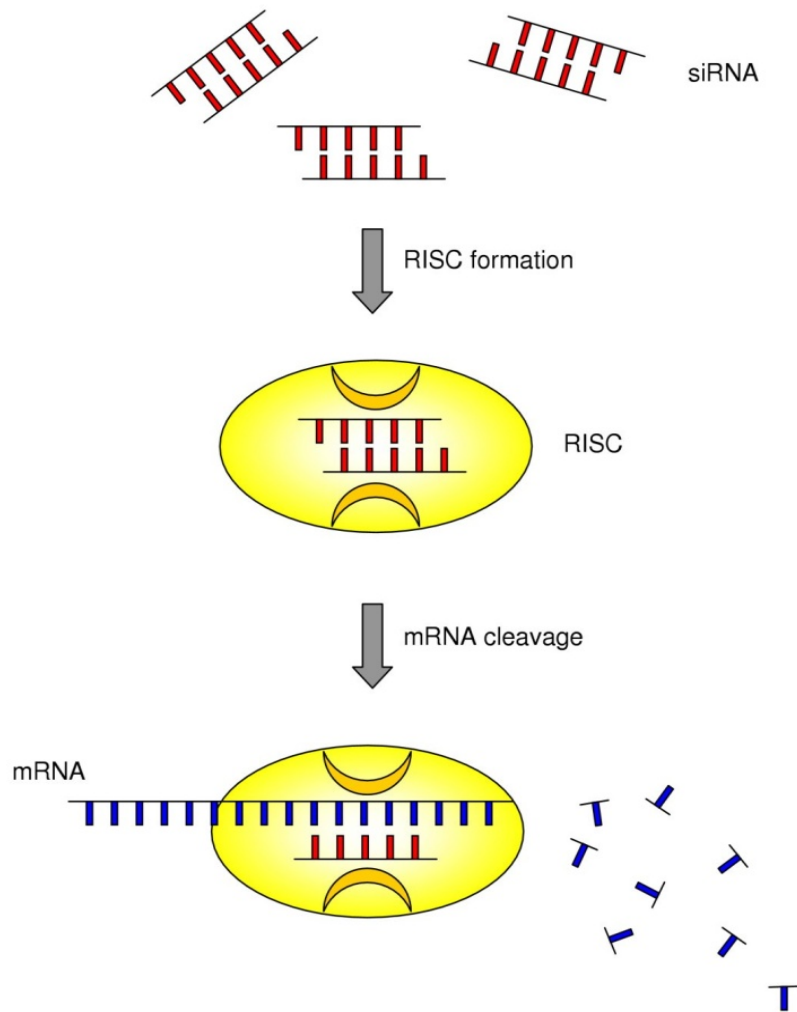


Figure 5. Mechanism of RNA interference through small interfering RNA (siRNA). Exogenously administered small interfering RNA (siRNA) pairs (double-stranded ~22-nucleotide), which exploit the endogenous RNA interference (RNAi) machinery. It directly associates with the cellular enzyme called RNA-induced silencing complex (RISC), that uses one strand of the siRNA to bind to mRNA through base pair complementary sequence. The nuclease activity of RISC then degrades the mRNA and leads to target gene knockdown (modified from Mocellin & Provenzano, 2004).

Argonaute 2 (Ago2), the enzymatic component of RISC, cleaves and discards one strand of the siRNA, which is called passenger or sense strand and retains the other strand which is known as guide or antisense strand to activate the mature RISC complex. Then, the RISC is delivered to the target mRNA molecule, which contains a complementary nucleic acid sequence, by the guide strand. siRNA guide

strand binds to the mRNA molecule through Watson–Crick base pairing in the complementary region (Rand et al., 2004; Matranga et al., 2005). Thereafter, endonuclease region of RISC cleaves the mRNA. Furthermore, cleaved mRNA is degraded by intracellular nucleases, and it is no longer available for translation of the corresponding protein. Since all eukaryotic cells contain the RNAi machinery, it is easy to target any gene to investigate its function (Caplen, 2004; Hannon and Rossi, 2004; Minhyung, 2009) and this technique also holds great potential to suppress disease-related gene expression (Dykxhoon and Lieberman, 2005; Vilgelm, 2006; Bumcrot, 2006; de Fougères et al., 2007).

1.9.2.2 An aniridia cell model based on gene silencing

In 2019, Latta et al established a siRNA and primary cell based aniridia cell model, applying RNA interference technique to knock down the PAX6 gene. Cells were transfected with lipofectamine and 5 nM siRNA against PAX6. This model was used to investigate the effect of the reduced PAX6 expression on some target genes such as TP63, ABCG2, ADH7, ALDH1A1, PITX1, DKK1, DSG1, KRT12, KRT3, KRT13, SPINK6, SPINK7, CSTV and SERPINB (Latta et al., 2019).

mRNA expression of differentiation markers KRT3, KRT13 and protease inhibitor SPINK7 showed significant reduction during quantitative analysis of siRNA- based primary aniridia cell model, while SPINK6, CSTV, SERPINB1, DKK1 and PITX1 expression behaved differently from mRNA sequencing result of patient cells.

DSG1 mRNA expression was reduced in siRNA- based primary aniridia cell model, similar to aniridia patient's epithelial cells (Latta et al., 2017), and similar to description of other studies describing the effect of PAX6 knockdown (Davis et al., 2003). However, there was no correlation between differentiation marker KRT12 and PAX6 expression, either in LECs control experiments or in the siRNA- based primary aniridia cell model (Latta et al., 2019, Rubelowski et al., 2020). Retinoic acid signaling component ADH7 and ALDH1A1 showed significant reduction upon PAX6 knockdown in the siRNA- based primary aniridia cell model at mRNA level, and in LECs of aniridia patients (Latta et al., 2019). There was a correlation between PAX6 and ADH7 or ALDH1A1 expression. Therefore, these were the proposed PAX6 (or AAK)-related gene targets, which should be extensively studied. PAX6 might drive the corneal epithelial differentiation process through direct or indirect regulation of RA signaling components and therefore, might be involved in AAK pathogenesis.

1.10 Differentiation triggering role of calcium in different cell types

Calcium is traditionally considered to trigger differentiation process. It has been used in different human cells such as epidermal keratinocytes, salivary acinar cells and human limbal epithelial cells. It has also

been used in murine cells such as epidermal keratinocytes and limbal epithelial cells to trigger differentiation (Ma and Liu et al., 2011; Siegenthaler et al., 1992; 1994).

1.10.1 Differentiation triggering in salivary acinar cells

In primary human salivary acinar cells, a culture medium supplemented with 1.0 mM Ca^{2+} triggered differentiation of acinar cells and supported the maintenance of the differentiated state (Hiraki et al., 2002). These cells exhibited an undifferentiated phenotype, as these were cultured in 0.2 mM Ca^{2+} . In addition, under these conditions, there were reduced cell-cell contacts. Nevertheless, using higher calcium concentration in the medium (up to 1.0 mM) cell-cell contacts increased and translocation of desmosomal protein from the cytoplasm to the cell membrane was induced. It has been suggested that 1.0 mM Ca^{2+} supplementation is optimal for differentiation of salivary gland cells and to maintain the differentiated state.

1.10.2 Differentiation triggering in skin keratinocytes

Another study proved that 1.2 mM Ca^{2+} calcium supplementation triggers differentiation of skin keratinocytes (Siegenthaler et al., 1994). There is a link between epidermal fatty acid binding protein (E-FABP) expression and keratinocyte differentiation. E-FABP expression was low in keratinocytes cultured under low calcium medium, but its expression increased to its twice using calcium supplemented medium, in differentiated keratinocytes. CRABP2 expression, a component of retinoic acid metabolism was also increased using calcium supplementation, referring to the more differentiated phenotype of these cells. Cells with weak CRABP2 expression were undifferentiated (Siegenthaler et al., 1992; 1994).

D'Souza used 0.1 and 1.0 mM two Ca^{2+} concentration to induce keratinocyte differentiation (D'Souza et al., 2001). In cell culture, differentiation process was triggered by 0.1 mM Ca^{2+} supplementation and it was maintained using 1.0 mM Ca^{2+} supplementation. Keratin 1 (KRT1) expression (early differentiation marker) and involucrin expression (late differentiation marker) increased through calcium supplementation in keratinocytes.

1.10.3 Differentiation triggering role of calcium in limbal epithelial cells

For corneal epithelial cells, Kawatika and Ma used calcium supplementation. Murine corneal and corneal-limbal epithelial cell differentiation could be promoted by increasing Ca^{2+} concentrations, using serum-free medium (Kawakita et al., 2004; Ma and Liu, 2011).

In 2004, Kawatika developed a method to culture mouse corneal-limbal cells and to study the effect of extracellular calcium supplementation on growth and differentiation of the epithelial cell culture. Therefore, the keratinocyte serum-free medium (KSFM) was modified by increasing Ca^{2+} concentration

to 0.9 mM. The corneal-limbal epithelial differentiation was promoted, whereas cell growth was suppressed at this concentration. This was verified by analysis of cytokeratin 12 (K12), connexin 43 (Cx43), cytokeratin10 (K10) and involucrin protein expression of the epithelial cells.

Ma and Liu also analysed the effect of extra Ca^{2+} on proliferation and differentiation of mouse corneal epithelial cells. Low Ca^{2+} concentration and 0.9 mmol/L Ca^{2+} supplementation have been used. Beside low Ca^{2+} concentration, p63 (nuclear transcription factor) and K19 (Keratin 19) expression was increased, which indicate epithelial progenitor phenotype.

Using 0.9 mmol/L Ca^{2+} supplementation, involucrin mRNA and protein expression increased (Ma and Liu et al., 2011). Therefore, use of a culture medium supplemented with 0.9 Ca^{2+} may trigger differentiation and promote growth in limbal epithelial stem cells cultures.

1.11 THESIS AIMS

PAX6 haploinsufficiency related aniridia is characterized by progression of aniridia related keratopathy (ARK) and is associated with disorder of limbal epithelial cells (LECs). PAX6 is expressed in mature corneal and conjunctival epithelial cells of healthy subjects. Screening of aniridia patients' limbal and conjunctival epithelial cells, deregulated mRNAs of RA signaling components *ADH7*, *RDH10*, *ALDH1A1*, *ALDH3A1*, *STRA6*, *CYP1B1*, *RBPI*, *CRABP2*, *FABP5*, *PPARG*, *VEGFA* and *ELOVL7* were identified. Changes at mRNA level are detected prior changes at protein level in undifferentiated primary LECs.

While combining a small interfering RNA (siRNA) based aniridia cell model (PAX6 knock down) with a differentiation triggering growth condition (Ca²⁺ supplementation) we aimed to visualize the expression of differentiation markers and retinoic acid signaling components at mRNA and protein level.

In addition, we aimed to visualize the expression of differentiation markers and retinoic acid signaling components at mRNA and protein level in the T-LSCs PAX6^{+/-} cells (aniridia cell model based on genome editing) with Ca²⁺ supplementation as differentiation triggering growth condition.

CHAPTER 2:

MATERIALS AND METHODS

2.1 MATERIAL

Laboratory materials, siRNA used in experiments, instruments and software, chemicals and kits, medias and buffers, primers used for qPCRs and antibodies used for western blots are listed below (**Tables 1-7**).

Name	Manufacturer
Acu Punch (1.5 mm)	Acuderm Inc.; Florida, USA
Cell-Tricks	Sysmex Europe GmbH
Cellstar serological pipette	Greiner Bio One International GmbH; Kremsmünster, Österreich
Cellstar tubes (15,50 ml)	Greiner Bio One International GmbH; Kremsmünster, Österreich
Eppendorf Reference Pipette	Eppendorf AG; Hamburg, Deutschland
Kryo-Tubes	Sarstedt AG & Co.KG; Nurbrecht, Deutschland
PCR-Tubes	Greiner Bio One International GmbH; Kremsmünster, Österreich
Petridishes	Greiner Bio One International GmbH; Kremsmünster, Österreich
Pipetteboy acu 2	INTEGRA Biosciences AG; Zizers, Schweiz
6 & 24 well plate	Sarstedt AG & Co.KG; Nurbrecht, Deutschland
Scraper	Sarstedt AG & Co.KG; Nurbrecht, Deutschland

Table 1. Laboratory material.

SiRNA	Basesequence	Manufacturer
Control si RNA	5'AGGUAGUGUAAUCGCCUUGUU	MWG Eurofins, Luxembourg, Luxembourg
PAX6 si RNA	5'CCUGGCUAGCGAAAAGCAAUU and 5' UGGGCGGAGUUAUGAUACCUU	MWG Eurofins, Luxembourg, Luxembourg

Table 2. siRNA used in experiments.

Name	Manufacturer
Primoververt invert light microscope	Carl Zeiss Microscopy GmbH; Jena, Deutschland
Cell culture bench	Thermofischer Scientific, Waltham, Massachusetts, USA
Heraeus Pico 17 Centrifuge	Thermofischer Scientific, Waltham, Massachusetts, USA
Megafuge Heraeus 16R	Thermofischer Scientific, Waltham, Massachusetts, USA
Incubator HERA Cell 240i	Thermofischer Scientific, Waltham, Massachusetts, USA
Nanodrope 1000 spectrophotometer	Thermofischer Scientific, Waltham, Massachusetts, USA
Thermocycler CFX Connect	Bio-rad Laboratories, München, Deutschland
Quant Studio 5 Real-Time-PCR	Thermofischer Scientific, Waltham, Massachusetts, USA
Thermoblock TB2	Biometra GmbH Analytik, Jena, Deutschland
Transblot Turbo Transfer System	Bio-rad Laboratories, München, Deutschland
Vortex-Genie 2	Scientific Industries, Inc., Newyork, USA
Shaker Dos-10 L	Neo Lab Migge GmbH; Heidelberg, Deutschland
Imaging System LAS 4000	GE Healthcare Life Science, Little Chalfon,UK

Table 3. Instruments and softwares.

Name	Manufacturer
Collagenase A	Roch Pharma AG, Schweiz
KSFM	Gibco, Life Technologies, Paisley, UK
Penicillin/Streptomycin	Sigma-Aldrich GmbH Deissenheim, Deutschland
EGF	Gibco, Life Technologies, Paisley, UK
BPE	Gibco, Life Technologies, Paisley, UK
DMEM	Sigma-Aldrich GmbH Deissenheim, Deutschland
Trypsin-EDTA	Sigma-Aldrich GmbH Deissenheim, Deutschland
Dulbeccos PBS	Sigma-Aldrich GmbH Deissenheim, Deutschland
Cryo-SFM	PromCell GmbH; Heidelberg, Deutschland

Lipofectamine 2000	ThermoFischer scientific, Waltham, Massachusetts, USA
Opti-MEM	Gibco Carlsbad, USA
Calcium chloride	Grüssing, Filsum, Germany
Syber Green master mix	Vazyme, Biotech, Nanjing
Dual-Colour-Marker	Bio-rad Laboratories, München, Deutschland
One Taq RT-PCR Kit	New England Biolabs, Frankfurt, Deutschland
RNA/DNA/Protein Isolation Kit	Norgen biotek Corp., Ontario, Canada
Glycerine	Medical store, Saarland Medical University
Bromophenolblue dye	Carls Roth GmbH & Co.KG, Karlsruhe, Deutschland
Western Froxx stripping Buffer	BioFroxx GmbH, Einhausen, Deutschland
Western Froxx solution B (anti-mouse HRP)	BioFroxx GmbH, Einhausen, Deutschland
Western Froxx solution B (anti-rabbit HRP)	BioFroxx GmbH, Einhausen, Deutschland
Western Froxx wash solution	BioFroxx GmbH, Einhausen, Deutschland
Chemiluminescence reagent	PerkinElmer Life Sciences, Deutschland
beta-Mercaptoethanol	Sigma-Aldrich GmbH Deissenheim, Deutschland
MOPS Buffer	ThermoFischer Scientific, Waltham, Massachusetts, USA
RNase-free DNase I Kit	Norgen Biotek Corp., Ontario, Canada
Syber green master mix	Vazyme Biotech, Nanjing
Nuclease free water	Sigma-Aldrich GmbH Deissenheim, Deutschland
Bradford reagent	Sigma-Aldrich, USA

Table 4. Chemicals and kits.

Name	Composition
Culture media for primary LECs	500 ml KSFM 2.5 µg EGF 25 mg BPE 1% penicillin/streptomycin

Culture media for cell line(T-LSCs and T-LSCs PAX6 ^{+/-})	500 ml KSFM 2.5 µg EGF 25 mg BPE 1% penicillin/streptomycin 0.4 mM CaCl ₂ 2mM Glutamine
0.9 mM Ca ²⁺ culture media	500 ml KSFM 2.5 µg EGF 25 mg BPE 1% penicillin/streptomycin 450 µl 100 mM CaCl ₂
Laemmli-Buffer	125 mM tris (P ^H 6.8) 60% Glycerine 2.5% SDS 0.01% Bromophenolblue 63 µl/ml Mercaptoethanol

Table 5. Medias and buffers.

Transcript name	Cat. No	Amplicon size (bp)	Manufacturer
PAX6	QT00071169	113 bp	QIAGEN GmbH, Hilden, Deutschland
ADH7	QT00000217	85 bp	QIAGEN GmbH, Hilden, Deutschland
ALDH1A1	QT00013286	97 bp	QIAGEN GmbH, Hilden, Deutschland
DSG1	QT00001617	96 bp	QIAGEN GmbH, Hilden, Deutschland
SPINK7	QT00039585	126 bp	QIAGEN GmbH, Hilden, Deutschland
GUSB	QT00046046	96 bp	QIAGEN GmbH, Hilden, Deutschland
TBP	QT00000721	132 bp	QIAGEN GmbH, Hilden, Deutschland
ALDH3A1	QT0240193	121bp	QIAGEN GmbH, Hilden, Deutschland
STRA6	QT00006748	74bp	QIAGEN GmbH, Hilden, Deutschland
RDH10	QT00029176	107bp	QIAGEN GmbH, Hilden, Deutschland
RBP1	QT01850296	126bp	QIAGEN GmbH, Hilden, Deutschland
CRABP2	QT00063434	140bp	QIAGEN GmbH, Hilden, Deutschland
CYP1B1	QT00209496	114bp	QIAGEN GmbH, Hilden, Deutschland
ELOVL7	QT01025976	89bp	QIAGEN GmbH, Hilden, Deutschland

CYP26A1	QT00026817	150bp	QIAGEN GmbH, Hilden, Deutschland
PPARG	QT00029841	113bp	QIAGEN GmbH, Hilden, Deutschland
VEGFA	QT01010184	273 bp	QIAGEN GmbH, Hilden, Deutschland
FABP5	QT00225561	97 bp	QIAGEN GmbH, Hilden, Deutschland

Table 6. Primers used for qPCR.

Antibody	Catalog No. / Manufacturer	Dilution
ACTB	Ab8227, Abcam, Cambridge, UK	1:500
DSG1	Sc-59904, Santa Cruz Biotechnology, California, USA	1:200
FABP5	SC-365236, Santa Cruz Biotechnology, California, USA	1:500
ALDH1A1	SC-374076, Santa Cruz Biotechnology, California, USA	1:200
PAX6	Sc-32766, Santa Cruz Biotechnology, California, USA	1:200
ADH7	PA5-26709, Thermo Fischer Scientific, Waltham, Massachusetts	1:500

Table 7. Antibodies used for western blot.

2.2 METHODS

2.2.1 Primary limbal epithelial cells

2.2.1.1 Isolation and culturing of primary limbal epithelial cells (pLECs)

The use of donor corneoscleral rims (human tissue) of the Klaus Faber Center for Corneal Diseases including Lions Eye Bank was approved by the Ethics Committee of Saarland/ Germany (no. 266/15) for our project.

Human tissues were handled according to the Declaration of Helsinki principles. Primary limbal epithelial cells were isolated from the limbal region as described before (Latta et al., 2018; Rubelowski et al., 2020), using collagenase digestion of limbal tissue (Chen et al., 2011; Gonzalez and Deng, 2013). Human corneoscleral rims were rinsed in phosphate buffer saline (PBS). After washing, the tissue was punched with 1.5 mm punch around the corneal limbus region, thereafter, it was incubated with 4 mg/ml collagenase overnight at 37°C. Further procedure was performed under cell culture bench and sterile conditions.

After overnight digestion, the tissue was triturated with the help of a pipette (10 times) and then it was placed back in the incubator for 10 minutes. Thereafter, the tissue suspension was filtered with a 2.0µM filter. After filtration, 10 ml PBS was added to wash the cells. Then, the filter was washed from its back side with 2.5 ml trypsin/ETDA in a well of a 6-well and the well was placed in the incubator for 5 min at 37°C. Then, it was triturated again with a pipette (10 times) and was kept for 5 minutes in incubator. Thereafter, 3 ml DMEM was added to the cell suspension, to stop the reaction. Then, the cell suspension was transferred into a falcon and was centrifuged at 800g for 5 minutes. Thereafter, the supernatant was discarded carefully. Cell pellet was washed with 1 ml PBS and again the cells were centrifuged with some medium at 800g for 5 min. After discarding the supernatant, the cell pellet was suspended in 500µl KSFM and was seeded in a well of a 24-well plate. We placed this plate back into the incubator. Medium was changed every 3-4 days until cells reached 90% confluence.

When the cells reached 90% confluence, the medium was discarded and the cells were rinsed with 1ml PBS. 500 µl trypsin/ETDA was added to the well and it was incubated at 37°C for 5 minutes in incubator. We aimed to detach the cells from the plate. Thereafter equal volume of DMEM was again added to the well to stop the reaction. Afterwards, cell suspension was transferred to an Eppendorf tube and was centrifuged at 800g for 5 minutes. The supernatant was discarded and the cells were suspended in 1 ml PBS and were centrifuged at 800g for 5 minutes again. The cell pellet was dissolved in 500µl KSFM medium and was seeded into one well of 6-well plate. 2.5ml KSFM medium was added to the same

well. Then we placed the well plate into the incubator. Medium was changed every 3-4 days until cells reached 90% confluence.

2.2.1.2 Cryopreservation of limbal epithelial cells

After reaching 90% confluence, medium was discarded and cells were rinsed with 1ml PBS. 500 μ l trypsin/ETDA was added to the well for 5 minutes at 37°C to detach the cells. Thereafter, 500 μ l DMEM was added to stop the reaction, and the cell suspension was transferred into an Eppendorf tube and was centrifuged at 800g for 5 minutes. The supernatant was discarded and the cells were suspended in 1 ml PBS and were centrifuged at 800g for 5 minutes again.

For further use, the cells were in part cryopreserved. Therefore, the cell pellet was dissolved in 500 μ l cryo-medium and was transferred to a cryotube, which was labeled and placed in a cryocontainer at -80°C. After the cells were frozen, the cryotube was transferred to a liquid nitrogen tank.

2.2.1.3 Ca^{2+} treatment and siRNA transfection of pLECs

Cells were thawed and seeded (or directly splitted without cryopreservation) into 4 wells of a 6 well plate. Thereafter, cells were divided into two groups, control and Ca^{2+} treated groups, respectively. We cultured the control group in serum free medium, with a low Ca^{2+} concentration (KSFM medium). After reaching 90% confluence, cells were transfected with 5 nM non-specific control, siCtrl (5'AGGUAGUGUAAUCGCCUUGUU) (Ctrl pLECs) and for pax6 knock- down a combination of 5'CCUGGCUAGCGAAAAGCAAUU and 5'UGGGCG GAGUUAUGAUACCUU (siPAX6 pLECs), respectively (Latta et al., 2019). For this purpose, for each well, 5 μ l Lipofectamine dissolved in 150 μ l Opti- MEM + GlutaMAX -I was used.

On the same day, the Ca^{2+} treatment group was treated with KSFM, supplemented with 0.9 mmol/L Ca^{2+} for 72 hours subsequently. Then the next day, cells were transfected as described previously (Ca^{2+} Ctrl pLECs and Ca^{2+} siPAX6 pLECs). Incubation time for each transfection was 48 hours. All siRNAs used for our experiments were previously used in another study of our laboratory (Latta et al., 2019).

2.2.1.4 Harvesting of pLECs

After 48 hours of transfection, the medium was discarded and the cells were washed with 1 ml PBS. 300 μ l SKP lysis buffer was added to each well and the cells were lysed with the help of a scraper. Then, the lysed cells were transferred to a sterile Eppendorf tube for the further process. Thereafter, either lysed cells were stored at -80°C or were directly used for RNA and protein extraction.

2.2.2 Human telomerase-immortalized limbal epithelial stem cells (T-LSCs) and genome edited T-LSCs (T-LSCs PAX6^{+/-})

2.2.2.1 Culture of T-LSCs and T-LSCs PAX6^{+/-}

The cells were generously provided by Roux et al. (Paris, France) and cultured as described previously (Roux et al., 2018). T-LSCs were thawed and seeded in 25 cm² flask using 5 ml KSFM, supplemented with BPE, EGF, 0.4 mM CaCl₂, 2mM Glutamine and 100 U/ml Penicillin /Streptomycin. The flask was placed in incubator at 37°C and 5% CO₂. Medium was changed in every 3 days until cells reached 90% confluence. Same protocol was used for T-LSCs PAX6^{+/-} cells.

2.2.2.2 Splitting of T-LSCs and T-LSCs PAX6^{+/-}

When the cells reached 90% confluence, the medium was discarded and cells were rinsed with 3 ml PBS. Afterwards, 3 ml trypsin/ETDA was added to the flask and it was incubated for 5-6 minutes in incubator at 37°C to detach the cells from flask. Thereafter, 3 ml DMEM was added to the flask and cell suspension was prepared and centrifuged at 1500g for 5 min. The supernatant was discarded and cell pellet was suspended in 1 ml PBS and was centrifuged at 1500g for 5 minutes. Then, the cell pellet was suspended in culture medium and cell suspension was used for seeding of the cells in a 75 cm² flask using 5 ml culture medium. The flask was placed back in the incubator, at 37°C and 5% CO₂ until cells grow to desired confluency and in the meantime the medium was changed every 3 days.

When cells became 90% confluent, T-LSCs and T-LSCs PAX6^{+/-} were subcultured in 6×25 cm² cell culture flasks, using the same splitting protocol. The medium was changed every 3 days until cells reached 80-90% confluence.

2.2.2.3 Ca²⁺ treatment of T-LSCs and T-LSCs PAX6^{+/-}

At desired confluency, both T-LSCs and T-LSCs PAX6^{+/-} cells were incubated with a low Ca²⁺ concentration (KSFM medium) (control group) and with KSFM medium supplemented with 0.9 mmol/L Ca²⁺ (Ca²⁺ treated group) for 24 or 72 hours subsequently.

2.2.2.4 Harvesting of T-LSCs and T-LSCs PAX6^{+/-}

After incubation, medium was discarded from each flask and cells were incubated with 3 ml Trypsin-EDTA to detach the cells from flask. Thereafter, 3 ml DMEM was added to stop the enzymatic reaction and a cell suspension was prepared with the help of a pipette. Then cell suspension was transferred to centrifuge tube and was centrifuged at 1500g for 5 minutes. After discarding the supernatant, 1 ml PBS was used to wash the cells, using 1500g for 5 minutes again. Afterwards, cell pellet was directly used for RNA and protein extraction or was stored at -80°C.

2.2.3 RNA and protein isolation

In order to get RNA and protein, lysed cells and pellets were processed with a DNA/RNA/ Protein isolation kit according to the manufacturer's instruction. The Kit is based on silica column technology, for isolation of nucleic acid and protein. On column, DNA digestion was performed to avoid DNA residuals in the RNA sample. RNA from each sample was eluted in 40 μ l and protein was eluted in 50 μ l of elution buffer to get a more concentrated sample.

2.2.3.1 RNA concentration estimation

Purity and quantity of RNA from each sample was checked with Nanodrop 1000 which is based on UV/VIS spectroscopy principle. Spectrophotometer was calibrated with 1 μ l of H₂O and then same volume of the respective RNA sample was pipetted onto the lower measuring surface with a precision pipette. 260/280 and 260/230 value for each sample was checked carefully.

2.2.3.2 cDNA synthesis

500 ng RNA was used for synthesis of a first strand of cDNA with M-MuLV Enzyme Mix kit and oligo-dt primers (One Taq-kit, NEB), according to the manufacturer's protocol in two steps (**Table 8**). In the first step, 500 ng RNA and Oligo d(T)23 Primer were incubated at 70°C for 5 min for RNA denaturation, annealing of primer and then, as a second step, M-MuLV reaction mixture and enzyme mixture were added to the product of the first step and there was an incubation for 1 hour at 42°C. Then, the temperature was increased to 80°C for 5 min, for cDNA synthesis.

First step	
Reagent	Volume
RNA (500 ng)	1-6 μ l
Oligo d(T)23 Primer	2 μ l
Nuclease-free Water	to a total volume of 8 μ l
Second step	
Reaction mixture 1	8 μ l
M-MuLV Reaction Mixture	10 μ l
M-MuLV Enzyme Mixture	2 μ l
Nuclease-free Water	30 μ l
Total	50 μ l

Table 8. *Materials used for the first strand of the cDNA synthesis.*

2.2.3.3 Quantitative polymerase chain reaction (qPCR)

The qPCR experiments were carried out in 96-well plates as duplicates, using ACEq DNA SYBR Green Mix and a PCR Thermocycler CFX Connect. Samples were run in 10 μ l volume of reaction using 2.5 μ l cDNA and 7.5 μ l AceQ SYBER qPCR Master Mix with primers. Reaction mixture (**Table 9**) was prepared in two steps: As a first step (template mix), the template (first strand, cDNA) was diluted in nuclease-free water in one tube. In a second step (Primer mix), primers were mixed with SYBER master mix and were diluted with nuclease-free water in a separate tube. Afterwards, both 2.5 μ l volume diluted templates were added.

Template mix	
Reagent	Volume (for one reaction)
cDNA	0.5 μ l
Nuclease-free Water	2 μ l
Total	2.5 μ l
Primer mix	
Primer	1.25 μ l
SYBER master mix	5 μ l
Nuclease-free Water	1.25 μ l
Total	7.5 μ l

Table 9. Materials of the reagent mixture of the single reaction, used in the qPCR experiment.

The amplification conditions (**Table 3**) for all transcripts were as follows: initial denaturation 95°C for 5 min, denaturation 95 °C for 10 s and primer annealing 60 °C for 30s. These steps were repeated for 40 cycles. Elongation occurred (~72°C) during heating up for denaturation for melt curve. Reference genes GUSB and TBP were run under the same conditions in each case.

Step1 Holding stage	Step 2 Cycling stage (no of cycle = 40)	Step3 Melt curve
Initial denaturation- 95°C (5 min)	Denaturation- 95°C (10 s) Annealing- 60°C (30s) Elongation~72°C (during heating up for denaturation)	Denaturation - 95°C.

Table 10. Thermocycler profile for the qPCR experiment and melt curve analysis.

The relative expression was normalized with the average of the GUSB and TBP reference gene. Ct and $\Delta\Delta\text{Ct}$ values were calculated for each target gene compared to controls (siCtrl) using QuantStudio™ design and analysis software. Data analysis was performed with Excel, expression fold-changes ($2^{\Delta\Delta\text{Ct}}$ values) were calculated.

2.2.4 Protein estimation

Protein estimation was performed using Bradford Assay based on colorimetry. The absorbance was measured at different concentrations of a known protein: BSA was measured at 595 nm and a calibration curve was plotted between absorbance versus concentration. Regression analysis was performed to calculate the unknown value of X variables with the help of known value of Y variable using $Y = mX + C$ regression equation and to check how efficient data fit to this regression line, R^2 (Coefficient of Regression) was calculated.

2.2.4.1 Western blot

Proteins were separated by SDS- Polyacrylamide gel electrophoresis. 20 μg total protein from each lysate was boiled in denaturing buffer for 5 min at 95°C. Denatured samples and Dual colour marker were loaded to 4-12 % Nu Page™ Bis-Tris SDS Gel and were subjected to electrophoresis, allowed to run for 1 hour at 120 Volt. Separated proteins were transferred from polyacrylamide gel to nitrocellulose membrane, using semi dry method with the Trans-Blot Turbo Transfer System. After three washing steps for 5 min, the membrane was incubated with primary antibody. Primary antibodies were diluted in combined blocking buffer and secondary antibody solution of Western Foxx kit. After incubation, the membrane was again washed with washing solution, three times for 5 min. Afterwards, the membrane was incubated with Western lightening chemiluminescence reagent plus ECL for 1 min to develop stain. After detection, images were acquired with a LAS 4000 System and image was exported as TIFF. The western blot was reprobated with ACTB as loading control. Each western blot was repeated 3-4 times.

2.2.5 Statistical analysis

mRNA and protein expression values were compared to controls using one-way ANOVA followed by Bonferroni test. A p-value below 0.05 was considered statistically significant. Graph Pad Prism 7.04 software (CA, USA) was used for analysis and to draw the graphs. For signal quantification of protein expression, densitometric analysis of western blots was performed using Image Studio™ Lite 5.2 (LI-COR Biosciences).

CHAPTER 3:

RESULTS

To trigger differentiation in pLECs, 0.9 mM Ca^{2+} supplementation as primary tool has been used. Furthermore, I checked the morphology of the cells.

3.1 Cell culture and morphology of pLECs

Primary limbal epithelial cells cultured in KSFM were homogenous small cells with typical cobblestone morphology (**Figure 6a**), whereas cells in KSFM with high Ca^{2+} concentration were a heterogeneous mix of small and large differentiated cells (**Figure 6b**).

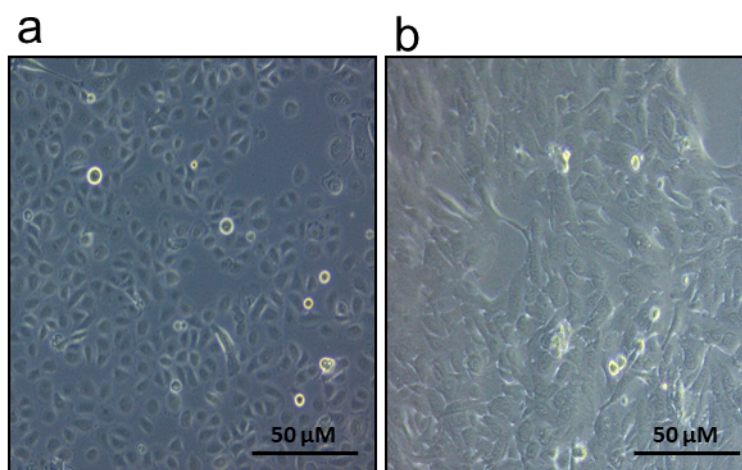


Figure 6. Morphology of the primary limbal epithelial cells (pLECs). In keratinocyte serum free medium (KSFM) cultured cells were homogeneous and small, with typical cobblestone morphology (**a**). In KSFM, with high Ca^{2+} concentration, there was a heterogeneous mixture of small and large differentiated cells (**b**).

3.2 Combination of Ca^{2+} treatment with primary siRNA cell model

Figures 7-11 display mRNA and protein expression of the analyzed genes.

3.2.1 Transcription factor *PAX6* and differentiation marker *DSG1* expression (qPCR and western blot)

The transcription factor *PAX6* (FC=1.3) and differentiation marker *DSG1* (FC=4.33) mRNA expression was significantly upregulated ($p=0.02$, $p=0.01$) after Ca^{2+} stimulation, compared to controls (**Figure 7a, b**). After siRNA treatment alone, *PAX6* expression (FC=0.23) was decreased ($p<0.0001$) and also

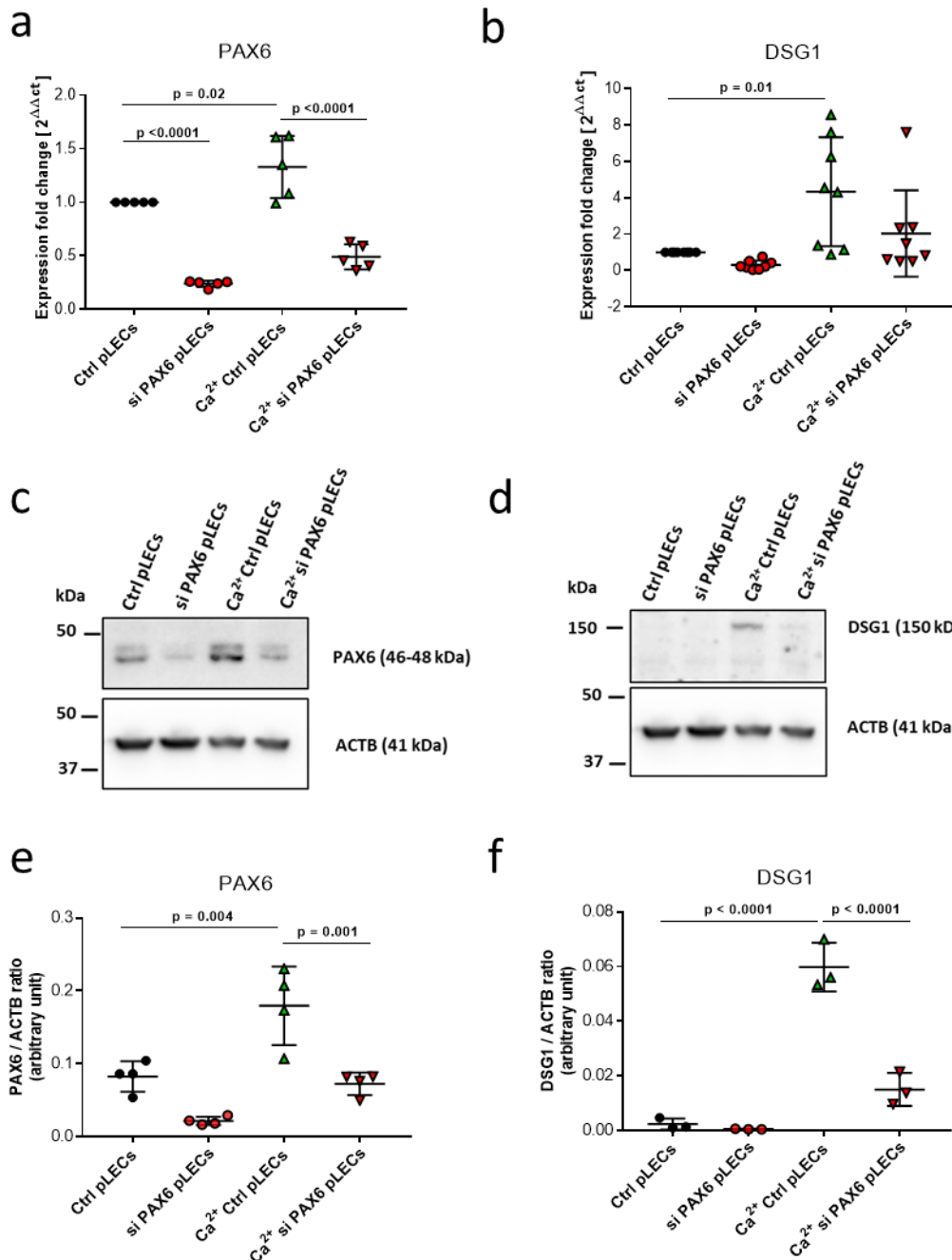


Figure 7. qRT-PCR and western blot analysis of differentiation markers PAX6 and DSG1 in primary limbal epithelial cells treated with Ctrl siRNA (Ctrl pLECs), in pLECs treated with siRNA against PAX6 (siPAX6 pLECs), in Ca^{2+} -stimulated primary limbal epithelial cells treated with Ctrl siRNA (Ca^{2+} pLECs) and in Ca^{2+} -stimulated pLECs, also treated with siRNA against PAX6 (Ca^{2+} si PAX6 pLECs). Expression fold changes (FC) were calculated relative to controls with the $\Delta\Delta Ct$ method (a-b) ($n=5$ for each). (c) and (d) display representative PAX6, DSG1 and β -actin (ACTB, control sample) Western blots for each treatment group/controls. For the western blot/densitometric analysis, quantification of the target transcripts was normalized to ACTB (ACTB control sample) ($n=3$ for each) (e-f). PAX6, DSG1 and ACTB were all detected in the same blot in parallel. mRNA and protein expression values were compared to controls using one-way ANOVA followed by Bonferroni test. A p-value below 0.05 was considered statistically significant.

decreased using Ca^{2+} stimulation, combined with siRNA treatment however, DSG1 expression did not change using siRNA treatment alone, or in combination with Ca^{2+} stimulation (**Figure 7a, b**) (n=5). PAX6, DSG1 and β -actin (ACTB, endogenous loading control) protein expression was measured using Western blot (**Figure 7c, d**) and densitometry (**Figure 7e, f**). PAX6 (p=0.004) and DSG1 (p<0.0001) protein expression increased in Ca^{2+} treated cells. After siRNA treatment alone, the mean PAX6 protein expression was about one third of those in controls (Ctrl pLECs), however, this change was not significant (p=0.08) and was significantly downregulated (p=0.004) using Ca^{2+} stimulation, combined with siRNA treatment, compared to Ca^{2+} stimulation alone. (**Figure 7c**). DSG1 was visible only in Ca^{2+} treated cells and was strongly reduced after PAX6 knock down (p<0.0001) (**Figure 7d**) (n=3).

3.2.2 Retinoic acid pathway components *ADH7*, *ALDH3A1* and *ALDH1A1* expression (qPCR and western blot)

ADH7 (FC=2.5), *ALDH1A1* (FC=4.55) showed increased mRNA expression after Ca^{2+} stimulation compared to controls (p<0.0001, p<0.0001) (**Figure 8a, b**). While *ADH7* mRNA expression was less than half of those in Ctrl pLECs, was not significantly downregulated (FC=0.33, p=0.07) but a combination of siRNA treatment and Ca^{2+} stimulation had a significant effect (p<0.0001), compared to Ca^{2+} stimulation treatment alone (**Figure 8a**). *ALDH1A1* mRNA expression following siRNA treatment alone was half of that in Ctrl pLECs, but was not significantly downregulated (FC=0.5, p=0.09). Nevertheless, it significantly decreased after combining this treatment with Ca^{2+} stimulation, compared to Ca^{2+} stimulation treatment alone (p=0.008) (**Figure 8b**). *ALDH3A1* mRNA expression remained unchanged using siRNA treatment alone and in combination with Ca^{2+} stimulation (**Figure 8c**) (n=5). *ADH7*, *ALDH1A1* and β -actin protein expression was analysed by Western blot. *ALDH1A1* protein expression was tended to be upregulated in presence of Ca^{2+} but did not change after siRNA treatment (**Figure 8e**). *ADH7* protein expression did not change under any growth conditions (p \geq 0.99) (**Figure 8d**) (n=3). Western blot was not performed for the *ALDH3A1* transcript.

3.2.3 Cellular binding protein *CRABP2*, *RBPI* and *FABP5* expression (qPCR and western blot)

Cellular binding proteins *CRABP2* (FC =3.21), *RBPI* (FC=1.39) and *FABP5* (FC=1.69) were significantly upregulated after Ca^{2+} treatment at mRNA level (p<0.0001, p=0.01, p=0.03) (**Figure 9a, b, c**). *RBPI* (FC=0.58) and *FABP5* (FC=0.22) mRNA expression showed a significant reduction after PAX6 knockdown, under normal growth conditions (p=0.006, p=0.01) (**Figure 9b, c**), while *CRABP2* mRNA expression was about half of that in Ctrl pLECs, but did not change significantly (FC=0.49, p=0.84) (**Figure 9a**). Using Ca^{2+} stimulation and siRNA treatment, *CRABP2* and *FABP5* mRNA expression was also downregulated, compared to Ca^{2+} stimulation alone (p=0.003, p= 0.002) (**Figure 9a, c**), but *RBPI* mRNA expression remain unchanged (**Figure 9b**).

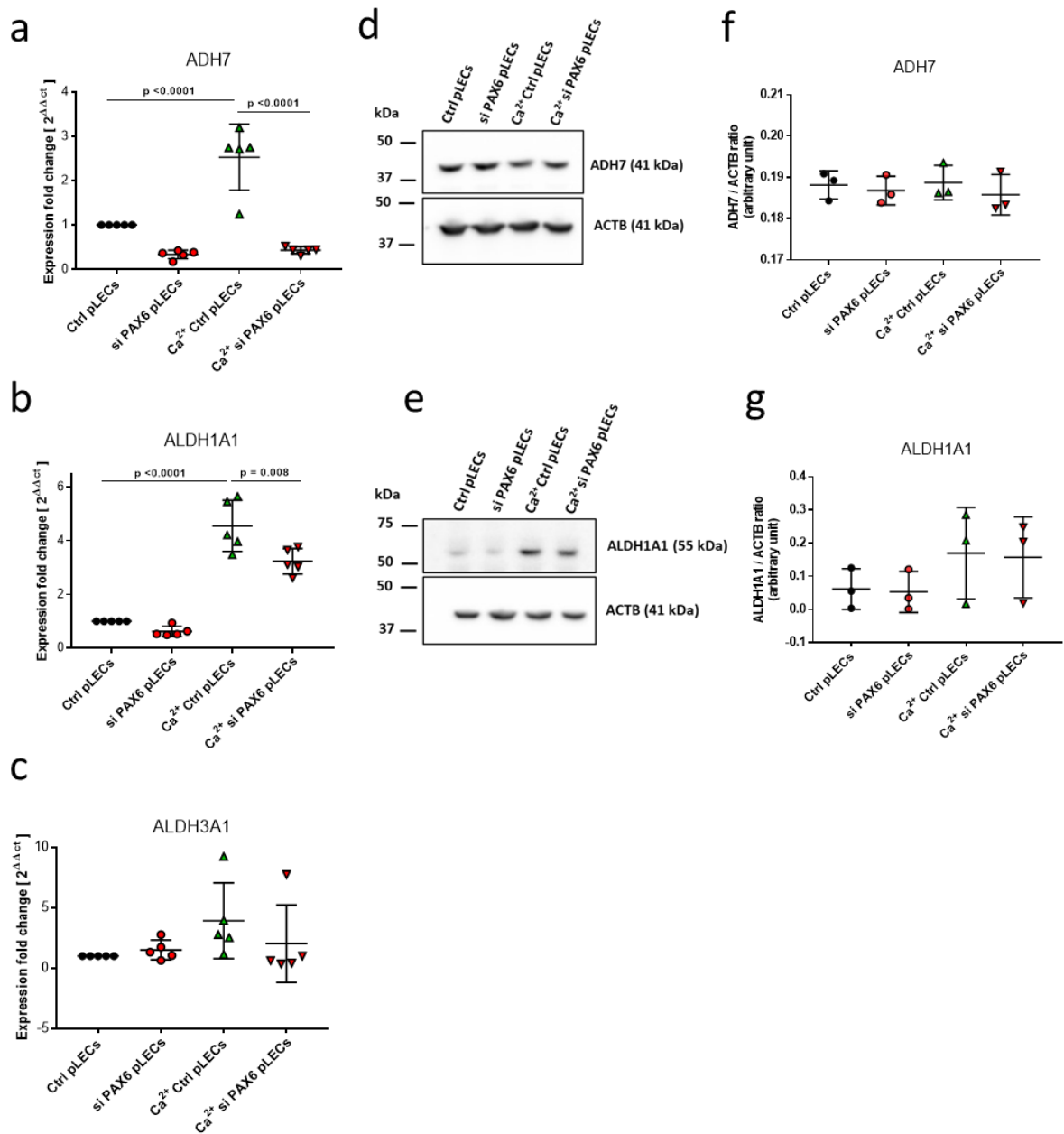


Figure 8. *qRT-PCR and western blot analysis of the metabolizing enzymes of retinoic acid signaling components ADH7, ALDH1A1 and qRT-PCR analysis of ALDH3A1 in primary limbal epithelial cells treated with Ctrl siRNA (Ctrl pLECs), in pLECs treated with siRNA against PAX6 (si PAX6 pLECs), in Ca^{2+} -stimulated primary limbal epithelial cells treated with Ctrl siRNA (Ca^{2+} pLECs) and in Ca^{2+} -stimulated pLECs, also treated with siRNA against PAX6 (Ca^{2+} si PAX6 pLECs). Expression fold changes (FC) were calculated relative to controls with the $\Delta\Delta Ct$ method (a-c) ($n=5$ for each). (d) and (e) display representative ADH7, ALDH1A1 and β -actin (ACTB, control sample) Western blots for each treatment group/controls (d-g) ($n=3$ for each). For the western blot analysis, quantification of the target transcripts was normalized to ACTB (ACTB control sample) (d-g). mRNA and protein expression values were compared to controls using one-way ANOVA followed by Bonferroni test. A p -value below 0.05 was considered statistically significant.*

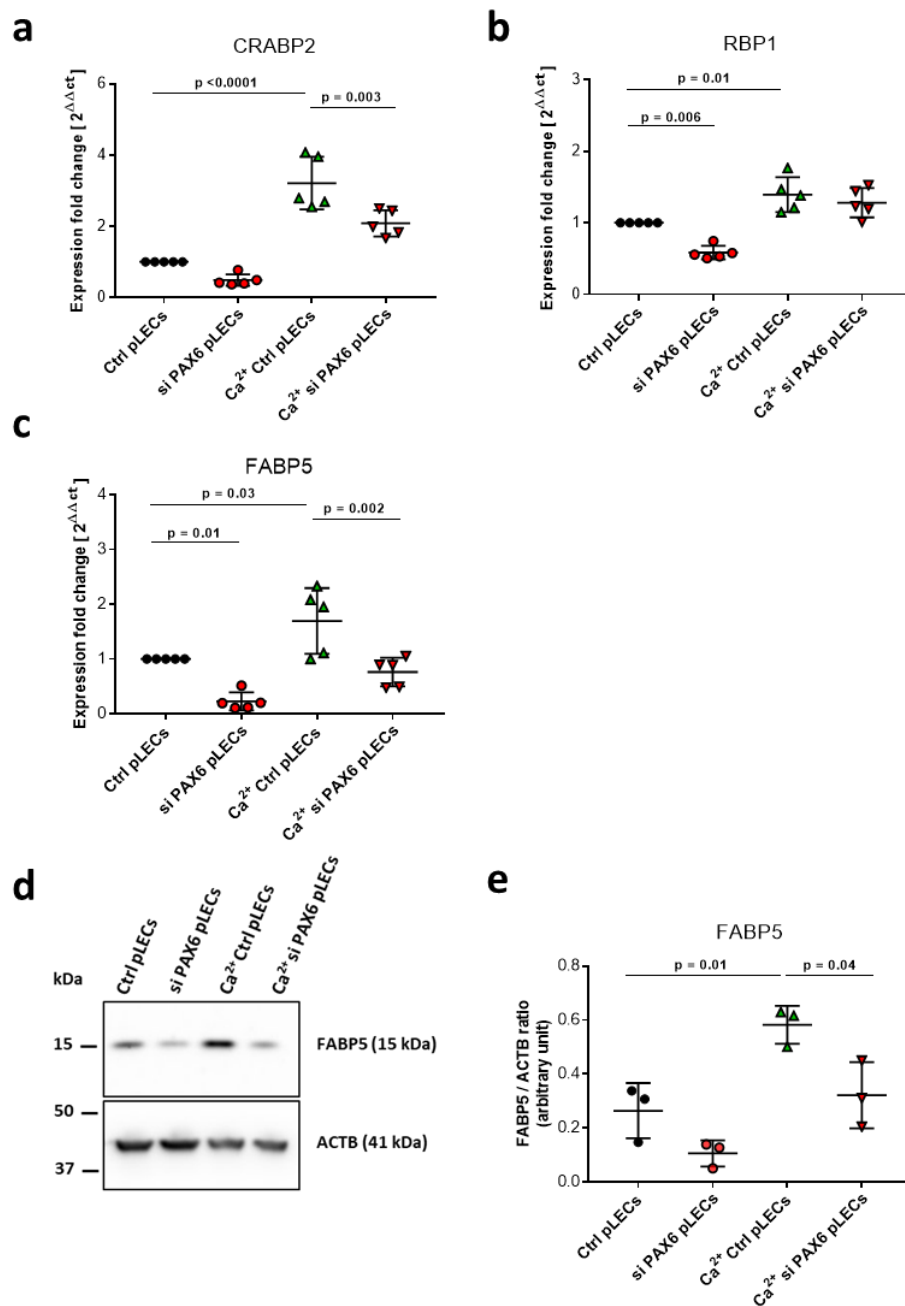


Figure 9. *qRT-PCR analysis of the cellular binding proteins CRABP2, RBP1 and qRT-PCR and Western blot analysis of the cellular binding protein/RA signaling component FABP5. Measurements in primary limbal epithelial cells treated with Ctrl siRNA (Ctrl pLECs), in pLECs treated with siRNA against PAX6 (si PAX6 pLECs), in Ca²⁺-stimulated primary limbal epithelial cells treated with Ctrl siRNA (Ca²⁺ pLECs) and in Ca²⁺-stimulated pLECs, also treated with siRNA against PAX6 (Ca²⁺ si PAX6 pLECs). Expression fold changes (FC) were calculated relative to controls with the $\Delta\Delta C_t$ method (a-c) ($n = 5$ for each). (d) displays FABP5 and β -actin (ACTB, control sample) representative western blots for each treatment group/controls. For the FABP5 western blot/densitometric analysis, quantification of the target transcript was normalized to ACTB (ACTB control sample) (e) ($n=3$). mRNA and protein expression values were compared to controls using one-way ANOVA followed by Bonferroni test. A p -value below 0.05 was considered statistically significant.*

Western blot analysis was not performed for CRABP2 and RBP1, as expression changes at mRNA level after PAX6 knockdown under normal growth conditions were not correlated with our prior screening data.

3.2.4 Retinoic acid pathway component *CYP1B1*, *PPARG*, *STRA6* and *VEGFA* (qPCR)

VEGFA (FC=0.48, p=0.70) and *STRA6* (FC=0.62, p=0.08) mRNA expression using Ca^{2+} supplementation and after PAX6 knockdown remained unchanged using both PAX6 knockdown and Ca^{2+} supplementation, compared to Ca^{2+} supplementation alone (FC=1.86, p>0.99 and FC=2.39, p=0.05) (Figure 10a, b) (n=5).

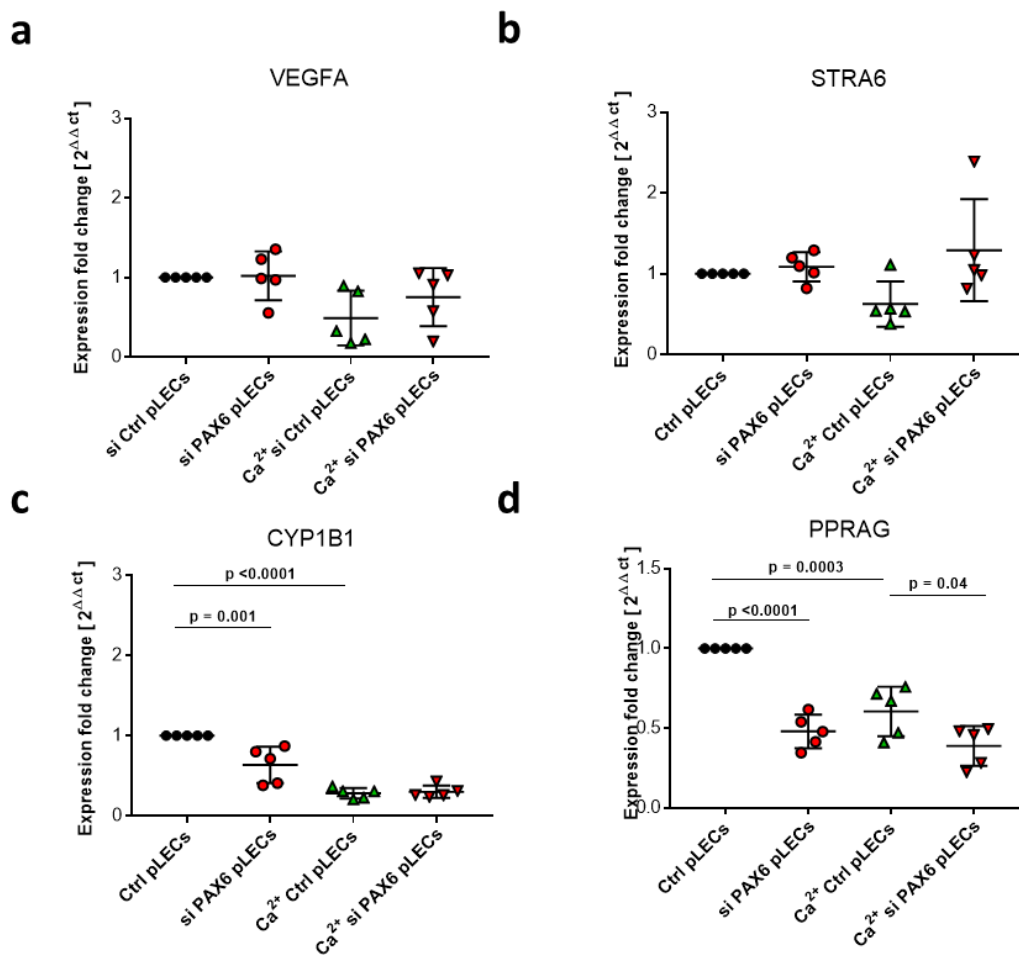


Figure 10. qRT-PCR analysis of the transcripts *VEGFA*, *STRA6*, *CYP1B1* and *PPRAG* (a-d) in primary limbal epithelial cells treated with Ctrl siRNA (Ctrl pLECs), in pLECs treated with siRNA against PAX6 (si PAX6 pLECs), in Ca^{2+} -stimulated primary limbal epithelial cells treated with Ctrl siRNA (Ca^{2+} pLECs) and in Ca^{2+} -stimulated pLECs, also treated with siRNA against PAX6 (Ca^{2+} si PAX6 pLECs). Expression fold changes (FC) were calculated relative to controls with the $\Delta\Delta\text{Ct}$ method (a-d) (n = 5 for each). mRNA expression values were compared to controls using one-way ANOVA followed by Bonferroni test. A p-value below 0.05 was considered statistically significant.

CYP11B1 (FC=0.28, $p < 0.0001$) and *PPARG* (FC=0.60, $p = 0.0003$) transcripts were significantly reduced after Ca^{2+} supplementation at mRNA level ($n=5$). *CYP11B1* (FC=0.63, $p = 0.001$) and *PPARG* mRNA was downregulated using siRNA treatment alone (**Figure 10c, d**), and *PPARG* mRNA (FC=0.38, $p = 0.04$) was also downregulated when combining siRNA treatment and Ca^{2+} supplementation, compared to Ca^{2+} supplementation alone (**Figure 10d**), but *CYP11B1* remained unchanged (**Figure 10c**) ($n=5$).

Western blot analysis was not performed for any of these markers, since expression changes at mRNA level using normal growth condition or Ca^{2+} supplementation and/or PAX6 knockdown was not correlated with transcriptional data obtained in aniridia patients

3.2.5 Lypogenic enzyme *ELOVL7*, *RDH10* and protease inhibitor *SPINK7* expression (qPCR)

After siRNA treatment alone, Ca^{2+} stimulation alone, or combining siRNA treatment and Ca^{2+} stimulation, *ELOVL7* (FC= 1.01) and *RDH10* (FC= 1.001) mRNA expression remained unchanged

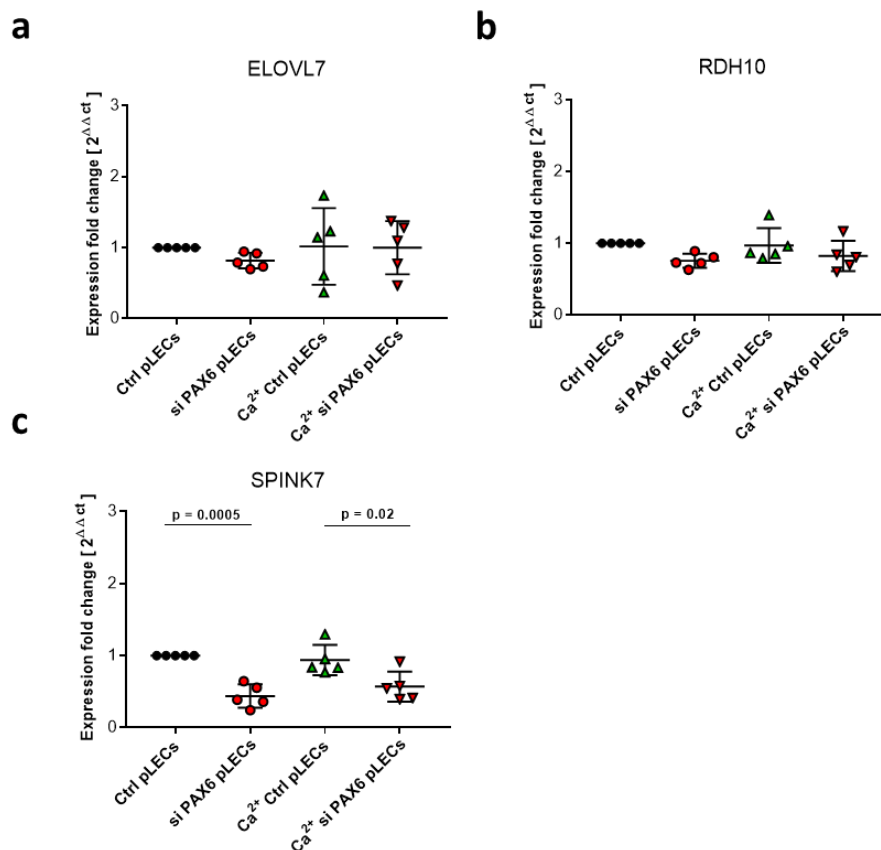


Figure 11. qRT-PCR analysis of transcripts *ELOVL7*, *RDH7* and *SPINK7* (a-c) in primary limbal epithelial cells treated with Ctrl siRNA (Ctrl pLECs), in pLECs treated with siRNA against PAX6 (si PAX6 pLECs), in Ca^{2+} -stimulated primary limbal epithelial cells treated with Ctrl siRNA (Ca^{2+} pLECs) and in Ca^{2+} -stimulated pLECs, also treated with siRNA against PAX6 (Ca^{2+} si PAX6 pLECs). Expression fold changes (FC) were calculated relative to controls with the $\Delta\Delta Ct$ method (a-c) ($n=5$ for each). mRNA expression values were compared to controls using one-way ANOVA followed by Bonferroni test. A p -value below 0.05 was considered statistically significant.

($p > 0.99$, $p > 0.99$) (**Figure 11a, b**). Serine protease inhibitor *SPINK7* mRNA expression (FC = 0.94) remained unchanged upon Ca^{2+} stimulation and was significantly downregulated after PAX6 knockdown, under normal (FC = 0.43) ($p = 0.0005$) and Ca^{2+} stimulated growth conditions (FC = 0.57) ($p = 0.02$) (**Figure 11c**) ($n = 5$ for each).

Western blot analysis was not performed for any of these markers, since altered expression changes were not observed at mRNA level after Ca^{2+} treatment alone.

3.3 Expression analysis of *FABP5* and *DSG1* gene in human telomerase-immortalized limbal epithelial stem cells (T-LCEs)

Figures 12 and **13** display mRNA expression of the analyzed genes. Western blot analysis was performed to compare mRNA and protein expression. Cellular binding protein FABP5 with differentiation markers PAX6 and DSG1 were investigated in this cell model to analyse the correlation between these target proteins and the master regulatory gene PAX6.

3.3.1 24 hours Ca^{2+} treatment (qPCR and western blot)

FABP5 mRNA (FC = 0.588, $p = 0.004$) and protein expression was significantly downregulated in mutated cells (PAX6^{+/-} T-LSCs), compared to wild type cells (T-LSCs), ($p < 0.0001$) (**Figure 12a, c**). After 24 hours Ca^{2+} treatment, both wild (FC = 2.01, $p < 0.0001$) and mutated LSCs (FC = 1.48, $p < 0.0001$) showed significant FABP5 mRNA upregulation (**Figure 12a**). After Ca^{2+} stimulation, FABP5 protein expression remained unchanged in both wild type and mutated cells, compared to untreated cells of same type (**Figure 12d**).

Differentiation marker PAX6 mRNA expression and protein expression remained unchanged, in both wild type and mutated cells compared to untreated cells of same type after Ca^{2+} stimulation, but both mRNA (FC = 0.538, $p = 0.01$) and protein expression was significantly reduced ($p = 0.0008$) in mutated cells (PAX6^{+/-} T-LSCs) compared to wild type cells (T-LSCs) (**Figure 12b, e**).

Junction protein/differentiation marker DSG1 mRNA expression (FC = 0.53) was significantly reduced ($p = 0.01$) in mutated cells (PAX6^{+/-} T-LSCs), compared to wild type cells (T-LSCs). After 24 hours Ca^{2+} treatment, DSG1 mRNA expression was significantly upregulated both in wild type (FC = 1.57) ($p = 0.004$) and mutated cells (FC = 1.93) ($p = 0.0006$), compared to untreated cells of same type (**Figure 12c**). In western blot, DSG1 protein was not visible either in wild type or mutated cells under both growth conditions (**Figure 12h**) ($n = 3$ for each).

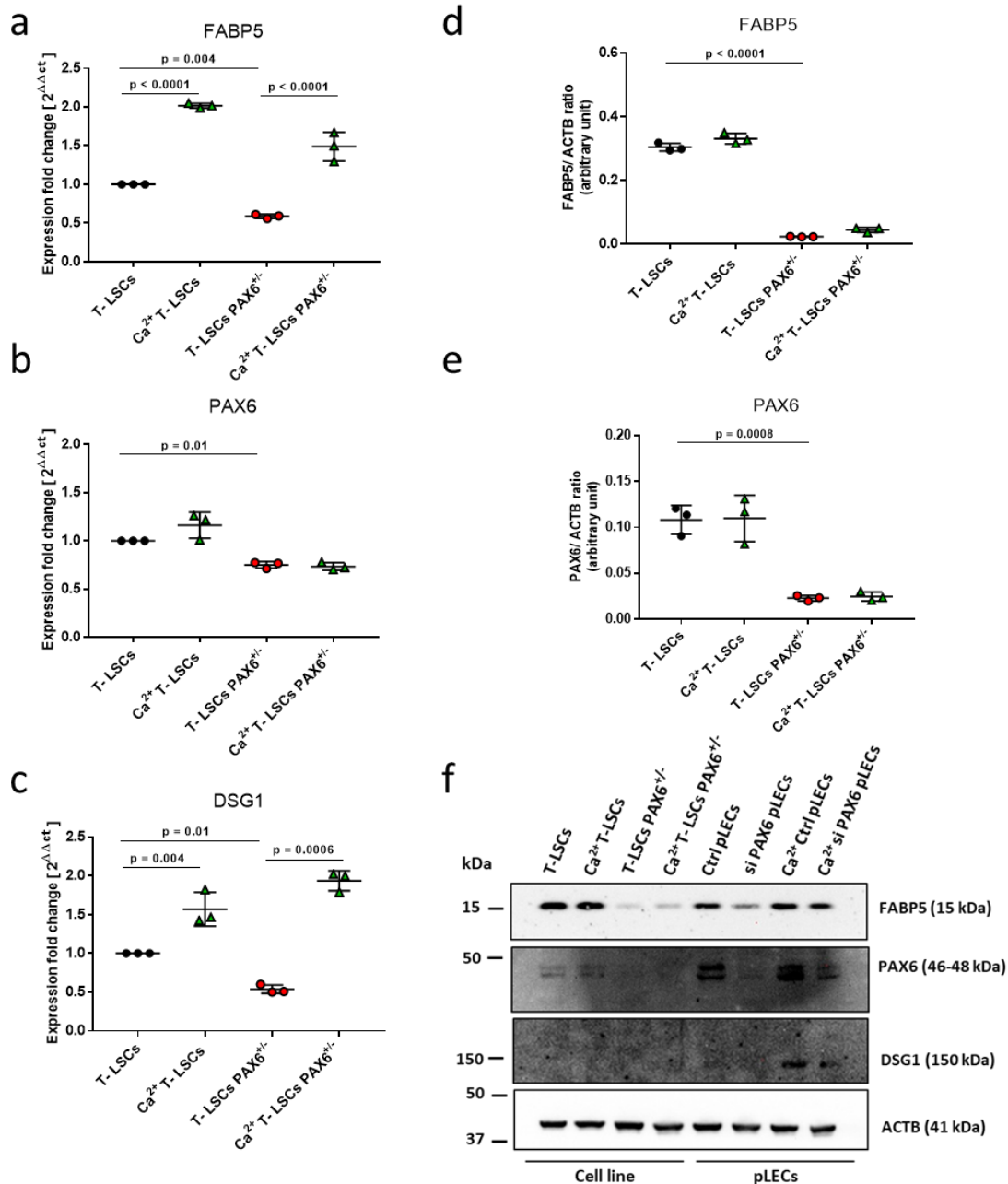


Figure 12. FABP5, PAX6, DSG1 qRT-PCR and western blot analysis - in human telomerase-immortalized limbal epithelial stem cells (T-LSCs), in Ca^{2+} -stimulated T-LSCs (Ca^{2+} T-LSCs), in CRISPR/Cas9 genome edited human telomerase-immortalized limbal epithelial stem cells (T-LSCs PAX6^{+/-}) and in Ca^{2+} -stimulated T-LSCs PAX6^{+/-} (Ca^{2+} T-LSCs PAX6^{+/-}) (a-f). Ca^{2+} stimulation was used in all cases for 24 hours. Expression fold changes (FC) were calculated relative to controls with the $\Delta\Delta Ct$ method (a, b, c) (n=3 for each). (f) displays representative FABP5, PAX6, DSG1, and β -actin (ACTB, control sample) western blots for each treatment group/controls. For the western blot/densitometric analysis, quantification of the target transcripts was normalized to ACTB (ACTB control sample) (d, e) (n=3 for each). mRNA and protein expression values were compared to controls using one-way ANOVA followed by Bonferroni test. A p-value below 0.05 was considered statistically significant.

3.3.2 72 hours Ca^{2+} treatment (qPCR and western blot)

After 72 hours Ca^{2+} treatment, FABP5 mRNA expression was significantly upregulated in wild type (FC = 1.77, $p=0.0005$) and mutated cells (FC=1.77, $p=0.007$), compared to untreated cells of same type (**Figure 13a**). FABP5 showed a restoration in T-LSCs PAX6^{+/-} cells compared to T-LSCs cells. The FABP5 protein expression changed parallel to changes in mRNA expression, with a significant upregulation in T-LSCs ($p < 0.0001$) and T-LSCs PAX6^{+/-} cells ($p < 0.0001$) through Ca^{2+} treatment (**Figure 13f, d**).

Expression of the differentiation marker PAX6 (FC=0.68) was significantly reduced in wild type cells at mRNA level ($p < 0.0001$) and remained unchanged in mutated cells after 72 hours Ca^{2+} treatment ($p > 0.99$) (**Figure 13b**). PAX6 expression was significantly reduced at mRNA (FC=0.35, $p < 0.0001$) and at protein level ($p < 0.0001$) in mutated cells (PAX6^{+/-} T-LSCs), compared to wild type cells (T-LSCs) (**Figure 13b, e**). There was a significant upregulation of PAX6 protein at the western blot and densitometric analysis both wild type ($p=0.0003$) and mutated cells ($p < 0.0001$) (**Figure 13e, f**).

DSG1 was significantly reduced (FC=0.60, $p=0.002$) in mutated cells (PAX6^{+/-} T-LSCs), compared to wild type cells (T-LSCs). After 72 hours Ca^{2+} treatment, DSG1 mRNA expression decreased in wild type cells (FC = 0.196, $p < 0.0001$) and in mutated cells tended to reduce (FC = 0.424, $p=0.02$), compared to untreated cells of same type at mRNA level (**Figure 13c**). In western blot analysis, DSG1 protein was not visible in wild type or mutated cells under any of the growth conditions (**Figure 13f**).

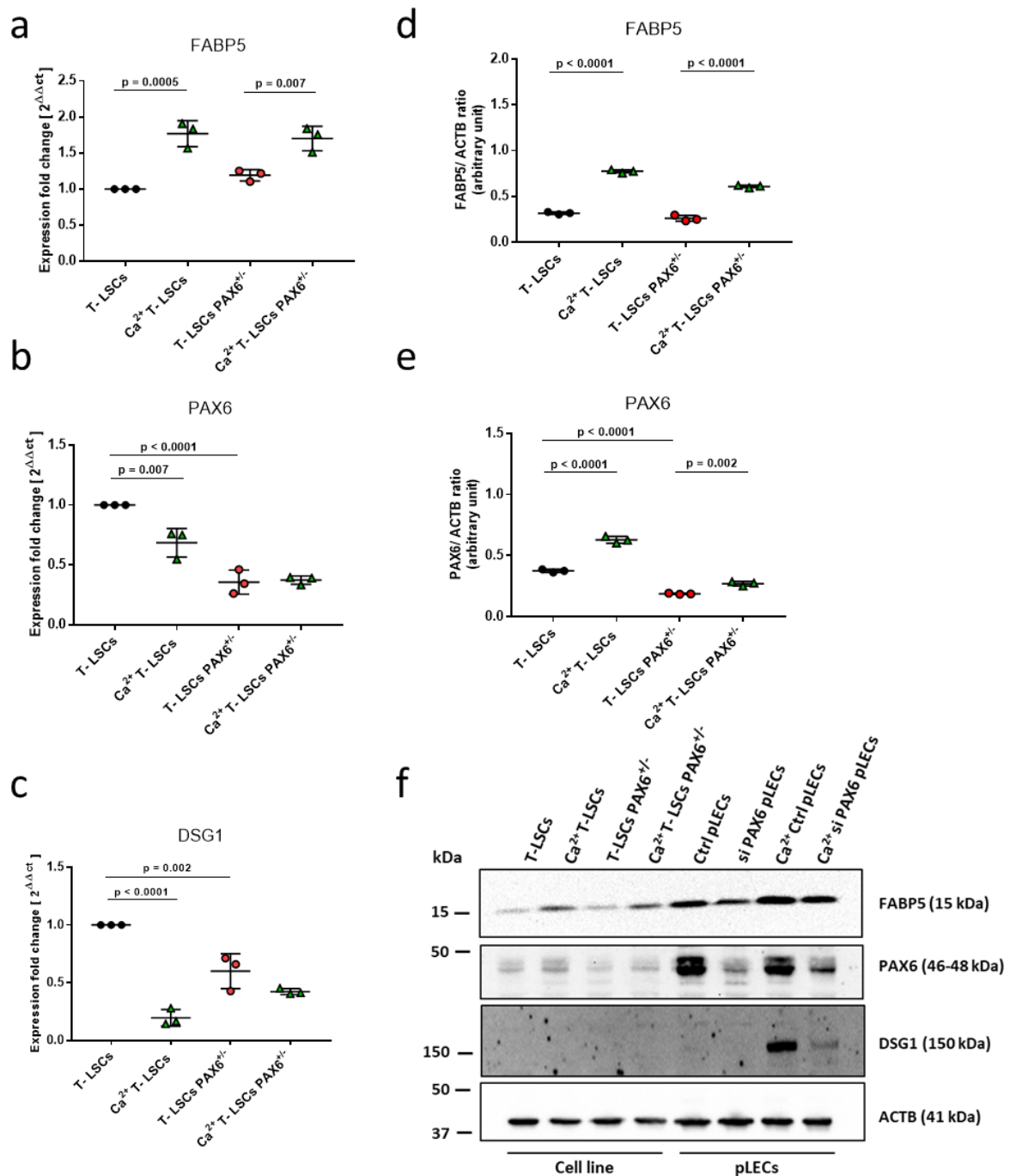


Figure 13. FABP5, PAX6, DSG1 qRT-PCR and western blot analysis -in human telomerase-immortalized limbal epithelial stem cells (T-LSCs), in Ca^{2+} stimulated T-LSCs (Ca^{2+} T-LSCs), in CRISPR/Cas9 genome edited human telomerase-immortalized limbal epithelial stem cells (T-LSCs PAX6^{+/-}) and in Ca^{2+} stimulated T-LSCs PAX6^{+/-} (Ca^{2+} T-LSCs PAX6^{+/-}) (a-f). Ca^{2+} stimulation was used in all cases for 72 hours. Expression fold changes (FC) were calculated relative to controls with the $\Delta\Delta Ct$ method (a, b, c) (n=3 for each). (f) displays representative FABP5, PAX6, DSG1, and β -actin (ACTB, control sample) western blots for each treatment group/controls. For the western blot/densitometric analysis, quantification of the target transcripts was normalized to ACTB (ACTB control sample) (d, e) (n=3 for each). mRNA and protein expression values were compared to controls using one-way ANOVA followed by Bonferroni test. A p-value below 0.05 was considered statistically significant.

CHAPTER 4:

DISCUSSION

In the present study, our expression data support the hypothesis, that the primary aniridia cell model (siRNA-based cell model), in combination with Ca^{2+} supplementation, could be utilized in order to investigate the genes, which are directly influenced by PAX6 and are involved in the differentiation process of the corneal epithelium. There are two main outcomes of the current study: First, the siRNA-based cell model in combination with Ca^{2+} supplementation could be a useful tool to analyse the gene expression not only at mRNA, but also at protein level. Second, using the siRNA-based cell model in combination with Ca^{2+} supplementation, evidence of the functional role of PAX6 in changes of RA signaling in limbal epithelial cells could be shown.

5.1 Morphological changes in LECs, using Ca^{2+} supplementation and siRNA-based cell model

After screening of conjunctival and limbal epithelial cells of aniridia patients, as a first step, we enhanced the differentiation through changing the culture conditions, since pLECs expressed a less differentiated phenotype and were not an ideal tool to study the differentiation process of corneal epithelial cells (Rubelowski et al., 2020). Several studies described that Ca^{2+} could trigger differentiation in several cell lines (Hiraki et al., 2002; D'Souza et al., 2001; Siegenthaler et al., 1994; Kawakita et al., 2004; Ma and Liu, 2011). We decided to culture cells in KSFM, supplemented with 0.9 mmol/L Ca^{2+} concentration. In our preliminary experiments, the Ca^{2+} supplementation group was treated with KSFM, supplemented with 0.9 mmol/L Ca^{2+} for 24 hours. However, following 24 hours Ca^{2+} supplementation, the morphology of the pLECs was unchanged. Therefore, the Ca^{2+} supplementation time was increased to 72 hours, which did result in changes of cell morphology. Then, we analysed the effect of the 72 hours Ca^{2+} supplementation on pLECs.

Through these culture conditions, morphology of the cells became heterogeneous, and they lost their homogeneous cobblestone morphology and increased their size, which indicated a triggered differentiation (**Figure 6**). The same morphological changes were observed after supplementation with 0.9 mmol/L Ca^{2+} , in murine corneal epithelial cells (Ma and Liu et al., 2011).

5.2 Increased expression of transcription factor PAX6 and differentiation marker DSG1 using Ca^{2+} supplementation and siRNA-based cell model

Both limbal and conjunctival epithelium express desmoglein 1, which is considered as differentiation marker (Rubelowski et al., 2020; Shi et al., 2020). DSG1 mRNA and protein expression increased in the siRNA-based cell model in combination with Ca^{2+} supplementation. Nevertheless, DSG1 was not detectable in pLECs (without the use of siRNA) (Rubelowski et al., 2020). Using Ca^{2+} supplementation,

the enhanced DSG1 expression at mRNA and protein level approved that Ca^{2+} supplementation could result in differentiation in pLECs. Therefore, Ca^{2+} supplementation is appropriate for studying the corneal epithelial differentiation process.

Our current study demonstrates upregulated PAX6 mRNA expression in Ca^{2+} supplemented, differentiated pLECs and downregulated PAX6 mRNA expression using the siRNA-based cell model. These profound changes were also detected at protein level (**Figure 7a, c, e**). Similarly, in previous studies a more pronounced PAX6 protein expression was detected in corneal epithelial cells, than in limbal epithelial cells, which supports the theory, that there is correlation between PAX6 gene expression and the differentiation process of the corneal epithelial cells (Kitazawa et al., 2019; Sivak et al., 2000; Li and Eccles, 2012). According to our expression data, PAX6 and DSG1 were both significantly upregulated in differentiated pLECs (Ca^{2+} supplemented pLECs) at protein level and were strongly reduced adding PAX6 knockdown (siRNA-based cell model) in each single pLECs preparation (**Figure 7**), which proves the siRNA-based aniridia cell model with Ca^{2+} supplementation an efficient tool to study aniridia epithelial phenotype.

Some previous studies showed, that DSG1 is required for differentiation of keratinocytes through suppression of signaling mechanisms, which trigger proliferation (Harmon et al., 2013; Getsios et al., 2009). In addition, an *in vivo* analysis in mouse already proved that DSG1 is important for corneal cell adhesion (Davis et al., 2003). We hypothesize that reduced DSG1 expression level could trigger proliferation, instead of differentiation in limbal epithelial cells and reduces their adhesion in parallel, which might lead to AAK, together with other factors/ mechanism.

5.3 Expression analysis of RA signaling components using Ca^{2+} supplementation and siRNA-based cell model

In prior mRNA sequencing of limbal and conjunctival epithelial cells of aniridia patients, deregulated RA signaling components have been identified (Latta et al., 2021) and in a previous study based on aniridia patients' limbal epithelial cells, there was decreased mRNA expression of RA signaling components ADH7 and ALDH1A1, which belong to the family of metabolizing enzymes, involved in retinol and retinaldehyde oxidation, respectively (Napoli et al., 2017; Duester, 2009). These markers are also considered as corneal differentiation markers (Rubelowski et al., 2020; Shi et al., 2020) and their expression decreased in the siRNA-based cell model and in aniridic patients (Latta et al., 2019). However, there was no correlation between ADH7 and ALDH1A1 mRNA and protein expression either in aniridia LECs or in the siRNA-based cell model, as the expression of these markers remained at a low level (Latta et al., 2019).

Using Ca^{2+} supplementation, the ADH7 and ALDH1A1 mRNA expression was significantly increased, parallel to an elevated PAX6 mRNA level. Both ADH7 and ALDH1A1 mRNA expression were reduced

in differentiated cells after siRNA treatment, showing an aniridic limbal cell phenotype (**Figure 8**). Although ALDH3A1 mRNA expression did not show clear expression changes under PAX6 knockdown, its expression tended to reduce in differentiated cells. This minor expression change in ALDH3A1 expression may be related to a very poor ALDH3A1 expression in LECs. ADH7 protein expression did not change, but ALDH1A1 protein tended to be upregulated after Ca²⁺ supplementation, referring to mildly triggered differentiation, without PAX6 knockdown. However, it was not downregulated after PAX6 knockdown under both growth conditions. It seems that ALDH1A1 is involved in the corneal epithelial differentiation process, but it is not directly regulated by PAX6. Since retinoic acid is important for corneal cell homeostasis (Kumar et al., 2017; Sommer, 1983), reduced expression of these markers could lead to a reduced amount of retinoic acid in cells, which might disturb the differentiation process and homeostasis of the corneal epithelium and could contribute to progression of AAK.

ADH7 and ALDH1A1 markers were significantly reduced in normal primary limbal epithelial cells after PAX6 knockdown in a previous study (Latta et al 2019). In the current study, these markers were only downregulated in calcium treated, differentiated cells. For these differences between both studies, the different statistical methods may be responsible. In the current study, we performed one-way ANOVA followed by Bonferroni test for multiple comparison, while in the previous study Wilcoxon signed ranked test was used to check the significant difference between the groups. Nevertheless, the fold changes were in the same range in the previous (Latta et al. 2019) and in the present study for ADH7 and ALDH1A1 mRNA expression. In addition, broader genetic variations between human cells and variability in siRNA treatment may also be responsible.

Cellular binding proteins RBP1, CRABP2 and FABP5 play an important role in uptake, metabolism and transportation of retinoic acid (Napoli et al., 2017). RBP1 and CRABP2 expression were upregulated in aniridia patients' conjunctival epithelium, but RBP1 was not detected and CRABP2 was downregulated during limbal cell screening (Latta et al., 2019; 2020). In our primary aniridia cell model, these transcripts were downregulated at mRNA level (**Figure 9**), which is apposite to screening results of the conjunctival epithelium. mRNA expression of both transcripts was significantly upregulated after Ca²⁺ treatment, but through additional PAX6 knockdown, these were downregulated similarly to normal pLECs (**Figure 9a, b**). These results support our hypothesis and refer to a more differentiated status of pLECs, but does not resemble to screening results, so we did not perform protein expression analysis.

FABP5 is involved in regulation of biological processes like differentiation, proliferation, migration and in apoptosis in various tissues (Ju et al., 2018; Arai et al., 2005; Ohata et al., 2017). FABP5 was strongly downregulated at mRNA level in patients' aniridic limbal and conjunctival cells (Latta et al., 2019; 2020)

and in aniridia primary cell model, as well as using Ca^{2+} supplementation and siRNA-based cell model (**Figure 9c**). FABP5 has shown the same strong expression changes at protein level, in western blot analysis of pLECs (**Figure 9d, e**). FABP5 is also involved in differentiation of keratinocytes (Siegenthaler et al., 1994; Ogawa et al., 2011) and in cell migration (Ju et al., 2018). Another member of the FABP family, the FABP7 has been proven as a downstream gene of PAX6 (Arai et al., 2005). A previous study described triggered differentiation of keratinocytes, following Ca^{2+} treatment which increased FABP protein expression 2-fold (Ogawa et al., 2011). These findings, in addition to our present results reveal a strong correlation between PAX6 and FABP5 expression. FABP5 could be a potential target for future studies, as a gene which may be directly regulated by PAX6 and may also be responsible for the alteration of differentiation processes.

Reduced expression of FABP5 in limbal epithelial cells could reduce the differentiation process of these cells into transient amplifying cells and may cause deficiency of these cells. In parallel, the reduced FABP5 expression could decrease the centripetal migration of the transient amplifying cells to differentiated corneal epithelial cells, which is necessary to maintain the corneal epithelium (Ju et al., 2018; Arai et al., 2005; Ohata et al., 2017). A combination of these effects may lead to a thin and fragile corneal epithelium, which is one of the symptoms of ARK.

STRA6 is a membrane receptor, which mediates cellular uptake of vitamin A (Noy, 2016; Chen et al., 2016). STRA6 mRNA expression remained unchanged after PAX6 knockdown and it was downregulated using Ca^{2+} supplementation and siRNA-based cell model (in differentiated cells). This indicates a disturbed endogenous RA signaling instead of disturbed cellular retinol uptake in the used model.

CYP1B1, a member of the cytochrome p450 family has been proposed as a retinoic acid synthesis component (Chambers et al., 2007). Its mRNA expression decreased using Ca^{2+} supplementation and siRNA-based cell model. We speculate that after Ca^{2+} supplementation, there were more differentiated cells, which were able to produce enough RA and therefore, CYP1B1 mRNA expression decreased by unknown regulatory mechanisms to balance the retinoic acid homeostasis, in the cells.

A previous study suggested that upregulated PPARG and VEGFA are involved in tissue neovascularization process (Forootan et al., 2016). We also found upregulated PPARG and VEGFA mRNA expression in our transcriptional data from limbal and conjunctival cells of aniridia patients (Latta et al., 2021). To further characterize the FABP5-PPARG-VEGF signaling pathway (Forootan et al., 2016), which could regulate the corneal neovascularisation, in case of aniridia related keratopathy, we analysed the effect of Ca^{2+} supplementation on the angiogenic factor VEGFA and on PPARG expression level. Surprisingly, both VEGFA and PPARG mRNA expression were downregulated,

which indicates that these genes are not directly controlled by PAX6, but may be affected by AAK secondarily.

5.4 Expression analysis of other putative markers using Ca²⁺ supplementation and siRNA-based cell model

Notably, in our expression study some gene expressions remained unchanged after Ca²⁺ supplementation. ELOVL7 (Fatty Acid Elongase 7) is a lipogenic enzyme, which is required for long chain fatty acid synthesis (Shi et al., 2019). In screening of conjunctival and limbal epithelial cells of aniridia patients, it was upregulated. We speculated, that upregulation of this marker could increase synthesis of retinoic acid, and the increased retinoic acid concentration may inhibit amplification of transient amplifying cells, thus affecting corneal epithelial maintenance. Nevertheless, ELOVL7 mRNA expression did not change under differentiation triggering growth conditions or following siRNA treatment in the present study.

RDH10 is a retinol dehydrogenase, which converts all-trans-retinol into all-trans-retinal and plays a critical role in synthesis of embryonic retinoic acid (Farjo et al., 2011). Its mRNA expression was upregulated in aniridic patient conjunctival epithelial cells (Latta et al., 2020). However, in limbal epithelial cells, its expression remained unchanged (mRNA sequencing). After Ca²⁺ supplementation, its mRNA expression also remained unchanged and only tended to decrease upon additional PAX6 knockdown. So we speculate that the expression of this transcript is very stable in pLECs and it is not directly regulated by PAX6.

Studies showed that both RDH10 and ELOVL7 are important for fatty acid synthesis and both are linked to fatty acid signaling. But our experiments showed that these genes may not directly contribute to the corneal epithelial differentiation processes and these genes might be regulated by other mechanisms, apart PAX6.

SPINK7 is a kallikrein protease inhibitor, which also cleaves DSG1 (Borgono et al., 2007). RNA sequencing results of patients and the siRNA-based cell model showed a strong reduction in its expression, which indicate its PAX6 dependency (Latta et al., 2019). We investigated SPINK7 expression in order to find out, whether there is a correlation between an altered SPINK7 expression and a disturbed corneal epithelial differentiation process. Its expression remained unchanged following Ca²⁺ supplementation alone, but its mRNA expression decreased upon PAX6 knockdown in both undifferentiated and differentiated cells. Therefore, this gene is not directly modulated by PAX6, but by other mechanisms also.

5.5 Human telomerase-immortalized limbal epithelial stem cells (T-LSCs) and genome edited T-LSCs (T-LSCs PAX6 +/-)

We investigated the master regulatory gene PAX6, the junction protein/differentiation marker DSG1 and the cellular binding protein FABP5 also in the PAX6^{+/-} T-LSCs cell model, to compare that to the siRNA-based cell model (both without and with Ca²⁺ supplementation). For both aniridia cell models the same culture conditions have been used.

FABP5 and DSG1 mRNA expression was strongly downregulated in PAX6^{+/-} T-LSCs and the same effect was visible at protein level for FABP5. However, under the same conditions, DSG1 protein expression was not detectable. Downregulation of FABP5 mRNA expression was similar to the siRNA-based cell model, with or with our Ca²⁺ supplementation. The same effect was only visible at protein level in the siRNA-based cell model, using Ca²⁺ supplementation (**Figure 9d**). After 24 hours of Ca²⁺ supplementation, there was no PAX6 upregulation in wild type or mutated cells, and it happened similar for FABP5 protein expression (**Figure 12d, e**). In contrast, results obtained after 72 hours incubation (**Figure 13d, e**) showed a marked upregulation of PAX6 and FABP5 protein, in both wild type and mutated cells. Here we argue that 24 hours might not be enough to trigger differentiation and changes at protein level. PAX6 and DSG1 mRNA expression were downregulated in a similar manner after long incubation, instead of upregulation. This could be a compensatory mechanism to balance PAX6 and DSG1 protein expression.

Expression data from this cell model and from our previous siRNA aniridia cell model (**Figure 9d, e**) strongly indicate, that FABP5 expression is PAX6 dependent. This is also supported by literature data (Arai et al., 2005; Matsumata et al., 2012). However, we could not verify the correlation between DSG1 and PAX6 expression, since DSG1 is not detectable at protein level in the PAX6^{+/-} T-LSC cell line, not even after 72 hours of Ca²⁺ supplementation. PAX6 expression was also lower in PAX6^{+/-} T-LSCs cells in comparison to pLECs (**Figure 12f, 13f**). Thus, the PAX6^{+/-} T-LSCs cell line is not ideal for studying differentiation processes of the corneal epithelium at molecular bases, as it is difficult to clarify the relationship between mRNA and protein expression changes, since PAX6 and DSG1 markers are less expressed in PAX6^{+/-} T-LSCs cell model, than in pLECs at protein level.

Expression of putative markers was increased in our model, cells exhibited a differentiated phenotype and the relative expression level of differentiation markers compared to undifferentiated cells was high and we could get information about changes at protein level. While T-LSCs expressed less PAX6 and DSG1 in comparison to pLECs, DSG1 was not detectable at protein level even after long incubation with Ca²⁺ in case of T-LSCs.

CHAPTER 5:

CONCLUSIONS AND OUTLOOK TO THE FUTURE

We provide evidence that haploinsufficiency of the master regulatory gene PAX6 contributes to a differentiation defect in corneal epithelial cells and has a direct influence on LECs differentiation and RA signaling components. With the siRNA-based cell model with Ca^{2+} supplementation, as enhanced aniridia cell model, we could confirm our hypothesis and identified target genes, which might be directly regulated by PAX6. In short, these experimental data provide perspective for further studies to better understand the differentiation process in LECs and are able to explain the insufficient cell function in AAK. An idealistic model could be developed combining differentiation triggering growth condition and using the siRNA-based cell model, to track molecular changes leading to differentiation and to investigate the signaling cascade involved in this process.

The result strongly indicated that the siRNA-based cell model with Ca^{2+} supplementation is efficient and has many advantages to study the corneal epithelial differentiation process. Nevertheless, for some genes it was difficult to obtain the same significant results after PAX6 gene silencing, as in aniridia patient cells due to cell confluence or strong effect of Ca^{2+} or maybe both conditions. In addition, human cells exhibit genetic variations on a large scale in comparison to mice, which could also be an explanation for the variability of the results.

In summary, Ca^{2+} treatment can be combined with PAX6 siRNA treatment to mimic aniridia cellular behavior, observed in patients. This may be restricted to some of the chosen markers. Upon PAX6 knockdown, mRNA expression of differentiation marker DSG1 and RA component FABP5 decreases. The similar effect becomes apparent at protein level though differentiation triggering Ca^{2+} treatment in siRNA-based aniridia cell model.

In the future, the interaction between PAX6 and DSG1 or RA component FABP5 should be analyzed since expression of these markers is altered parallel to PAX6 expression changes. DSG1 and FABP5 might be regulated by PAX6, since PAX6 has an affinity to bind with other transcription factors through promotor region and modulate their expression. These genes could be directly regulated by PAX6 and may be responsible for the altered differentiation process of LECs.

CHAPTER 6:

REFERENCES

- Ahmad S (2012) Concise review: Limbal stem cell deficiency, dysfunction, and distress. *Stem Cells Transl Med.* 1: 110–115.
- Anderson TR, Hedlund E, Carpenter EM (2002) Differential Pax6 promoter activity and transcript expression during forebrain development. *Mech. Dev.* 114: 171–175.
- Asselineau D, Bernard BA, Bailly C, Darmon M (1989) Retinoic acid improves epidermal morphogenesis. *Dev Biol.* 133:322-35.
- Arai Y, Funatsu N, Numayama-Tsuruta K, Nomura T, Nakamura S, Osumi N (2005) Role of *Fabp7*, a downstream gene of Pax6, in the maintenance of neuroepithelial cells during early embryonic development of the rat cortex. *J Neurosci.* 25:9752-61.
- Azuma N, Nishina S, Yanagisawa H, Okuyama T, Yamada M (1996) PAX6 missense mutation in isolated foveal hypoplasia [letter]. *Nat. Genet.* 13, 141–142.
- Baulmann DC, Ohlmann A, Flügel-Koch C, Goswami S, Cvekl A, Tamm ER (2002) Pax6 heterozygous eyes show defects in chamber angle differentiation that are associated with a wide spectrum of other anterior eye segment abnormalities. *Dev.* 118:3-17.
- Borgono CA, Michael IP, Komatsu N, Jayakumar A, Kapadia R, Clayman GL, Sotiropoulou G, Diamandis EP (2007) A potential role for multiple tissue kallikrein serine proteases in epidermal desquamation. *J Biol Chem.* 282:3640-52.
- Bossenbroek NM, Sulahian TH, Ubels JL (1998) Expression of nuclear retinoic acid receptor and retinoid X receptor mRNA in the cornea and conjunctiva. *Curr Eye Res.* 17:462-9.
- Brown A, McKie M, van Heyningen V, Prosser J (1998) The human PAX6 mutation database. *Nucleic Acids Res.* 26:259-64.
- Bumcrot D, Manoharan M, Kotliansky V, Sah DWY (2006) RNAi therapeutics: a potential new class of pharmaceutical drugs, *Nat. Chem. Biol.* 2:711–719.
- Callaerts P, Halder G and Gehring WJ (1997) PAX-6 in development and evolution. *Annu Rev Neurosci.* 20: 483-532.
- Caplen NJ (2004) Gene therapy progress and prospects. Downregulating gene expression: the impact of RNA interference. *Gene Ther;* 11:1241–1248.
- Carriere C, Plaza S, Martin P, Quatannens B, Bailly M, Stehelin D, Saule S (1993) Characterization of quail Pax-6 (Pax-QNR) protein expressed in the neuroretina. *Mol Cell Biol.* 13: 7257–7266.

- Chaloin-Dufau C, Sun TT, Dhouailly D (1990) Appearance of the keratin pair K3/K12 during embryonic and adult corneal epithelial differentiation in the chick and in the rabbit. *Cell Differ Dev.* 32(2):97-108.
- Chambers D, Wilson L, Maden M, Lumsden A (2007) RALDH-independent generation of retinoic acid during vertebrate embryogenesis by CYP1B1. *Development.* 134: 13 69-83.
- Chen Y, Clarke OB, Kim J, Stowe S, Kim YK, Assur Z, Cavalier M, Godoy-Ruiz R, von Alpen DC, Manzini C, Blaner WS, Frank J, Quadro L, Weber DJ, Shapiro L, Hendrickson WA, Mancina F (2016) Structure of the STRA6 receptor for retinol uptake. *Science.* 353: aad8266.
- Chen SY, Hayashida Y, Chen MY, Xie HT, Tseng SC (2011) A new isolation method of human limbal progenitor cells by maintaining close association with their niche cells. *Tissue Eng Part C Methods.* 17:537-48.
- Clagett-Dame M, DeLuca HF (2002) The role of vitamin A in mammalian reproduction and embryonic development. *Annu Rev Nutr.* 22:347-81.
- Clinch TE, Goins KM, Cobo LM (1992) Treatment of contact lens-related ocular surface disorders with autologous conjunctival transplantation. *Ophthalmology.*99:634–638.
- Corden LD, Swensson O, Swensson B, Smith FJ, Rochels R, Uitto J, McLEAN WH (2000) Molecular genetics of Meesmann's corneal dystrophy: ancestral and novel mutations in keratin 12 (K12) and complete sequence of the human KRT12 gene. *Exp Eye Res.* 70:41-9.
- Collinson JM, Chanas SA, Hill RE, West JD (2004) Corneal development, limbal stem cell function, and corneal epithelial cell migration in the Pax6 (+/-) mouse. *Invest Ophthalmol Vis Sci.* 45:1101-8.
- Davis JA, Reed RR (1996) Role of Olf-1 and Pax-6 transcription factors in neurodevelopment. *J Neurosci.* 16(16):5082-94.
- Davis J, Duncan MK, Robison WG Jr, Piatigorsky J (2003) Requirement for Pax6 in corneal morphogenesis: a role in adhesion. *J Cell Sci.*116:2157-67.
- Davanger M, Evensen A (1971) Role of the pericorneal papillary structure in renewal of corneal epithelium *Nature.* 229:560-1.
- de Fougères A, Vornlocher HP, Maraganore J, Lieberman J (2007) Interfering with disease: a progress report on siRNA-based therapeutics. *Nat. Rev. Drug Discov.* 6: 443– 453.
- DelMonte DW, Kim T (2011) Anatomy and physiology of the cornea *J Cataract Refract Surg.* 37:588-98.
- Desvergne B, Wahli W (1999) Peroxisome proliferator-activated receptors: nuclear control of metabolism. *Endocr Rev.* 20:649-88.
- D'Souza SJ, Pajak A, Balazsi K, Dagnino L (2001) Ca²⁺ and bmp-6 signaling regulate e2f during epidermal keratinocyte differentiation. *J Biol Chem.* 276:23531-8.
- Dua HS, Saini JS, Azuara-Blanco A, Gupta P (2000) Limbal stem cell deficiency: concept, aetiology, clinical presentation, diagnosis and management. *Ind J Ophthalmol.* 48:83–92.

- Dua HS, Shanmuganathan VA, Powell-Richards AO, Tighe PJ, Joseph A (2005) Limbal epithelial crypts: a novel anatomical structure and a putative limbal stem cell niche. *Br J Ophthalmol.* 89:529-32.
- Duester G (2009) Retinoic acid synthesis and signaling during early organogenesis. *Cell.* 134: 921-31.
- Dykxhoorn DM, Lieberman J (2005) The silent revolution: RNA interference as basic biology, research tool, and therapeutic, *Annu. Rev. Med.* 56: 401–423.
- Ehlers N, Heegaard S, Hjortdal J, Ivarsen A, Nielsen K, Prause JU (2010) Morphological evaluation of normal human corneal epithelium. *Acta Ophthalmol.* 88: 858-61.
- Elbashir SM, Harborth J, Lendeckel W, Yalcin A, Weber K, Tuschl T (2001) Duplexes of 21-nucleotide RNAs mediate RNA interference in cultured mammalian cells. *Nature.* 411:494-501.
- Epstein JA, Glaser T, Cai J, Jepeal L, Walton DS, Maas RL (1994) Two independent and interactive DNA-binding subdomains of the Pax6 paired domain are regulated by alternative splicing. *Genes Dev.* 8: 2022–2034.
- Espana EM, Grueterich M, Romano AC (2002) Idiopathic limbal stem cell deficiency. *Ophthalmology.* 109:2004–2010.
- Farjo KM, Moiseyev G, Nikolaeva O, Sandell LL, Trainor PA, Ma JX (2011) RDH10 is the primary enzyme responsible for the first step of embryonic Vitamin A metabolism and retinoic acid synthesis. *Dev Biol.* 357:347-55.
- Faye PA, Poumeaud F, Chazelas P, Duchesne M, Rassat M, Miressi F, Lia AS, Sturtz F, Robert PY, Favreau F, Benayoun Y (2021) Focus on cell therapy to treat corneal endothelial diseases. *Exp Eye Res.* 23:108462.
- Forootan FS, Forootan SS, Gou X, Yang J, Liu B, Chen D, Al Fayi MS, Al-Jameel W, Rudland PS, Hussain SA, Ke Y (2016) Fatty acid activated PPAR γ promotes tumorigenicity of prostate cancer cells by up regulating VEGF via PPAR responsive elements of the promoter. *Oncotarget.* 7:9322-39.
- Freeman WM, Walker SJ, Varana KE (1999) Quantitative RT-PCR: pitfalls and potential. *Bio techniques.* 26:112-22, 124-5.
- Gehring WJ (1996) The master control gene for morphogenesis and evolution of the eye. *Genes Cells.* 1(1):11-5.
- Getsios S, Simpson CL, Kojima S, Harmon R, Sheu LJ, Dusek RL, Cornwell M, Green KJ (2009) Desmoglein 1-dependent suppression of EGFR signaling promotes epidermal differentiation and morphogenesis. *J Cell Biol.* 2009 Jun 29;185(7):1243-58.
- Ghyselinck NB, Duester G (2019) Retinoic acid signaling pathways. *Development.* 146: 167502.
- Glaser T, Walton DS, Maas RL (1992) Genomic structure, evolutionary conservation and aniridia mutations in the human PAX6 gene. *Nat Genet.* 2: 232–239.

- Glaser T, Jepeal L, Edwards JG, Young SR, Favor J, Maas RL (1994) PAX6 gene dosage effect in a family with congenital cataracts, aniridia, anophthalmia and central nervous system defects. *Nat Genet.* 7:463-71.
- Gonzalez S, Deng SX (2013) Presence of native limbal stromal cells increases the expansion efficiency of limbal stem/progenitor cells in culture. *Exp Eye Res.* 116:169-76.
- Gorlov IP, Saunders GF (2002) A method for isolating alternatively spliced isoforms: isolation of murine Pax6 isoforms. *Anal Biochem.* 308: 401–404.
- Grant WM, Walton DS (1974) Progressive changes in the angle in congenital aniridia, with development of glaucoma. *Trans Am Ophthalmol Soc.*72:207-28.
- Grindley JC, Davidson DR, Hill RE (1995) The role of Pax-6 in eye and nasal development. *Development.*121:1433-42.
- Haagdoorens M, Van Acker SI, Van Gerwen V, Ní Dhubhghaill S, Koppen C, Tassignon MJ, Zakaria N (2016) Limbal Stem Cell Deficiency: Current Treatment Options and Emerging Therapies. *Stem Cells Int.*2016:9798374.
- Hannon, GJ, Rossi JJ (2004) Unlocking the potential of the human genome with RNA interference. *Nature* 431: 371–378.
- Hall HN, Williamson KA, FitzPatrick DR (2019) The genetic architecture of aniridia and Gillespie syndrome. *Hum Genet.*138:881-898.
- Han H (2018) RNA Interference to Knock Down Gene Expression. *Methods Mol Biol.* 1706: 293–302.
- Hanna C, Bicknell DS, O'Brien JE (1961) Cell turnover in the adult human eye. *Arch Ophthalmol.* 65:695-8.
- Harmon RM, Simpson CL, Johnson JL, Koetsier JL, Dubash AD, Najor NA, Sarig O, Sprecher E, Green KJ (2013) Desmoglein-1/Erbin interaction suppresses ERK activation to support epidermal differentiation. *J Clin Invest.*123:1556-70.
- Hill RE, Favor J, Hogan BL, Ton CC, Saunders GF, Hanson IM, Prosser J, Jordan T, Hastie ND, van Heyningen V (1991) Mouse small eye results from mutations in a paired-like homeobox containing gene. *Nature.* 354: 522-525.
- Hiraki A, Shirasuna K, Ikari T, Shinohara M, Garrod DR (2002) Calcium induces differentiation of primary human salivary acinar cells. *J Cell Physiol.* 193:55-63.
- Hogan B L, Horsburgh G, Cohen J, Hetherington CM, Fisher G, Lyon MF (1986) Small eyes (Sey): a homozygous lethal mutation on chromosome 2 which affects the differentiation of both lens and nasal placodes in the mouse. *J Embryol Exp Morphol.* 97: 95-110.
- Huang SK, Xiao HQ, Kleine-Tebbe J, Paciotti G, Marsh DG, Lichtenstein LM, Liu MC (1995a) IL-13 expression at the sites of allergen challenge in patients with asthma. *J Immun.* 155: 2688-2694.

- Huang SK, Yi M, Palmer E, Marsh DG (1995b) A dominant T cell receptor beta-chain in response to a short ragweed allergen, Amb a 5. *J Immunol.* 154:6157-62.
- Ihnatko R, Eden U, Fagerholm P, Lagali N (2016) Congenital aniridia and the ocular surface. *Ocul Surf.* 14:196-206.
- Irvine AD, Corden LD, Swensson O, Swensson B, Moore JE, Frazer DG, Smith FJ, Knowlton RG, Christophers E, Rochels R, Uitto J, McLean WH (1997) Mutations in cornea-specific keratin K3 or K12 genes cause Meesmann's corneal dystrophy. *Nat Genet.* 16:184-7.
- Johnson JL, Koetsier JL, Sirico A, Agidi AT, Antonini D, Missero C, Green KJ (2014) The desmosomal protein desmoglein 1 aids recovery of epidermal differentiation after acute UV light exposure. *J Invest Dermatol.* 134:2154-2162.
- Ju J, Wang N, Wang J, Wu F, Ge J, Chen F (2018) 4- Amino-2-trifluoromethyl-phenylretinate inhibits proliferation, invasion, and migration of breast cancer cells by independently regulating CRABP2 and FABP5. *Drug Des Devel Ther.* 12:997-1008.
- Käsmann-Kellner B, Latta L, Fries FN, Viestenz A, Seitz B (2018) Diagnostic impact of anterior segment angiography of limbal stem cell insufficiency in PAX6-related aniridia. *Clin Anat.* 31: 392-397.
- Kawakita T, Espana EM, He H, Yeh LK, Liu CY, Tseng SC (2004) Calcium-induced abnormal epidermal-like differentiation in cultures of mouse corneal-limbal epithelial cells. *Invest Ophthalmol Vis Sci.* 45:3507-12.
- Kelly M, von Lintig J (2015) STRA6: role in cellular retinol uptake and efflux. *Hepatobiliary Surg Nutr.* 4(4):229-42.
- Kim J, Lauderdale JD (2006) Analysis of Pax6 expression using a BAC transgene reveals the presence of a paired-less isoform of Pax6 in the eye and olfactory bulb. *Dev Biol.* 292: 486-505.
- Kim SW, Seo KY, Rhim T, Kim EK (2012) Effect of retinoic acid on epithelial differentiation and mucin expression in primary human corneal limbal epithelial cells. *Curr Eye Res.* 37: 33-42.
- Kitazawa K, Hikichi T, Nakamura T, Sotozono C, Kinoshita S, Masui S (2016) PAX6 regulates human corneal epithelium cell identity. *Exp Eye Res.* 154:30-38
- Koroma, BM, Yang JM, Sundin OH (1997) The Pax-6 homeobox gene is expressed throughout the corneal and conjunctival epithelia. *Invest. Invest Ophthalmol Vis Sci.* 38:108-20.
- Kruse FE, Tseng SC (1994) Retinoic acid regulates clonal growth and differentiation of cultured limbal and peripheral corneal epithelium. *Invest Ophthalmol Vis Sci.* 35:2405-20.
- Kleinjan DA, Seawright A, Elgar G, van Heyningen V (2002) Characterization of a novel gene adjacent to PAX6, revealing synteny conservation with functional significance. *Mamm Genome.* 13: 102–107.

- Kulkarni BB, Tighe PJ, Mohammed I, Yeung AM, Powe DG, Hopkinson A, Shanmuganathan VA, Dua HS (2010) Comparative transcriptional profiling of the limbal epithelial crypt demonstrates its putative stem cell niche characteristics. *BMC Genomics*. 11:526.
- Lagali N, Edén U, Utheim TP, Chen X, Riise R, Dellby A, Fagerholm P (2013) In vivo morphology of the limbal palisades of vogt correlates with progressive stem cell deficiency in aniridia-related keratopathy. *Invest Ophthalmol Vis Sci*. 54: 5333–5342.
- Landsend ES, Utheim ØA, Pedersen HR, Lagali N, Baraas RC, Utheim TP (2018) The genetics of congenital aniridia-a guide for the ophthalmologist. *Surv Ophthalmol*. 63: 105-113.
- Latta L, Nordström K, Stachon T, Langenbacher A, Fries FN, Szentmáry N, Seitz B, Käsmann-Kellner B (2019) Expression of retinoic acid signaling components ADH7 and ALDH1A1 is reduced in aniridia limbal epithelial cells and a siRNA primary cell based aniridia model. *Exp Eye Res*. 179:8-17.
- Latta L, Ludwig N, Krammes L, Stachon T, Fries FN, Mukwaya A, Szentmáry N, Seitz B, Wowra B, Kahraman M, Keller A, Meese E, Lagali N, Käsmann-Kellner (2020) Abnormal neovascular and proliferative conjunctival phenotype in limbal stem cell deficiency is associated with altered microRNA and gene expression modulated by PAX6 mutational status in congenital aniridia. *Ocul Surf*16: 1542-0124.
- Latta L, Viestenz A, Stachon T, Colanesi S, Szentmáry N, Seitz B, Käsmann-Kellner (2018) Human aniridia limbal epithelial cells lack expression of keratins K3 and K12. *Exp Eye Res*. 167:100-109.
- Lavker RM, Tseng SCG, Sun TT (2004) Corneal epithelial stem cells at the limbus: looking at some old problems from a new angle. *Exp Eye Res*. 78:433-46.
- Le Q, Deng SX, Xu J (2013) In vivo confocal microscopy of congenital aniridia-associated keratopathy. *Eye*. 27: 763–766.
- Lee DD, Stojadinovic O, Krzyzanowska A, Vouthounis C, Blumenberg M, Tomic-Canic M (2009) Retinoid-responsive transcriptional changes in epidermal keratinocytes. *J Cell Physiol*. 220:427-439.
- Lee H, Khan R, O'Keefe M (2008) Aniridia: current pathology and management. *Acta Ophthalmol*. 86:708-15.
- Li G, Xu F, Zhu J, Krawczyk M, Zhang Y, Yuan J, Patel S, Wang Y, Lin Y, Zhang M, Cai H, Chen D, Zhang M, Cao G, Yeh E, Lin D, Su Q, Li W-w, Sen G L, Afshari N, Chen S, Maas RL FuX-D, Zhang K, Liu Y, Ouyang H (2015) Transcription factor PAX6 (Paired Box 6) controls limbal stem cell lineage in development and disease. *J Biol Chem*. 290:20448-54.
- Lima Cunha D, Arno G, Corton M, Moosajee M (2019) The spectrum of PAX6 mutations and genotype-phenotype correlations in the eye. *Genes (Basel)*. 10:1050.
- Li T, Lu L (2005) Epidermal growth factor-induced proliferation requires down-regulation of Pax6 in corneal epithelial cells. *J Biol Chem*. 280:12988-95.

- Lichtinger A, Pe'er J, Frucht-Pery J (2010) Limbal stem cell deficiency after topical mitomycin C therapy for primary acquired melanosis with atypia. *Ophthalmology*. 117: 431–437.
- Li W, Chen YT, Hayashida Y, Blanco G, Kheirkah A, He H, Chen SY, Liu CY, Tseng SC (2008) Down-regulation of Pax6 is associated with abnormal differentiation of corneal epithelial cells in severe ocular surface diseases. *J Pathol*. 214:114-22.
- Love MI, Huber W, Anders S (2014) Moderated estimation of fold change and dispersion for RNA-seq data with DESeq2. *Genome Biol*.15:550.
- Mangelsdorf DJ (1994) Vitamin A receptors. *Nutr Rev*. 52 (2 Pt 2): S32-44.
- Martin P, Carriere C, Dozier C, Quatannens B, Mirabel MA, Vandenbunder B, Stehelin D, Saule S (1992) Characterization of a paired box- and homeobox-containing quail gene (Pax-QNR) expressed in the neuroretina. *Oncogene*.7(9):1721-8.
- Matsumata M, Sakayori N, Maekawa M, Owada Y, Yoshikawa T, Osumi N (2012) The effects of Fabp7 and Fabp5 on postnatal hippocampal neurogenesis in the mouse. *Stem Cells*. 30:1532-43.
- Matsuo T, Osumi-Yamashita N, Noji S, Ohuchi H, Koyama E, Myokai F, Matsuo N, Taniguchi S, Doi H, Iseki S (1993) A mutation in the Pax-6 gene in rat small eye is associated with impaired migration of midbrain crest cells. *Nat Genet*. 3:299-304.
- Matranga C, Tomari Y, Shin C, Bartel DP, Zamore PD (2005) Passenger-strand cleavage facilitates assembly of siRNA into Ago2-containing RNAi enzyme complexes. *Cell*. Nov 18;123(4):607-20.
- Ma XL, Liu HQ (2011) Effect of calcium on the proliferation and differentiation of murine corneal epithelial cells in vitro. *Int J Ophthalmol*.4:247-9.
- Michalik L, Wahli W (2007) Guiding ligands to nuclear receptors. *Cell*. 129:649-51.
- Minhyung L (2009) Gene regulation for effective gene therapy. *Advanced Drug Delivery Reviews*. 61: 487-488.
- Mishra R, Gorlov IP, Chao LY, Singh S, Saunders GF (2002) PAX6, paired domain influences sequence recognition by the homeodomain. *J Biol Chem*. 277: 49488–49494.
- Mocellin S, Provenzano MJ (2004) RNA interference: learning gene knock-down from cell physiology. *J Transl Med*. 2:39.
- Napoli JL (2017) Cellular retinoid binding-proteins, CRBP, CRABP, FABP5: Effects on retinoid metabolism, function and related diseases. *Pharmacol Ther*. 173:19-33.
- Nakatsu MN, Ding Z, Ng MY, Truong TT, Yu F, Deng SX (2011) Wnt/ β catenin signaling regulates proliferation of human cornea epithelial stem/progenitor cells. *Invest Ophthalmol Vis Sci*. 52:4734-41.
- Nelson LB, Spaeth GL, Nowinski TS, Margo CE, Jackson L (1984) Aniridia A review. *Surv Ophthalmol*. 28:621-42.

- Nishida K, Kinoshita S, Ohashi Y, Kuwayama Y, Yamamoto S (1995) Ocular surface abnormalities in aniridia. *Am J Ophthalmol.* 120: 368–375.
- Notara M, Alatzas A, Gilfillan J (2010) In sickness and in health: corneal epithelial stem cell biology, pathology and therapy. *Exp Eye Res.* 90:188-95.
- Notara M, Lentzsch A, Coroneo M, Cursiefen C (2018) The role of limbal epithelial stem cells in regulating corneal (lymph) angiogenic privilege and the microenvironment of the limbal niche following UV Exposure. *Stem Cells Int.* 2018:8620172.
- Noy N (2016) Vitamin A transport and cell signaling by the retinol-binding protein receptor STRA6. *Subcell Biochem.* 81: 77-93.
- Ohata T, Yokoo H, Kamiyama T, Fukai M, Aiyama T, Hatanaka Y, Hatanaka K, Wakayama K, Orimo T, Kakisaka T, Kobayashi N, Matsuno Y, Taketomi A (2017) Fatty acid-binding protein 5 function in hepatocellular carcinoma through induction of epithelial–mesenchymal transition. *Cancer Med.* 6:1049-1061.
- Ogawa E, Owada Y, Ikawa S, Adachi Y, Egawa T, Nemoto K, Suzuki K, Hishinuma T, Kawashima H, Kondo H, Muto M, Aiba S, Okuyama R (2011) Epidermal FABP (FABP5) regulates keratinocyte differentiation by 13(S)-HODE-mediated activation of the NF-κB signaling pathway. *J Invest Dermatol.* 131:604 -12.
- Ouyang H, Xue Y, Lin Y, Zhang X, Xi L, Patel S, Cai H, Luo J, Zhang M, Zhang M, Yang Y, Li G, Li H, Jiang W, Yeh E, Lin J, Pei M, Zhu J, Cao G, Zhang L, Yu B, Chen S, Fu X-D, Liu Y, Zhang K (2014) WNT7A and PAX6 define corneal epithelium homeostasis and pathogenesis. *Nature.* 511:358-61.
- Pinson J, Simpson TI, Mason JO, Price DJ (2006) Positive autoregulation of the transcription factor Pax6 in response to increased levels of either of its major isoforms, Pax6 or Pax6(5a), in cultured cells. *BMC Dev Biol.* 25: 25.
- Plaza S, Saule S, Dozier C (1999) High conservation of cis-regulatory elements between quail and human for the Pax-6 gene. *Dev Genes Evol.* 209: 165–173.
- Prosser J, van Heyningen V (1998) PAX6 mutations reviewed. *Hum Mutat.* 11:93-108.
- Puangsricharern V, Tseng SC (1995) Cytologic evidence of corneal diseases with limbal stem cell deficiency. *Ophthalmology.* 102:1476–1485.
- Quinn JC, West JD, Hill RE (1996) Multiple functions for Pax6 in mouse eye and nasal development. *Genes Dev.* 10:435-46.
- Rhinn M, Dollé P (2012) Retinoic acid signalling during development. *Development.* 139: 43-58.
- Ramaesh T, Collinson JM, Ramaesh K, Kaufman MH, West JD, Dhillon B (2003) Corneal abnormalities in Pax6^{+/-} small eye mice mimic human aniridia-related keratopathy. *Invest Ophthalmol Vis Sci.* 44:1871-8.

- Ramaesh K, Ramaesh T, Dutton GN, Dhillon B (2005a) Evolving concepts on the pathogenic mechanisms of aniridia related keratopathy. *Int J Biochem Cell Biol.* 37: 547-57.
- Rand TA, Ginalski K, Grishin NV, Wang X (2004) Biochemical identification of Argonaute 2 as the sole protein required for RNA-induced silencing complex activity. *Proc Natl Acad Sci U S A.* Oct 5;101(40):14385-9.
- Ross M (2019) Aniridia. <https://emedicine.medscape.com/article/1208379-overview>.
- Rubelowski AK, Latta L, Katiyar P, Stachon T, Käsman-Kellner B, Seitz B, Szentmáry N (2020) HCE-T cell line lacks cornea-specific differentiation markers compared to primary limbal epithelial cells and differentiated corneal epithelium. *Graefes Arch Clin Exp Ophthalmol.* 258:565-575.
- Samarawickrama C, Chew S, Watson S (2015) Retinoic acid and the ocular surface. *Surv Ophthalmol.* 60:183-95.
- Schlötzer-Schrehardt U, Kruse FE (2005) Identification and characterization of limbal stem cells. *Exp Eye Res.* 81:247-64.
- Schug TT, Berry DC, Shaw NS, Travis SN, Noy N (2007) Opposing effects of retinoic acid on cell growth result from alternate activation of two different nuclear receptors. *Cell.* 129:723-33.
- Schug TT, Berry DC, Toshkov IA, Cheng L, Nikitin AY, Noy N (2008) Overcoming retinoic acid-resistance of mammary carcinomas by diverting retinoic acid from PPARbeta/delta to RAR. *Proc Natl Acad Sci U S A.* 105(21):7546-51.
- Siegenthaler G, Tomatis I, Chatellard-Gruaz D, Jaconi S, Eriksson U, Saurat JH (1992) Expression of CRABP-I and -II in human epidermal cells. Alteration of relative protein amounts is linked to the state of differentiation. *Biochem J.* 287:383-9.
- Siegenthaler G, Hotz R, Chatellard-Gruaz D, Didierjean L, Hellman U, Saurat J H (1994) Purification and characterization of the human epidermal fatty acid-binding protein: Localization during epidermal cell differentiation in vivo and in vitro. *Biochem J.* 302:363-71.
- Shi H, Wang L, Luo J, Liu J, Loo JJ, Liu H (2019) Fatty Acid Elongase 7 (ELOVL7) plays a role in the synthesis of long-chain unsaturated fatty acids in goat mammary epithelial cells. *Animals (Basel).* 9:389.
- Shi L, Stachon T, Käsman-Kellner B, Seitz B, Szentmáry N, Latta L (2020) Keratin 12 mRNA expression could serve as an early corneal marker for limbal explant cultures. *Cytotechnology.* 72:239-245.
- Shortt AJ, Secker GA, Munro PM, Khaw PT, Tuft SJ, Daniels JT (2007) Characterization of the limbal epithelial stem cell niche: Novel imaging techniques permit in vivo observation and targeted biopsy of limbal epithelial stem cells. *Stem Cells.* 25:1402–1409.
- Secker GA, Daniels UT (2008) Limbal epithelial stem cells of the cornea. *StemBook.* PMID:20614614.

- Singh S, Mishra R, Arango NA, Deng JM, Behringer RR, Saunders GF (2002) Iris hypoplasia in mice that lack the alternatively spliced Pax6(5a) isoform. *Proc Natl Acad Sci U S A.* 99:6812-5.
- Singer VL, Lawlor TE, Yue S (1999) Comparison of SYBR Green I nucleic acid gel stain mutagenicity and ethidium bromide mutagenicity in the Salmonella/mammalian microsome reverse mutation assay (Ames test)". *Mut Res.*439: 37–47.
- Sommer A (1983) Effects of vitamin A deficiency on the ocular surface. *Ophthalmology.* 90:592-600.
- Sommer A (1990) Xerophthalmia, keratomalacia and nutritional blindness. *Int Ophthalmol.*14 (3):195-9.
- Sotozono C, Ang LP, Koizumi N, Higashihara H, Ueta M, Inatomi T, Yokoi N, Kaido M, Dogru M, Shimazaki J, Tsubota K, Yamada M, Kinoshita S (2007) New grading system for the evaluation of chronic ocular manifestations in patients with Stevens-Johnson syndrome. *Ophthalmology.* 114:1294-302.
- Sridhar MS (2018) Anatomy of cornea and ocular surface. *Ind J Ophthalmol.*66: 190–194.
- Sun TT, Lavker RM (2004) Corneal epithelial stem cells: past, present, and future. *J Investig Dermatol Symp Proc.* 9:202-7.
- Terzic J, Saraga-Babic M (1999) Expression pattern of PAX3 and PAX6 genes during human embryogenesis. *Int J Dev Biol.* 43:501-8.
- Thatcher JE, Isoherranen N (2009) The role of CYP26 enzymes in retinoic acid clearance. *Expert Opin Drug Metab Toxicol.* 5:875-86.
- Ton CC, Hirvonen H, Miwa H, Weil MM, Monaghan P, Jordan T, van Heyningen V, Hastie ND, Meijers-Heijboer H, Drechsler M (1991) Positional cloning and characterization of a paired box- and homeobox-containing gene from the aniridia region. *Cell.* 67:1059-74.
- Ton CC, Miwa H, Saunders GF (1992) Small eye (Sey): cloning and characterization of the murine homolog of the human aniridia gene. *Genomics.* 13: 251–256.
- Townsend W M (1991) The limbal palisades of Vogt. *Trans Am Ophthalmol Soc.* 89:72 1-56.
- Tripathy K, Salini B (2020) Aniridia. In: *StatPearls [Internet].* Treasure Island (FL): StatPearls Publishing; 2020 Jan.
- Tseng SC (1989) Concept and application of limbal stem cells. *Eye (Lond).*3:141-57.
- Tzoulaki I, White IM, Hanson IM (2005) PAX6 mutations: genotype-phenotype correlations. *BMC Genet.* 6:27.
- Vilgelm AE, Chumakov SP, Prassolov VS (2006) RNA interference: biology and prospects of application in biomedicine and biotechnology. *Mol. Biol.* 40:339-354.
- Walther C, Gruss P (1991) Pax-6, a murine paired box gene, is expressed in the developing CNS. *Development.* 113: 1435–1449.

- Wittrup A, Liberman J (2015) Knocking down disease: a progress report on siRNA therapeutics. *Nat Rev Genet.* 16:543-52.
- Xia SL, Wu ML, Li H, Wang JH, Chen NN, Chen XY, Kong QY, Sun Z, Liu J (2015) CRABP-II- and FABP5-independent responsiveness of human glioblastoma cells to all-trans retinoic acid. *Oncotarget.* 6:5889-902.
- Xu PX, Zhang X, Heaney S, Yoon A, Michelson AM, Maas RL (1999) Regulation of Pax6 expression is conserved between mice and flies. *Development.* 126: 383–395.
- Xu ZP, Saunders GF (1997) Transcriptional regulation of the human PAX6 gene promoter. *J Biol Chem.* 272: 3430–3436.
- Yu S, Levi L, Siegel R, Noy N (2012) Retinoic acid induces neurogenesis by activating both retinoic acid receptors (RARs) and peroxisome proliferator-activated receptor β/δ (PPAR β/δ). *J Biol Chem.* 287:42195-205.
- Zhang W, Cveklova K, Oppermann B, Kantorow M, Cvekl A (2001) Quantitation of PAX6 and PAX6(5a) transcript levels in adult human lens, cornea, and monkey retina. *Mol. Vis.* 7: 1–5.
- Ziouzenkova O, Plutzky J (2008) Retinoid metabolism and nuclear receptor responses: New insights into coordinated regulation of the PPAR-RXR complex. *FEBS Lett.* 582:32-8.

ACKNOWLEDGEMENTS

It is a great pleasure to mention all people who contributed and assisted me directly and indirectly to complete my doctoral study.

First and foremost, I would like to express my highest, most sincere thanks to my supervisor **Prof. Dr. Nóra Szentmáry**, who gave me an opportunity to pursue my dissertation under her guidance. She was always ready for discussing my results and open to my ideas. Without her valuable advice, encouragement and moral support, it would not have been possible to complete the work. I am highly obliged for her support and critical amendments during the whole work, including my dissertation and manuscript preparation.

I express my sincere regards and respect to **Prof. Dr. Berthold Seitz** for allowing me to carry out my project work in his prestigious laboratory, constructive comments and fruitful suggestions regarding the manuscripts.

I would like to thank **Dr. Lorenz Latta** for teaching me scientific techniques, his valuable advice and scientific discussions.

I am deeply thankful to my colleague and co-author **Dr. Tanja Stachon** for her valuable advices, technical support and friendly behaviour. She was always ready for help and support during my entire research work.

I would like to acknowledge **Prof. Dr. Achim Langenbacher** for his help in statistical analysis of the experimental data.

I gratefully acknowledge the funding source, **HOMFOR** that made my thesis work possible.

I am also thankful to my sister **Dr. Rashmi Katiyar** and my friend **Dr. Shweta Suiwal** for her constant support during my research work and thesis writing.

At last, but not the least I am grateful to **Karin Schiestel-Stammwitz, Alfreda Zäch-Welsch** and **Claudia Bücklein** for their administrative support.

There is no such word to express my heartiest gratitude to **my parents, sister, brother-in-law, brother** and **friends** for being a source of inexhaustible encouragement and inspiration to build up my education, a warm thanks to all.

CURRICULUM VITAE

The curriculum vitae was removed from the electronic version of the doctoral thesis for reason of data protection.

LIST OF PUBLICATIONS

- Wal P, **Katiyar P**, Pandey R, Mehra R (2014) Oral insulin delivery system and recent advances in insulin delivery. *Ejbps* Volume 1, Issue 3, 242-255.
- Rubelowski AK, Latta L, **Katiyar P**, Stachon T, Käsmann-Kellner B, Seitz B, Szentmáry N (2020) HCE-T cell line lacks cornea-specific differentiation markers compared to primary limbal epithelial cells and differentiated corneal epithelium. *Graefes Arch Clin Exp Ophthalmol*; 258: 565-575.
- **Katiyar P**, Stachon T, Fries FN, Langenbacher A, Seitz B, Käsmann-Kellner B, Latta L, Szentmáry N (2021). FABP5 and DSG1 protein expression are PAX6 dependent or driven by PAX6 in limbal epithelial cells. *Exp Eye Res*, *under revision*.
- Latta L, Knebel I, Bleil C, Stachon T, **Katiyar P**, Zussy C, Fries FN, Käsmann-Kellner B, Seitz B, Szentmáry N (2021). Similarities in DSG1 and KRT3 downregulation through RA treatment and PAX6 knockdown: Does PAX6 affect RA signaling in limbal epithelial cells? *Biomolecules*, *under preparation*.



HCE-T cell line lacks cornea-specific differentiation markers compared to primary limbal epithelial cells and differentiated corneal epithelium

Anna-Klara Rubelowski¹ · Lorenz Latta¹ · Priya Katiyar¹ · Tanja Stachon¹ · Barbara Käsmann-Kellner¹ · Berthold Seitz¹ · Nóra Szentmáry^{1,2}

Received: 22 August 2018 / Revised: 25 November 2019 / Accepted: 9 December 2019
© Springer-Verlag GmbH Germany, part of Springer Nature 2020

Abstract

Purpose Human corneal epithelial cell-transformed (HCE-T) cell line is used as a widely accepted barrier model for pharmacological investigations in the context of eye application. The differentiation of (limbal) corneal epithelial into mature corneal epithelium coincides with the expression of established differentiation markers. If these differentiation mechanisms are disturbed, it will lead to ocular surface disease. In this study, we want to compare the expression of differentiation markers in the HCE-T cell line to differentiated primary epithelial cells (pCECs) and primary limbal epithelial cell (LEC) culture. This is necessary in order to decide whether HCE-T cells could be a tool to study the differentiation process and its regulatory networks in corneal epithelium.

Methods Primary limbal epithelial cells (LECs) for cell culture and primary corneal epithelial cells (pCECs) as differentiated tissue samples were obtained from the limbus or central cornea region of corneal donors. HCE-T cell line was purchased from RIKEN Institute RCB-2280. Expression levels of conjunctival- and corneal-specific keratin and adhesion markers (KRT3, KRT12, KRT13, KRT19, DSG1), stem cell and differentiation markers (PAX6, ABCG2, ADH7, TP63, ALDH1A1), and additional (unvalidated) putative differentiation and stem cell markers (CTSV, SPINK7, DKK1) were analyzed with qPCR. Additionally, KRT3, KRT12, DSG1, and PAX6 protein levels were analyzed with Western blot.

Results KRT3, KRT12, DSG1, PAX6, ADH7, and ALDH1A1 mRNA expressions were higher in LECs and magnitudes higher in pCECs compared to HCE-T cells. KRT3, KRT12, PAX6, ALDH1A1, ADH7, TP63, and CTSV mRNAs have shown increasing mRNA expression from HCE-T < HCE-T cultured in keratinocyte serum-free medium (KSFM) < LEC < to pCEC. KRT3 and KRT12 protein expressions were only slightly increased in LEC compared to HCE-T samples, and the strongest signals were seen in pCEC samples. DSG1 protein expression was only detected in pCECs. PAX6 protein expression was hardly detected in HCE-T cells, and no difference could be seen between LECs and pCECs.

Conclusions The HCE-T cell line is even less differentiated than LECs regarding the investigated markers and therefore might also lack the ability to express differentiation markers at protein level. Hence, this cell line is not suitable to study corneal differentiation processes. Primary LECs in the way cultured here are not an ideal system compared to differentiated epithelium in organ culture but should be preferred to HCE-T cells if corneal differentiation markers are investigated. Other cell models or differentiation protocols should be developed in the future to gain new tools for research on ocular surface diseases.

Keywords HCE-T · Limbal epithelial cells · Primary corneal epithelium · Cornea-specific differentiation markers · Cell line

Anna-Klara Rubelowski and Lorenz Latta contributed equally to this work.

Electronic supplementary material The online version of this article (<https://doi.org/10.1007/s00417-019-04563-0>) contains supplementary material, which is available to authorized users.

✉ Lorenz Latta
lorenz.latta@uks.eu

¹ Department of Ophthalmology, Saarland University Medical Center, Homburg, Saar, Germany

² Department of Ophthalmology, Semmelweis University, Budapest, Hungary

Introduction

The HCE-T cell line was developed in 1995 by Araki-Sasaki et al. [1]. These cells express 64 kDa keratin (KRT3) upon a longer cultivation period (7 days+), and this epithelial cell line shows similar properties to differentiated corneal epithelial cells derived from organs. Aldehyde dehydrogenase activity is used as an abundant protein marker for differentiated corneal epithelial cells and its activity was only slightly decreased in the HCE-T cell line compared to a human corneal epithelial sheet [1]. Since its development, several other properties of the HCE-T cell line have been investigated but mostly for drug screening purposes.

Permeability and toxicity

Using the HCE-T cell line for toxicity and ocular permeability tests is to date regarded as the most appropriate cell line for both kinds of analyses. This application may also be enhanced by an artificial stroma equivalent [2]. Becker et al. reported that HCE-T cells stay more undifferentiated regarding morphology and marker permeability compared to a commercially available viral-based cell system from primary corneal epithelial cells [3]. Other groups reported that the HCE-T cell line builds desmosomes, tight junctions, and basal cells, which explains its wide use in drug permeability assays [4, 5]. HCE-T is an immortalized cell line. In vitro studies are also likely to be performed with immortalized cell lines, especially the well-established HCE-T line because of its easy handling in order to generate comparable results. However, results using monolayered cell cultures of various origins have limitations in several aspects and it is difficult to translate their results to complex in vivo situations, e.g., in human eyes (review see: [6]).

Genetic stability

Since a cell line can change its properties over time, the genetic stability of HCE-T cells was investigated. Subcloning and genetic analysis revealed that these cells are heterogenous and genetically unstable. They should therefore be individually tested as to whether they match the genetically intended research purpose [7].

Description at molecular level

Only very few systematic studies characterized the HCE-T cell line at a molecular level. Drug metabolism enzymes are not altered in the HCE-T cell line [8] but ABC-transporter expression differs from human corneal epithelial cells [9, 10]. Furthermore mechanistic studies of various groups exist. Several biological processes were studied by these groups but not related to corneal differentiation [11–24].

There is not much information on corneal identity of the HCE-T cell line regarding differentiation markers known from literature and from our own studies (Table 1). To our knowledge, only one study performed a gene expression analysis comparing air-lifted HCE-T cells with primary corneal epithelial cells by microarrays identifying downregulated corneal differentiation markers [25].

Cells from primary limbal epithelial cell (LEC) culture exhibit an undifferentiated phenotype at protein level making it difficult to judge the proportion of corneal or conjunctival progenitors. As for the human corneal epithelial cell-transformed cell line (HCE-T), it is reported to express corneal differentiation markers. We choose primary corneal epithelial cell (pCE) as a reference for experiments. Those pCE cells were peeled off directly from organ culture and should therefore show maximum corneal differentiation. We used a common set of differentiation markers as described in Table 1.

We assume LECs as undifferentiated and pCECs as highly differentiated reference cells. HCE-T cells are derived from the primary corneal epithelium and were therefore expected to exhibit an expression profile more similar to corneal differentiation markers expressed in pCECs. We expected them to show an intermediate phenotype compared to the other two cell types (LECs and pCECs). The study aims to generate a semi-quantitative description of differentiation marker expression in HCE-T cells, LECs, and pCECs to determine the convenience of these cell types and cell line in studying cell differentiation processes.

The purpose of this study was to analyze expression levels of corneal- and conjunctival-specific keratin and adhesion markers (KRT3, KRT12, KRT13, KRT19, DSG1), stem cell and differentiation markers (TP63, ABCG2, PAX6, ADH7, ALDH1A1), and additional (unvalidated) putative differentiation and stem cell markers (CTSV, SPINK7, DKK1) using qPCR and KRT3, KRT12, DSG1, and PAX6 protein levels with Western blot in HCE-T, LECs, and pCECs. The barrier function is well established for the HCE-T cell line, but was also included in mRNA expression analysis (CHD1, CLDN1, OCLN1, TJP1) since cell junction properties of the HCE-T cell line is regarded suitable to test for barrier function in vitro. They should not show huge differences in expression levels. For better comparability, HCE-T cells were additionally cultured in keratinocyte serum-free medium (KSFM) since this medium was used for LEC culture.

Materials and methods

This project (work with human tissue) was approved by the Ethics Committee of Saarland/Germany (no. 226/15).

Table 1 Summary of stem cell and differentiation markers investigated in our study [12–15]

Marker (gene)	Full name	Description	Citation for the description of this marker
KRT3	Keratin, type II cytoskeletal 3	Corneal differentiation marker	[26]
KRT12	Keratin, type I cytoskeletal 12	Corneal differentiation marker	[17]
KRT13	Keratin, type I cytoskeletal 13	Conjunctival differentiation marker	[27]
KRT19	Keratin, type I cytoskeletal 19	Conjunctival differentiation marker	[27, 28]
DSG1	Desmoglein-1	Higher expression in corneal epithelium compared to conjunctival epithelium, downregulated in PAX6 [±] mouse corneal epithelial cells	[29, 30]
PAX6	Paired box protein Pax-6	Transcription factor critical for eye development; downregulated in keratopathic eye surfaces, controls expression of some corneal differentiation markers	[29, 31–33]
ABCG2	ATP-binding cassette subfamily G member 2	Putative limbal epithelial stem cell marker	[34]
ADH7	Alcohol dehydrogenase class 4 mu/sigma chain	Higher expressed differentiated corneal epithelium compared to conjunctiva epithelium	[30, 35]
TP63	Tumor protein 63	Putative limbal stem cell marker (Δ TP63 α isoform)	[36–38]
ALDH1A1	Retinal dehydrogenase 1	Maybe involved in regulation differentiation of corneal epithelial cells	[1, 30, 39, 40]
CTSV	Cathepsin L2	Major proteinase of corneal epithelium upregulated in corneal epithelium compared to conjunctiva epithelium	[30, 41]
SPINK7	Serine protease inhibitor Kazal-type 7	Involved in skin epithelial homeostasis; expression may be influenced by PAX6 (own unpublished data)	[42, 43]
DKK1	Dickkopf-related protein 1	Upregulated in limbus region	[44]

Cell culture

Human corneal epithelial cell line (HCE-T)

The HCE-T cell line is available at RIKEN cell bank (RCB 2280). Cells were seeded in 75 cm² cell culture flasks in culture medium which consisted of DMEM (Sigma-Aldrich GmbH Deisenheim, Germany) and supplemented with 5% fetal calf serum (FCS) (Fisher Scientific GmbH Schwerte, Germany), 10 ng/ml epithelial growth factor (EGF), and 1% insulin, transferrin, and selenium (ITS). The medium was changed every 2 to 3 days until the cells reached confluence. After reaching confluence, the cells were harvested ($n = 5$) using Trypsin-EDTA (0.05% trypsin, 0.002% EDTA, Sigma-Aldrich GmbH Deisenheim, Germany). Another batch of HCE-T cells was seeded in cell culture flasks with keratinocyte serum-free medium (KSFM) (Gibco, Carlsbad, USA) using the same procedure as described above ($N = 5$).

Limbal epithelial cells (LECs)

Primary limbal epithelial cells were extracted by punching small biopsies \varnothing 1.5 mm around the corneal limbus. The limbal biopsies were incubated with collagenase (5 mg/ml) for 12 h at 37 °C, filtered, washed, and trypsinated. For growth, the isolated cells were seeded into single wells of a 24-well plate with KSFM (Gibco, Carlsbad, USA). The medium was exchanged every 3 days. Before reaching confluence, the cells were passaged by trypsinization into 6-well

plates. After reaching confluence in 6-wells, the cells were passaged to four 6-well plates and were pooled for cell harvesting and lysis ($n = 5$).

Primary corneal epithelial cells (pCECs)

A mechanical separation with a scalpel was used to isolate the corneal epithelia from the donor corneas used for endothelial transplantation. These donor tissues exhibit intact corneal epithelium which could be isolated for research purposes. Epithelia of 5–7 corneas were pooled for one pCEC preparation without further cultivation to obtain differentiated cells ($n = 5$). The cells were stored at -80 °C until RNA and protein extraction.

Primary conjunctival epithelial cells (pCJEC)

As reference for conjunctival markers, pieces of conjunctiva of corneal donors were submerged in lysis buffer of RNA/DNA/protein isolation kit (Isolate II, Bioline, London, UK). Tissue was vortexed with lysis buffer and debris was centrifuged down. Supernatant of clear lysis buffer containing conjunctival RNA and protein was used for RNA and protein extraction.

RNA and protein extraction and cDNA synthesis

Cells from all preparations were processed with a RNA/DNA/protein isolation kit (Isolate II, Bioline, London, UK) according to the manufacturer's instructions. RNA quantity was checked with an UV/VIS spectrophotometry (Nanodrop

Table 2 Qiagen QuantiTect Primer pairs used for qPCR

Targeted mRNA transcripts	Cat. no.	Amplicon size (bp)
ABCG2: NM_004827, NM_001257386	QT00073206	114 bp
ADH7: NM_000673, NM_001166504	QT00000217	85 bp
ALDH1A1: NM_000689	QT00013286	97 bp
CHD1: NM_004360	QT00080143	84 bp
CLDN1: NM_021101	QT00225764	122 bp
CTSV: NM_001201575, NM_001333, XM_006716960	QT00015113	111 bp
DKK1: NM_012242	QT00009093	137 bp
DSG1: NM_001942	QT00001617	96 bp
KRT 13: NM_002274, NM_153490	QT00068747	60 bp
KRT12: NM_000223	QT00011949	104 bp
KRT19: NM_002276	QT00081137	117 bp
KRT3: NM_057088	QT00050365	118 bp
KRT4: NM_002272	QT00052500	66 bp
OCLN: NM_001205254, NM_001205255, NM_002538	QT00081844	69 bp
PAX6: NM_000280, NM_001127612, NM_001604, NM_001258462, NM_001258463, NM_001258464, NM_001258465	QT00071169	113 bp
SPINK7: NM_032566	QT00039585	126 bp
TBP: NM_001172085, NM_003194	QT00000721	132 bp
TJP1: NM_003257, NM_175610, NM_001301025, NM_001301026	QT00077308	75 bp
Tp63: NM_001114978, NM_001114979, NM_001114980, NM_001114981, NM_001114982, NM_003722	QT02424051	116 bp

1000, PeqLab, Erlangen, Germany). The protein concentration was analyzed with a Bradford kit (Merck Darmstadt, Germany).

OneTaq RT-PCR kit (New England Biolabs Inc., Frankfurt, Germany) was used to convert total RNA to cDNA with M-MuLV Enzyme Mix and oligo dT primers. Five hundred nanograms of total RNA was used for one cDNA reaction.

Quantitative PCR (qPCR)

Primer sets (Table 2) were mixed with ACEq DNA SYBR Green Mix (Vazyme) for qPCR. Samples were run in 25 μ l volume using 1 μ l cDNA and primer concentration according to the manufacturer's instructions. The qPCR experiments ($n = 5$) were carried out in 96-well plates as duplicates and were measured with a PCR Thermocycler CFX Connect (BioRad Laboratories, München, Germany). The amplification conditions were 95 °C for 10 s, 58 °C for 10 s, and 72 °C for 45 s and 44 cycles. For KRT13, an annealing temperature of 64 °C was used. TATA-binding protein (TBP) was used as a reference gene and was run under the same conditions. The C_q values were analyzed from BioRad CFX Manager Software 3.1. Fold changes were calculated using the $\Delta\Delta C_q$ method. Data analysis was performed with Excel 2016 (Microsoft Redmond, WA, USA), and expression fold changes ($2^{\Delta\Delta C_q}$) were converted to log₂ of fold changes.

Graphs were drawn with Graph Pad Prism software (Prism 7; GraphPad Software Inc., La Jolla, CA, USA).

Western blot

A list of antibodies used for Western blot analysis is summarized in Table 3. The samples of 20 μ g total protein were boiled in a sample buffer for 5 min at 95 °C. The samples were loaded and the proteins were separated on a precast 4–12% NuPage™ Bis-Tris SDS Gel (Invitrogen, Waltham, MA, USA). Following separation, the proteins were transferred onto a nitrocellulose membrane with the Trans-Blot Turbo Transfer System (BioRad, Hercules CA, USA).

Table 3 List, catalog number, manufacturer/distributor, and dilution of antibodies used for Western blot

Antibody	Catalog number, manufacturer/distributor	Dilution
ACTB (β -actin)	Ab8227, Abcam	1:5000
DSG1	sc-59904, Santa Cruz Biotechnology	1:200
KRT12	sc-515882, Santa Cruz Biotechnology	1:200
KRT13	sc-101460, Santa Cruz Biotechnology	1:200
KRT19	sc-53003, Santa Cruz Biotechnology	1:200
KRT3	CBL218, EMD Millipore	1:500
KRT4	Ab9004 [6B10] Abcam	1:1000
PAX6	sc-32766, Santa Cruz Biotechnology	1:200

WesternFroxx Washing buffer, stripping buffer blocking, and secondary antibody solution were purchased from BioFroxx GmbH, Einhausen, Germany. Blots were processed according to the manufacturer's instruction. Primary antibodies (Table 3) were diluted in combined blocking and secondary antibody solution. Each Western blot experiment was repeated 4 times. After stripping, the membrane was reprobed with anti-mouse ACTB antibodies (Table 3) as a loading control. Western lightning chemiluminescence reagent plus ECL

(PerkinElmer Life Sciences) was used for detection. The images were acquired with a LAS 4000 System (GE Healthcare, Little Chalfon, England).

Results

Figures 1, 2, and 3 display mRNA expression as \log_2 value of the fold change (\log_2 FC) of the analyzed genes. Western blot

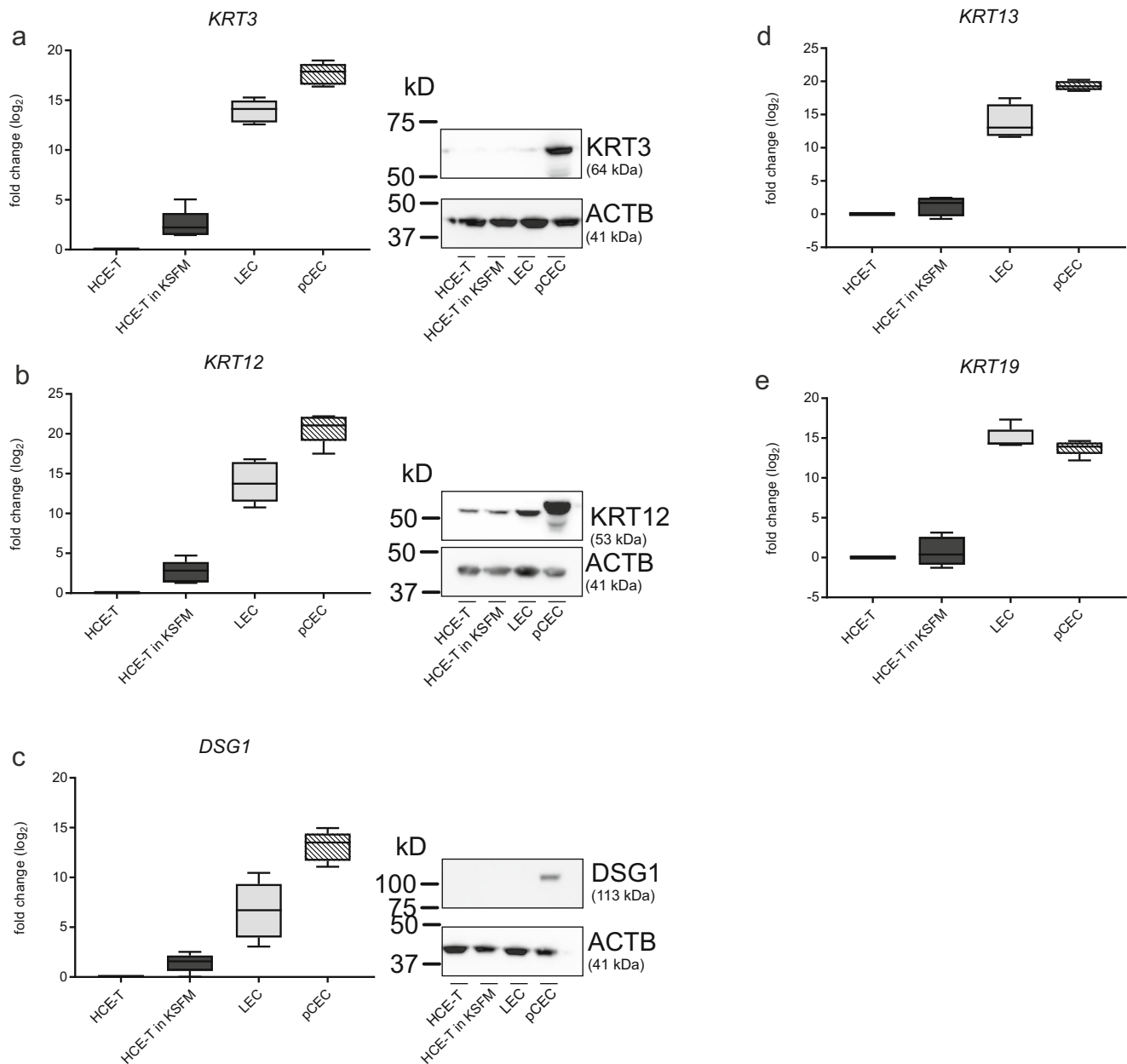
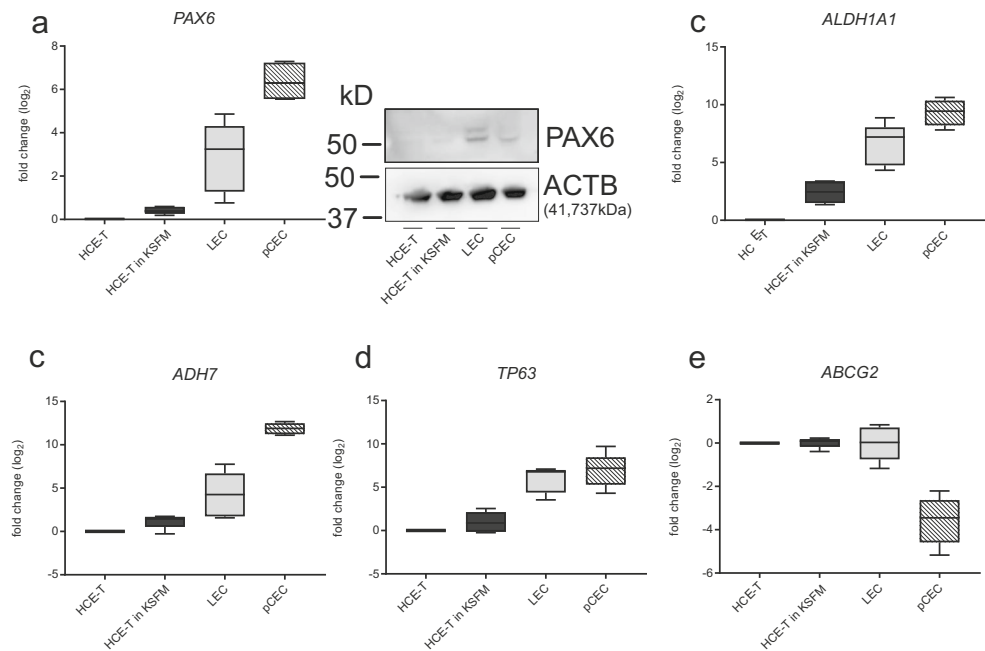


Fig. 1 qPCR results of different target genes (KRT3 (a), KRT12 (b), DSG1 (c), KRT13 (d), and KRT19 (e)) as \log_2 fold change. The \log_2 fold change of each target gene was plotted for the following cell types: cell line (HCE-T; HCE-T in KSFM), primary limbal epithelial cell (LEC) culture, and primary corneal epithelial cells (pCECs). Values were

normalized to HCE-T ($\Delta\Delta\text{CT}$ method). Corresponding protein expression of selected target genes was assayed by Western blot (a–c). The loaded protein amount of each lane was similar to the indicated loading control (ACTB, β -actin)

Fig. 2 qPCR results of different target genes (PAX6 (a), ALDH1A1 (b), ADH7 (c), TP63 (d), and ABCG2 (e)) as \log_2 fold change. The \log_2 fold change of each target gene was plotted for the following cell types: cell line (HCE-T; HCE-T in KSFM), primary limbal epithelial cell (LEC) culture, and primary corneal epithelial cells (pCECs). Values were normalized to HCE-T ($\Delta\Delta CT$ method). Corresponding protein expression of the selected target gene was assayed by Western blot (a). The loaded protein amount of each lane was similar to the indicated loading control (ACTB, β -actin)



analysis was performed to compare mRNA and protein expression between the cell types for several genes.

Conjunctival- and corneal-specific keratin and adhesion markers (qPCR)

As shown in Fig. 1, HCEC, in KSFM medium-cultured HCEC, LEC, and pCEC exhibit 5-fold to 1 millionfold difference in mRNA expression of the target genes (KRT3, KRT12, KRT13, KRT19, DSG1) (Fig. 1a–e). pCECs and LECs express thousandfold ($>10 \log_2$ FC) higher KRT3, KRT12, KRT13, and KRT19 expressions than HCE-T (Fig. 1a, b, d, e). DSG1 expression was around $6.6 \pm 2.5 \log_2$ FC in LEC and $13.1 \pm 1.3 \log_2$ FC in pCEC compared to HCE-T (Fig. 1c). In all samples, corneal differentiation markers KRT3, KRT12, and DSG1 showed magnitudes higher mRNA expression values in pCEC compared to LEC. Conjunctival differentiation markers KRT13 and KRT19 showed similar or reduced expression in pCECs compared to LECs (Fig. 1e).

Conjunctival- and corneal-specific keratin and adhesion markers (Western blot)

KRT3 Western blot analysis showed only faint signals for LEC but strong signals in pCEC samples (Fig. 1a). KRT3 and KRT12 protein expressions were only slightly increased in LEC compared to HCE-T samples. The strongest signals for KRT3 and KRT12 were seen in pCEC samples (Fig. 1b). DSG1 protein expression was only detected in pCECs but not in any other cell types (Fig. 1c).

Stem cell and differentiation markers (qPCR)

PAX6, ALDH1A1, ADH7, and TP63 mRNAs showed increasing mRNA expression from HCE-T $<$ HCE-T in KSFM $<$ LEC $<$ pCEC (Fig. 2a–e). PAX6 expression in LECs (\log_2 FC 2.9 ± 1.4) was lower as in pCECs (\log_2 FC 6.4 ± 0.7). There was no difference in TP63 mRNA expression between LEC and pCEC (Fig. 2a, d).

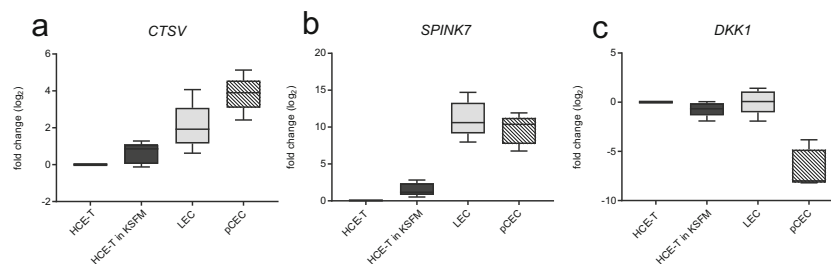


Fig. 3 qPCR results of different target genes (CTSV (a), SPINK7 (b), and DKK1 (c)) as \log_2 fold change. The \log_2 fold change of each target gene was plotted for the following cell types: cell line (HCE-T; HCE-T in

KSFM), primary limbal epithelial cell (LEC) culture, and primary corneal epithelial cells (pCECs). Values were normalized to HCE-T ($\Delta\Delta CT$ method)

ACBG2 mRNA expression in HCE-T, HCEC in KSFM, and LECs was at a similar level but its expression in pCEC was even lower (\log_2 FC -3.6 ± 0.9) than in all other cell types (Fig. 2e).

Stem cell and differentiation markers (Western blot)

There was no reproducible difference in PAX6 protein expression between LEC and pCEC. In HCE-T cells, PAX6 was only detected as a weak shadow (Fig. 2).

Additional (unvalidated) putative differentiation and stem cell markers (qPCR)

CTSV mRNA expression has shown increasing tendency from HCE-T < HCE-T in KSFM < LEC < to pCEC (Fig. 3).

The highest CTSV mRNA expression was found in pCEC (Fig. 3a). SPINK7 mRNA expression was similar in LEC (\log_2 FC 11.1 ± 2.2) and in pCEC (\log_2 FC 9.7 ± 1.8) (Fig. 3b). DKK1 mRNA expression was the lowest in pCEC and was similar for HCE-T, HCE-T in KSFM, and LEC (Fig. 3c).

Markers of cell junction (qPCR)

CDH1 (E-cadherin) and CLDN1 (Claudin-1) mRNA expression displayed an increasing tendency from HCE-T < HCE-T

in KSFM < LEC < to pCEC. In contrast, TJP1 (ZO-1) and OCLN (occludin) were lower expressed in LECs and only slightly higher expressed in pCECs (Fig. 4).

Conjunctival markers at mRNA and protein level

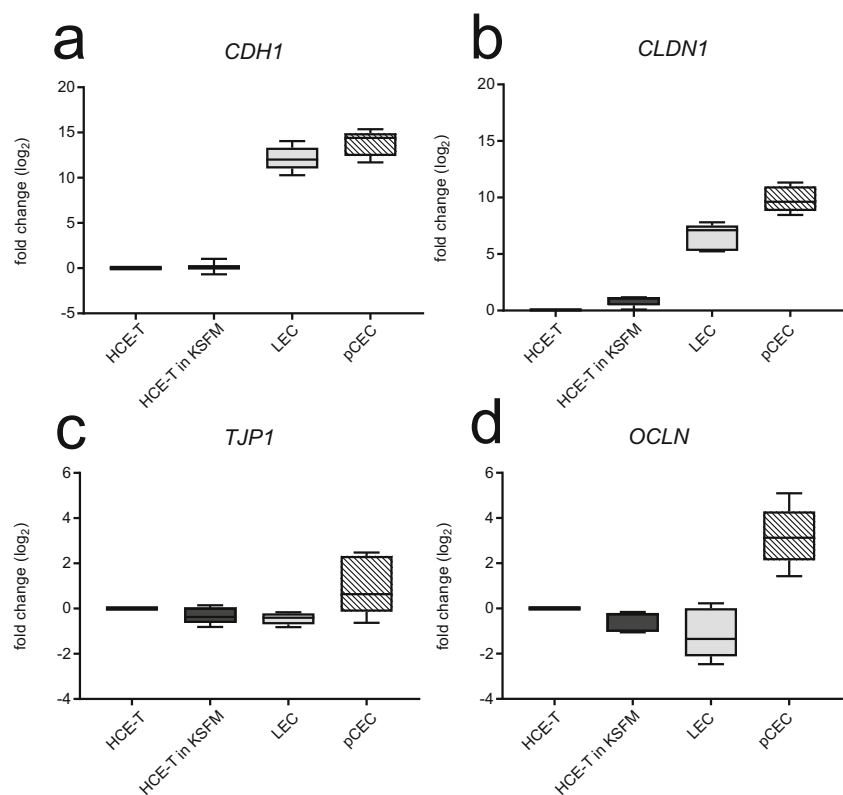
To evaluate possible conjunctival contamination in LEC culture, expression of conjunctival markers was compared to an independent set of LEC, HCE-T, and pCEC and pCjEC ($n = 3$). mRNA of conjunctival markers KRT13 and KRT4 mRNA and protein level increased from LEC to pCjEC (Fig. S1).

Discussion

Our expression data supports the hypothesis that HCE-T cells are not differentiated regarding corneal-specific expression markers. In addition, the KSFM medium had no effect on HCE-T cell line differentiation concerning the investigated gene expression.

All observed keratin markers and desmoglein (KRT3, KRT12, KRT13, KRT19, and DSG1) were higher expressed in LECs and magnitudes higher expressed in pCECs compared to HCE-T cells. Therefore, HCE-T cells are surprisingly less differentiated than LEC regarding the investigated mRNA expression levels. Western blot analysis of keratins (KRT3 and KRT12) and desmoglein 1 (DSG1) proved the correlation

Fig. 4 qPCR results of different target genes (CHD1 (a), CLDN1 (b), TJP1 (c), and OCLN1 (d)) as \log_2 fold change. The \log_2 fold change of each target gene was plotted for the following cell types: cell line (HCE-T; HCE-T in KSFM), primary limbal epithelial cell (LEC) culture, and primary corneal epithelial cells (pCECs). Values were normalized to HCE-T ($\Delta\Delta$ CT method)



of mRNA and protein production (Fig. 1a–c). The corresponding proteins (KRT3, KRT12, and DSG1) were detected in pCEC with the strongest intensity. DSG1 could only be detected in pCECs. So in contrast to its cDNA, DSG1 protein expression in LECs was not detectable. Robust mRNA expression changes in differentiation markers seemed to have low effects on protein levels as shown by comparing HCE-T and LEC levels for KRT3 and KRT12. Therefore, slight expression changes, especially in undifferentiated individual LEC preparations, are difficult to visualize at protein level with Western blot. The increasing expression of corneal differentiation markers from HCE-T < LEC < pCEC is also supported by the markers ALDH1A1, AHD7, and CTSV which were found to be increased in corneal epithelium (compared to conjunctival epithelium) [49]. SPINK7, which might be a PAX6- and cornea-dependent marker (unpublished data), showed no additional increase in pCEC. Therefore, SPINK7 is not suitable as a corneal differentiation marker.

The used HCE-T cell-culturing conditions with KSFM culture medium might suppress further differentiation of the cells. Literature search for quantitative effects of airlift culture on HCE-T cell differentiation supports our findings that the lack of differentiation is a feature of this cell line [25]. HCE-T cells showed similar differences in a study performing mRNA microarray comparison of air-lifted HCE-T cells and pCECs [25]. Additionally, this shows that our result is not caused by genetic instability, or as a result of subcloning of HCE-T cell line in our batch, which could be likely to occur [7].

Since HCE-T cells lack corneal-specific expression markers, the conjunctival-specific markers KRT13 and KRT19 were also investigated. KRT13 and KRT19 expression was magnitudes higher in LEC and pCEC compared to HCE-T cells. Other investigators [] did a stringent differentiation of corneal and conjunctival phenotype using antibodies against KRT13 and KRT4. This is true for direct comparison of corneal and conjunctival tissue. However, there is a basal expression of KRT4, KRT13, and KRT19 in pCEC and in LEC. Since pCEC and LEC also express conjunctival markers in basal quantities at mRNA and protein level, but in smaller quantities compared to pCEC (Fig. S1), it remains difficult to estimate in which ratio conjunctival precursor cells might contaminate limbal epithelial cell culture. In order to answer this question, the fate of corneal epithelial cells and conjunctival progenitor cells would have to be analyzed at the level of single mRNA and protein level during the differentiation process to mature epithelial cells. KRT19 as a conjunctival marker is under discussion since it is also identified as a stem cell marker and shows elevated expression in the limbus region compared to the cornea [48]. A conjunctival contamination of pCEC is highly unlikely since the cells were isolated from the cornea, which was spatially separated from the conjunctiva, but the marker

expression could be changed due to organ culture process before pCECs were harvested. It should be also taken into consideration that all keratins observed in HCE-T cell line showed extreme low mRNA expression values. Keratins are regulated by different transcription factors [49]. Hence, it remains unclear why all investigated keratins show very low mRNA expression levels in the HCE-T cell line.

Especially at lower mRNA expression levels, our results point to a poor correlation of mRNA and protein expression of common corneal differentiation markers. Expression changes of differentiation markers on mRNA level have to be judged carefully for biological relevance if protein expression cannot be measured accurately.

ABCG2 and DKK1 expression levels were similar in HCE-T and LEC cells. Since higher ABCG2 and DKK1 expression is characteristic for LECs and stem cells, HCE-T cells exhibit stem cell-like phenotypes for these markers. TP63 was reduced in HCE-T compared to LECs and pCECs. The critical TP63 isoform identifying undifferentiated cells might be Δ TP63 α [50]. Since Δ TP63 α isoform cannot be measured by qPCR, measuring all TP63 splice variants together might result in similarities between LECs and pCECs regarding TP63 expression.

PAX6 exhibits a $2.8 \pm 1.4 \log_2$ fold change (FC) difference in LEC and a $6.3 \pm 0.7 \log_2$ fold change (FC) difference in pCEC compared to HCE-T. This profound change in mRNA expression between LECs and pCECs could not be detected at protein level with Western blot. However, both PAX6 protein isoforms could be detected using this method. The observed variability between LEC and pCEC regarding PAX6 protein isoform expression ($n = 4$) prohibits conclusions if PAX6 isoform expression drives differentiation from LECs to pCECs. A combined isoform expression analysis by qPCR and Western blot in LEC and pCEC should be performed in the future since isoform-specific PAX6 expression has shown to regulate different target genes [50–52].

Most interestingly, the described HCE-T phenotype in this experiment has several similarities with aniridia primary cultures (undifferentiated phenotype), with a mouse aniridia model and with epithelial cell samples from patients with keratopathy [48, 53, 54]. The use of CRISPR/Cas technology to knock out PAX6 also lacks differentiation for the described differentiation markers in primary corneal epithelial cells [55]. However, another group using CRISPR/Cas knockdown of one PAX6 allele in immortalized human limbal epithelial cells did not detect changes in the markers discussed above [56].

The expression of cell junction markers was higher in HCE-T cells. Claudins (like CLDN1) were linked to electrical resistance [57]. TJPI and OCLN showed no strong repression in HCE-T compared to pCEC. The

expression changes in junction markers are not as pronounced in comparison to expression changes in keratin markers. This is studied in a more detailed way by Greco et al. [25]. The barrier function is studied after confluence, making it more difficult to compare to our experimental setup. Time dependence of investigated differentiation markers after reaching confluence should also be studied for keratin expression in the future.

Conclusions

The HCE-T cell line (or at least the passages we obtained from RIKEN institute) is not a good model to study the differentiation process of corneal epithelial cells, especially the expression of keratins. One should keep in mind that the differentiation of corneal epithelial cells, in vitro, cannot mimic in vivo differentiation of these cells on an intact ocular surface. Primary corneal cells obtained from donors should always be included to reference the endpoint of the differentiation process and to find better cell models to study differentiation and investigate the signaling cascades involved. In future studies, the role of cell junction and related signaling should be included, resulting in the inclusion of more time and environmentally derived factors during the differentiation process. This approach may lead to better models to understand surface keratopathy pathology and allow for better platforms in drug screening. Primary corneal cells treated with viruses to prolong their life span may be a good starting point since they are commercially available [3].

An idealistic model could be developed using limbal epithelial cells driving their differentiation close to the differentiation status of pCECs and thereby tracking molecular changes leading to differentiation. Other described models are based on viral transfection of pCECs mentioned above and should also be considered for a comparative analysis in the future.

Acknowledgments This work was supported by The Dr. Rolf M. Schwiete Foundation and HOMFOR.

The authors thank Prof. Flockerzi, Department of Experimental and Clinical Pharmacology and Toxicology, for providing the Western blot imaging system and Nanodrop. They would also like to thank Prof. Hoth, Department of Biophysics, Saarland University, for providing the qPCR system.

Funding This study was funded by The Rolf M. Schwiete Stiftung and HOMFOR.

Compliance with ethical standards

Ethical approval This article does not contain any studies with human participants or animals performed by any of the authors.

Conflict of interest The authors declare that they have no conflict of interest.

References

1. Araki-Sasaki K, Ohashi Y, Sasabe T, Hayashi K, Watanabe H, Tano Y, Handa H (1995) An SV40-immortalized human corneal epithelial cell line and its characterization. *Invest Ophthalmol Vis Sci* 36(3):614–621
2. Reichl S (2008) Cell culture models of the human cornea - a comparative evaluation of their usefulness to determine ocular drug absorption in-vitro. *J Pharm Pharmacol* 60(3):299–307. <https://doi.org/10.1211/jpp.60.3.0004>
3. Becker U, Ehrhardt C, Schneider M, Muys L, Gross D, Eschmann K, Schaefer UF, Lehr CM (2008) A comparative evaluation of corneal epithelial cell cultures for assessing ocular permeability. *Altern Lab Anim* 36(1):33–44
4. Toropainen E, Ranta V-P, Talvitie A, Suhonen P, Urtti A (2001) Culture model of human corneal epithelium for prediction of ocular drug absorption. *Invest Ophthalmol Vis Sci* 42(12):2942–2948
5. Juretic M, Jurisic Dukovski B, Krtalic I, Reichl S, Cetina-Cizmek B, Filipovic-Grcic J, Lovric J, Pepic I (2017) HCE-T cell-based permeability model: a well-maintained or a highly variable barrier phenotype? *Eur J Pharm Sci* 104:23–30. <https://doi.org/10.1016/j.ejps.2017.03.018>
6. Ronkko S, Vellonen KS, Jarvinen K, Toropainen E, Urtti A (2016) Human corneal cell culture models for drug toxicity studies. *Drug Deliv Transl Res* 6(6):660–675. <https://doi.org/10.1007/s13346-016-0330-y>
7. Yamasaki K, Kawasaki S, Young RD, Fukuoka H, Tanioka H, Nakatsukasa M, Quantock AJ, Kinoshita S (2009) Genomic aberrations and cellular heterogeneity in SV40-immortalized human corneal epithelial cells. *Invest Ophthalmol Vis Sci* 50(2):604–613. <https://doi.org/10.1167/iovs.08-2239>
8. Kolln C, Reichl S (2012) mRNA expression of metabolic enzymes in human cornea, corneal cell lines, and hemicornea constructs. *J Ocul Pharmacol Ther* 28(3):271–277. <https://doi.org/10.1089/jop.2011.0124>
9. Becker U, Ehrhardt C, Daum N, Baldes C, Schaefer UF, Ruprecht KW, Kim KJ, Lehr CM (2007) Expression of ABC-transporters in human corneal tissue and the transformed cell line, HCE-T. *J Ocul Pharmacol Ther* 23(2):172–181. <https://doi.org/10.1089/jop.2006.0095>
10. Verstraelen J, Reichl S (2014) Multidrug resistance-associated protein (MRP1, 2, 4 and 5) expression in human corneal cell culture models and animal corneal tissue. *Mol Pharm* 11(7):2160–2171. <https://doi.org/10.1021/mp400625z>
11. Ho JH, Chuang CH, Ho CY, Shih YR, Lee OK, Su Y (2007) Internalization is essential for the antiapoptotic effects of exogenous thymosin beta-4 on human corneal epithelial cells. *Invest Ophthalmol Vis Sci* 48(1):27–33. <https://doi.org/10.1167/iovs.06-0826>
12. Ho JH, Tseng KC, Ma WH, Chen KH, Lee OK, Su Y (2008) Thymosin beta-4 upregulates anti-oxidative enzymes and protects human cornea epithelial cells against oxidative damage. *Br J Ophthalmol* 92(7):992–997. <https://doi.org/10.1136/bjo.2007.136747>
13. Hogerheyde TA, Stephenson SA, Harkin DG, Bray LJ, Madden PW, Woolf MI, Richardson NA (2013) Evaluation of Eph receptor and ephrin expression within the human cornea and limbus. *Exp Eye Res* 107:110–120. <https://doi.org/10.1016/j.exer.2012.11.016>
14. Klinggam W, Fu R, Janga SR, Edman MC, Hamm-Alvarez SF (2018) Cathepsin S alters the expression of pro-inflammatory cytokines and MMP-9, partially through protease-activated receptor-2,

- in human corneal epithelial cells. *Int J Mol Sci* 19(11). <https://doi.org/10.3390/ijms19113530>
15. Kurpakus MA, Daneshvar C, Davenport J, Kim A (1999) Human corneal epithelial cell adhesion to laminins. *Curr Eye Res* 19(2): 106–114
 16. Lang R, Song PI, Legat FJ, Lavker RM, Harten B, Kalden H, Grady EF, Bunnett NW, Armstrong CA, Ansel JC (2003) Human corneal epithelial cells express functional PAR-1 and PAR-2. *Invest Ophthalmol Vis Sci* 44(1):99–105
 17. Nagai N, Fukuoka Y, Ishii M, Otake H, Yamamoto T, Taga A, Okamoto N, Shimomura Y (2018) Instillation of sericin enhances corneal wound healing through the ERK pathway in rat debrided corneal epithelium. *Int J Mol Sci* 19(4). <https://doi.org/10.3390/ijms19041123>
 18. Nagai N, Inomata M, Ito Y (2008) Contribution of aldehyde dehydrogenase 3A1 to disulfiram penetration through monolayers consisting of cultured human corneal epithelial cells. *Biol Pharm Bull* 31(7):1444–1448
 19. Seomun Y, Joo CK (2008) Lumican induces human corneal epithelial cell migration and integrin expression via ERK 1/2 signaling. *Biochem Biophys Res Commun* 372(1):221–225. <https://doi.org/10.1016/j.bbrc.2008.05.014>
 20. Tong L, Png E, Aihua H, Yong SS, Yeo HL, Riau A, Mendoz E, Chaurasia SS, Lim CT, Yiu TW, Iismaa SE (2013) Molecular mechanism of transglutaminase-2 in corneal epithelial migration and adhesion. *Biochim Biophys Acta* 1833(6):1304–1315. <https://doi.org/10.1016/j.bbamcr.2013.02.030>
 21. Verstraelen J, Reichl S (2015) Upregulation of P-glycoprotein expression by ophthalmic drugs in different corneal in-vitro models. *J Pharm Pharmacol* 67(5):605–615. <https://doi.org/10.1111/jph.12357>
 22. Wang M, Munier F, Araki-Saski K, Schorderet D (2002) TGFBI gene transcript is transforming growth factor-beta1-responsive and cell density-dependent in a human corneal epithelial cell line. *Ophthalmic Genet* 23(4):237–245
 23. Yamada T, Ueda T, Ugawa S, Ishida Y, Imayasu M, Koyama S, Shimada S (2010) Functional expression of transient receptor potential vanilloid 3 (TRPV3) in corneal epithelial cells: involvement in thermosensation and wound healing. *Exp Eye Res* 90(1):121–129. <https://doi.org/10.1016/j.exer.2009.09.020>
 24. Zimowska G, Shi J, Munguba G, Jackson MR, Alpatov R, Simmons MN, Shi Y, Sugrue SP (2003) Pinin/DRS/memA interacts with SRp75, SRm300 and SRrp130 in corneal epithelial cells. *Invest Ophthalmol Vis Sci* 44(11):4715–4723
 25. Greco D, Vellonen KS, Turner HC, Hakli M, Tervo T, Auvinen P, Wolosin JM, Urtti A (2010) Gene expression analysis in SV-40 immortalized human corneal epithelial cells cultured with an air-liquid interface. *Mol Vis* 16:2109–2120
 26. Schermer A, Galvin S, Sun TT (1986) Differentiation-related expression of a major 64K corneal keratin in vivo and in culture suggests limbal location of corneal epithelial stem cells. *J Cell Biol* 103(1):49–62
 27. Ramirez-Miranda A, Nakatsu MN, Zarei-Ghanavati S, Nguyen CV, Deng SX (2011) Keratin 13 is a more specific marker of conjunctival epithelium than keratin 19. *Mol Vis* 17:1652–1661
 28. Ramos T, Scott D, Ahmad S (2015) An update on ocular surface epithelial stem cells: cornea and conjunctiva. *Stem Cells Int* 2015: 601731. <https://doi.org/10.1155/2015/601731>
 29. Davis J, Duncan MK, Robison WG Jr, Piatigorsky J (2003) Requirement for Pax6 in corneal morphogenesis: a role in adhesion. *J Cell Sci* 116(Pt 11):2157–2167. <https://doi.org/10.1242/jcs.00441>
 30. Turner HC, Budak MT, Akinci MA, Wolosin JM (2007) Comparative analysis of human conjunctival and corneal epithelial gene expression with oligonucleotide microarrays. *Invest Ophthalmol Vis Sci* 48(5):2050–2061. <https://doi.org/10.1167/iov.06-0998>
 31. Liu JJ, Kao WW, Wilson SE (1999) Corneal epithelium-specific mouse keratin K12 promoter. *Exp Eye Res* 68(3):295–301. <https://doi.org/10.1006/exer.1998.0593>
 32. Ramaesh K, Ramaesh T, Dutton GN, Dhillon B (2005) Evolving concepts on the pathogenic mechanisms of aniridia related keratopathy. *Int J Biochem Cell Biol* 37(3):547–557. <https://doi.org/10.1016/j.biocel.2004.09.002>
 33. Li G, Xu F, Zhu J, Krawczyk M, Zhang Y, Yuan J, Patel S, Wang Y, Lin Y, Zhang M, Cai H, Chen D, Zhang M, Cao G, Yeh E, Lin D, Su Q, W-w L, Sen GL, Afshari N, Chen S, Maas RL, Fu X-D, Zhang K, Liu Y, Ouyang H (2015) Transcription factor PAX6 (paired box 6) controls limbal stem cell lineage in development and disease. *J Biol Chem* 290(33):20448–20454. <https://doi.org/10.1074/jbc.M115.662940>
 34. Budak MT, Alpdogan OS, Zhou M, Lavker RM, Akinci MA, Wolosin JM (2005) Ocular surface epithelia contain ABCG2-dependent side population cells exhibiting features associated with stem cells. *J Cell Sci* 118(Pt 8):1715–1724. <https://doi.org/10.1242/jcs.02279>
 35. Satre MA, Zgombic-Knight M, Duester G (1994) The complete structure of human class IV alcohol dehydrogenase (retinol dehydrogenase) determined from the ADH7 gene. *J Biol Chem* 269(22): 15606–15612
 36. Ebrahimi M, Taghi-Abadi E, Baharvand H (2009) Limbal stem cells in review. *J Ophthalmic Vis Res* 4(1):40–58
 37. Forsdahl S, Kiselev Y, Hogseth R, Mjelle JE, Mikkola I (2014) Pax6 regulates the expression of Dkk3 in murine and human cell lines, and altered responses to Wnt signaling are shown in FlpIn-3T3 cells stably expressing either the Pax6 or the Pax6(5a) isoform. *PLoS One* 9(7):e102559. <https://doi.org/10.1371/journal.pone.0102559>
 38. Pellegrini G, Dellambra E, Golisano O, Martinelli E, Fantozzi I, Bondanza S, Ponzin D, McKeon F, De Luca M (2001) p63 identifies keratinocyte stem cells. *Proc Natl Acad Sci U S A* 98(6): 3156–3161. <https://doi.org/10.1073/pnas.061032098>
 39. Labrecque J, Dumas F, Lacroix A, Bhat PV (1995) A novel isoenzyme of aldehyde dehydrogenase specifically involved in the biosynthesis of 9-cis and all-trans retinoic acid. *Biochem J* 305(Pt 2): 681–684
 40. Kumar S, Dollé P, Ghyselinck NB, Duester G (2017) Endogenous retinoic acid signaling is required for maintenance and regeneration of cornea. *Exp Eye Res* 154:190–195. <https://doi.org/10.1016/j.exer.2016.11.009>
 41. Adachi W, Kawamoto S, Ohno I, Nishida K, Kinoshita S, Matsubara K, Okubo K (1998) Isolation and characterization of human cathepsin V: a major proteinase in corneal epithelium. *Invest Ophthalmol Vis Sci* 39(10):1789–1796
 42. Furio L, Hovnanian A (2011) When activity requires breaking up: LEKTI proteolytic activation cascade for specific proteinase inhibition. *J Invest Dermatol* 131(11):2169–2173. <https://doi.org/10.1038/jid.2011.295>
 43. Meyer-Hoffert U, Wu Z, Kantyka T, Fischer J, Latendorf T, Hansmann B, Bartels J, He Y, Glaser R, Schroder JM (2010) Isolation of SPINK6 in human skin: selective inhibitor of kallikrein-related peptidases. *J Biol Chem* 285(42):32174–32181. <https://doi.org/10.1074/jbc.M109.091850>
 44. Nakatsu MN, Ding Z, Ng MY, Truong TT, Yu F, Deng SX (2011) Wnt/β-catenin signaling regulates proliferation of human cornea epithelial stem/progenitor cells. *Invest Ophthalmol Vis Sci* 52(7): 4734–4741. <https://doi.org/10.1167/iov.10-6486>
 45. Schlotzer-Schrehardt U, Kruse FE (2005) Identification and characterization of limbal stem cells. *Exp Eye Res* 81(3):247–264. <https://doi.org/10.1016/j.exer.2005.02.016>
 46. Secker GA, Daniels JT (2008) Corneal epithelial stem cells: deficiency and regulation. *Stem Cell Rev* 4(3):159–168. <https://doi.org/10.1007/s12015-008-9029-x>

47. Kurpakus MA, Stock EL, Jones JC (1990) Expression of the 55-kD/64-kD corneal keratins in ocular surface epithelium. *Invest Ophthalmol Vis Sci* 31(3):448–456
48. Bath C, Muttuvelu D, Emmersen J, Vorum H, Hjortdal J, Zachar V (2013) Transcriptional dissection of human limbal niche compartments by massive parallel sequencing. *PLoS One* 8(5):e64244–e64244. <https://doi.org/10.1371/journal.pone.0064244>
49. Blumenberg M (2006) Transcriptional regulation of keratin gene expression. In: *Intermediate Filaments*. Springer US, Boston, pp 93–109. https://doi.org/10.1007/0-387-33781-4_7
50. Di Iorio E, Barbaro V, Ruzza A, Ponzin D, Pellegrini G, De Luca M (2005) Isoforms of DeltaNp63 and the migration of ocular limbal cells in human corneal regeneration. *Proc Natl Acad Sci U S A* 102(27):9523–9528. <https://doi.org/10.1073/pnas.0503437102>
51. Sasamoto Y, Hayashi R, Park S-J, Saito-Adachi M, Suzuki Y, Kawasaki S, Quantock AJ, Nakai K, Tsujikawa M, Nishida K (2016) PAX6 isoforms, along with reprogramming factors, differentially regulate the induction of cornea-specific genes. *Sci Rep* 6: 20807. <https://doi.org/10.1038/srep20807> <http://www.nature.com/articles/srep20807#supplementary-information>
52. Kiselev Y, Eriksen TE, Forsdahl S, Nguyen LH, Mikkola I (2012) 3T3 cell lines stably expressing Pax6 or Pax6(5a)—a new tool used for identification of common and isoform specific target genes. *PLoS One* 7(2):e31915. <https://doi.org/10.1371/journal.pone.0031915>
53. Latta L, Viestenz A, Stachon T, Colanesi S, Szentmáry N, Seitz B, Käsman-Kellner B (2018) Human aniridia limbal epithelial cells lack expression of keratins K3 and K12. *Exp Eye Res* 167 (Supplement C):100–109. doi:<https://doi.org/10.1016/j.exer.2017.11.005>
54. Li W, Chen YT, Hayashida Y, Blanco G, Kheirkah A, He H, Chen SY, Liu CY, Tseng SC (2008) Down-regulation of Pax6 is associated with abnormal differentiation of corneal epithelial cells in severe ocular surface diseases. *J Pathol* 214(1):114–122. <https://doi.org/10.1002/path.2256>
55. Kitazawa K, Hikichi T, Nakamura T, Sotozono C, Kinoshita S, Masui S (2017) PAX6 regulates human corneal epithelium cell identity. *Exp Eye Res* 154:30–38. <https://doi.org/10.1016/j.exer.2016.11.005>
56. Roux IP, Romain D, Jean-Paul C, Jieqiong Q, Huiqing Z, Alain J, Olivier F, Daniel A (2018) Modeling of aniridia-related keratopathy by CRISPR/Cas9 genome editing of human limbal epithelial cells and rescue by recombinant PAX6 protein. *Stem Cells* 36(9). <https://doi.org/10.1002/stem.2858>
57. Krause G, Winkler L, Mueller SL, Haseloff RF, Piontek J, Blasig IE (2008) Structure and function of claudins. *Biochim Biophys Acta* 1778(3):631–645. <https://doi.org/10.1016/j.bbamem.2007.10.018>

Publisher's note Springer Nature remains neutral with regard to jurisdictional claims in published maps and institutional affiliations.